# Synthons of UDP-*N*-acetyl-L-Fucosamine (UDP-L-FucNAc) as potential inhibitors of *Staphylococcus aureus* Capsular Polysaccharide Biosynthesis

by

Ngoje Owuor Philemon

Submitted in Partial Fulfillment of the Requirements

For the Degree of

Masters of Science in

Chemistry

program

YOUNGSTOWN STATE UNIVERSITY

August, 2015

**Synthons of UDP-*N*-acetyl-L-Fucosamine (UDP-L-FucNAc) as potential inhibitors of *Staphylococcus aureus* Capsular Polysaccharide Biosynthesis**

Ngoje Owuor Philemon

I herby release this thesis to the public. I understand that this thesis will be made available from the OhioLINK ETD Center and the MAAG Library Circulation Desk for public access. I also authorize the University or other individuals to make copies of this thesis as needed for scholarly research.

Signature:

_____

Ngoje O. Philemon Date

Approvals:

_____

Dr. Peter Norris, Thesis Advisor Date

_____

Dr. John A. Jackson, Committee Member Date

_____

Dr. Nina V. Stourman, Committee Member Date

_____

Dr. Sal Sanders, Dean of Graduate Studies & Research Date

## ABBREVIATIONS

| | |
|---|---|
| **PBP 2a** | Penicillin binding protein 2a |
| **THF** | Tetrahydrofuran |
| **TMSCl** | Trimethylsilyl chloride |
| **$CH_2Cl_2$** | Methylene chloride |
| **TLC** | Thin layer chromatography |
| ***DI*-$H_2O$** | De-ionized water |
| **$NaHCO_3$** | Sodium bicarbonate |
| **DPPE** | 1,2-Bis(diphenylphosphino)ethane |
| **$MgSO_4$** | Magnesium sulfate |
| **IR** | Infrared Spectroscopy |
| **$^1$H NMR** | Proton nuclear magnetic resonance |
| **$^{13}$C NMR** | Carbon-13 nuclear magnetic resonance |
| **$Cp_2TiCl_2$** | Titanocene dichloride |
| **Mn** | Manganese |

## Abstract

Non-traceless modified Staudinger reaction was utilized as a safe method in this work to synthesize novel synthons of UDP-*N*-acetyl-L-fucosamine as potential inhibitors of or substrates for bacterial glycosyltransfares, responsible for the biosynthesis of the capsular polysaccharide of *Staphyloccous aureus.* Carbon-13 and proton spectral techniques were used in the characterization of formed products.

**Acknowledgements**

Having had an intense time of work on this thesis, I would like to express my sincere gratitude to the people who have offered me great help in several ways.

First, I am deeply indebted to my research advisor, Dr. Peter Norris, for his guidance throughout my research at his group and for providing a unique opportunity to work on this interesting project. I also owe him thanks for important suggestions aimed to a scientific improvement of this thesis.

There are many present and past members of Norris group to whom I am grateful for their help and encouragement while undertaking the work described in this thesis. Special thanks to Dr. Stourman, Dr. Jackson, for being part of my thesis committee members, Dr. Zeller for his crystallographic assistance, Mr. Tim Styranec for his kind and devoted attention in providing us with the necessary lab utilities upon request.

Thanks to Dr. Wagner and all the people from the chemistry department for their wonderful job and their help, also many thanks to Lisa for her kind and generous attention and help. I would also like to thank the coordinator of chemistry graduate school Dr. Lovelace for her help and kindness.

My friends Mike, Cefas, Chris, Emmanuel, Jen, Collins and Rosyline, thanks a lot for being my friends, your friendship made my life at peace.

I dedicate this thesis to the most important people in my life: my family both in Kenya and USA. Without your unconditional support, encouragement and care none of this would be possible.

## Table of contents

Title page i

Signature page ii

Abbreviations iii

Abstract iv

Acknowledgement v

Table of contents vi

List of Schemes viii

List of Equations ix

List of Tables ix

List of Figures x

Introduction

*Staphylococcus aureus*: Pathogenesis 1

*Staphylococcus aureus* mechanism of antibiotic resistance

- Resistance to β-lactams 2
- Resistance to Glycopeptides 3
- Resistance to Macrolides 5
- Resistance to Quinolones 5
- Resistance to Tetracyclines 6
- Resistance to Trimethoprim/Sulfametoxazole 6

Development of new anti-infective agents for the treatment of Methicilin-Resistant *Staphylococcus aureus* Infections

Oxaxolidinones 8

Daptomycin and Telavancin 9

Quinupristin-Dalfopristin 9

Tigecycline 10

Ceftobiprole and Ceftaroline 10

Structure of Capsular Polysaccharide of *Staphylococcus aureus* 11

Biosynthesis of UDP-L-FucNAc 12

Azide-Phosphine Chemistry 14

Statement of the Problem 16

Results and discussion

1. Retrosynthestic analysis

1.1 Synthesis of 1-bromo-2,3,4-tri-*O*-acetyl-α-L-fucose **3** 17

1.2 Synthesis of 1,3,4-tri-*O*-acetyl-2-azidodeoxy-α,β-L-fucose **6** 19

1.3 Azidonitration of Glycals 20

1.4 Azidochlorination of Glycals 22

1.5 Conversion of azido nitrate to azido acetate 23

1.6 Synthesis of amides via Staudinger reaction 24

Conclusion 35

References 54

Appendix 1 59

Experimental

General procedures 36

Synthesis of compound **2** 37

Synthesis of compound **3** 38

Synthesis of compound **4** 39

Synthesis of compound **5** 40

Synthesis of compound **6** 42

General procedures for conversion of azides to amides via Staudinger reaction 44

Synthesis of compound **7** 45

Synthesis of compound **8** 46

Synthesis of compound **9** 51

Synthesis of compound **10** 47

Synthesis of compound **11** 49

Synthesis of compound **12** 50

Synthesis of compound **13** 48

Synthesis of compound **19** 52

## Schemes

**Scheme 1:** Staudinger reaction 15

**Scheme 2:** Synthesis of compound **3** 17

**Scheme 3:** Synthesis of compound **6** 19

**Scheme 4:** Mechanism for formation of fucal **4** 19

**Scheme 5:** Proposed mechanism for azidonitration reaction 21

**Scheme 6:** Modified Staudinder reaction 24

**Scheme 7:** Schematic representation of Oxazolidinone synthesis from **8** 27

## Equations

**Equation 1:** Formation of azide radical 21

**Equation 2:** Synthesis of compound **19** 22

**Equation 3:** Attempted synthesis of compound **20** 23

**Equation 4:** Synthesis of compound **7** 26

**Equation 5:** Synthesis of compound **8** 27

**Equation 6:** Synthesis of compound **9** 29

**Equation 7:** Synthesis of compound **10** 30

**Equation 8:** Synthesis of compound **11** 31

**Equation 9:** Synthesis of compound **12** 32

**Equation 10:** Synthesis of compound **13** 33

**Equation 11:** Attempted synthesis of compounds **16** and **17** 34

## Tables

**Table 1:** Synthesis of L-FucNAc derivatives from acyl chlorides 25

**Table 2:** Structures of L-FucNAc synthons 25

## Figures

**Figure 1:** β-Lactam anti-biotic derivatives 3

**Figure 2:** Vancomycin as a glycopeptide antibiotic 4

**Figure 3:** Quinolone antibiotic derivatives 6

**Figure 4:** Structure of Co-trimoxazole 7

**Figure 5:** Oxazolidinone antibiotic derivatives 8

**Figure 6:** CP's of serotype 5 and 8 11

**Figure 7:** Biosynthesis of UDP-L-FucNAc 13

**Figure 8:** Dihedral angle between **H1** and **H2** of compound **3** 18

**Figure 9:** Structure of compound **14** 29

**Figure 10:** $^{1}$H NMR spectrum for compound **2** 60

**Figure 11:** $^{13}$C NMR spectrum for compound **2** 61

**Figure 12:** COSY spectrum for compound **2** 62

**Figure 13:** $^{1}$H NMR spectrum for compound **3** 63

**Figure 14:** $^{13}$C NMR spectrum for compound **3** 64

**Figure 15:** COSY spectrum for compound **3** 65

**Figure 16:** $^{1}$H NMR spectrum for compound **4** 66

**Figure 17:** $^{13}$C NMR spectrum for compound **4** 67

**Figure 18:** COSY spectrum for compound **4** 68

**Figure 19:** $^{1}$H NMR spectrum for compound **5** 69

**Figure 20:** $^{13}$C NMR spectrum for compound **5** 70

**Figure 21:** COSY spectrum for compound **5** 71

**Figure 22:** IR spectrum for compound **5** 72

**Figure 23:** $^{1}$H NMR spectrum for compound **6** 73

**Figure 24:** $^{13}$C NMR spectrum for compound **6** 74

**Figure 25:** COSY spectrum for compound **6** 75

**Figure 26:** IR spectrum for compound **6** 76

**Figure 27:** $^{1}$H NMR spectrum for compound **7** 77

**Figure 28:** $^{13}$C NMR spectrum for compound **7** 78

**Figure 29:** $^{1}$H NMR spectrum for compound **8** 79

**Figure 30:** $^{13}$C NMR spectrum for compound **8** 80

**Figure 31:** IR spectrum for compound **8** 81

**Figure 32:** $^{1}$H NMR spectrum for compound **11** 82

**Figure 33:** $^{13}$C NMR spectrum for compound **11** 83

**Figure 34:** IR spectrum for compound **11** 84

**Figure 35:** $^{1}$H NMR spectrum for compound **12** 85

**Figure 36:** $^{13}$C NMR spectrum for compound **12** 86

**Figure 37:** IR spectrum for compound **12** 87

**Figure 38:** $^{1}$H NMR spectrum for compound **13** 88

**Figure 39:** $^{13}$C NMR spectrum for compound **13** 89

**Figure 40:** IR spectrum for compound **13** 90

**Figure 41:** $^{1}$H NMR spectrum for compound **19** 91

**Figure 42:** $^{13}$C NMR spectrum for compound **19** 92

**Figure 43:** IR spectrum for compound **19** 93

# INTRODUCTION

*Staphylococcus aureus,* a Gram-positive bacterium, has the ability of residing in the human body without causing any harm. However, this particular pathogen is also responsible for a large portion of hospital and community-acquired infections globally. These includes superficial skin and soft tissue infections, deep wound and internal organ infections, bacteremia, endocarditis, arthritis, osteomyelitis and sepsis.[1]

Pathogenicity of *S. aureus* is attributed to the dominant methicillin- and vancomycin-resistant strains which have enabled it to acquire resistance to nearly all antibiotics used to treat it. These strains feature capsular polysaccharides which which surrounds the peptidoglycan cell wall. The thick cell wall protects bacteria from phagocytic attack by the human polymorph nuclear leukocytes and adaptive immune responses while at the same time propagating *S. aureus* persistence in the human bloodstream.[2,3] In addition to the peptidoglycan cell wall, *S. aureus* colonizes human host by secreting proteinaceous surface adhesins such as ClfB (clumping factor B proteins) and, IsdA (iron-regulated surface determinant A proteins) as well as wall techoic acid that enable adhesion onto the human epithelial cells. Secretion of invasive enzymes such as staphylokinase and evasive toxins such as cytolytic toxin plays a key role in allowing the pathogen to penetrate human tissues with ease while constantly replicating itself.[4, 5]

## *Staphylococcus aureus* mechanism of antibiotic resistance

Methicillin-resistant *Staphylococcus aureus* (MRSA) is at present the most commonly identified antibiotic-resistant pathogen. Methicillin resistance does not mean that no drugs will work. It does mean that vancomycin is the only drug which will in most instances work against multidrug-resistant *staphylococci*. The above underlying statement could soon be rejected based on the emergence of vancomycin-resistant strains that have been observed in some individuals from the previous findings.[6]

## Resistance to beta-lactams

Resistance to β-lactam antibiotics (e.g. methicillin and penicillin, **Figure 1**) is due to the production of an altered penicillin-binding-protein, known as PBP 2a by the *mecA* gene. PBP 2a as a membrane-bound enzyme catalyzes the transpeptidation reaction that is required for the cross-linking of peptidoglycan bonds. In addition, the reduced affinity of PBP 2a to β-lactam antibiotics has been shown to facilitate survival of the pathogen under high concentration of these antibiotics. Most strains of *S. aureus* also produce a class of enzymes known as β-lactamases which can hydrolyze β-lactam antibiotic molecules by splitting the amide closed-ring bonds, thus inactivating the drug and rendering it inactive. It is believed that synthesis of β-lactamases is influenced by the sequential binding of the anti-repressor and the repressor protein that regulates *blaZ* gene that encodes β-lactamase. [7, 8, 9]

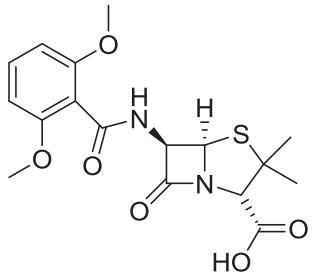


Methicilin

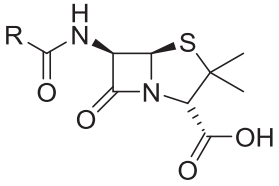


Penicilin core

**Figure 1**: β-Lactam antibiotic derivatives.

## Resistance to Glycopeptides

Glycopeptides are a group of drugs with high activity against Gram-positive micro-organisms resistant to methicillin. The bactericidal activity is limited to Gram-positive bacteria because the external membrane of Gram-negative bacteria is not permeable to these compounds, due to their hydrophobic characteristic. The mechanism of action of glycopeptides involves the inhibition of synthesis and assembly of the cell wall peptidoglycan polymers. The glycopeptides that historically have been used over the years are vancomycin (**Figure 2**) and teicoplanin. However, several recent reports have highlighted the limitations of vancomycin and teichoplanin, and their role in the management of serious infections.[10, 11]

Teicoplanin, formerly known as teichomycin A, is a lipoglycopeptide with a structural similarity to vancomycin and with high bactericidal activity against aerobic and anaerobic Gram-positive bacteria. Teicoplanin is involved in the inhibition of peptidoglycan formation. Recent findings have shown that Gram-negative strains are more resistant to this agent because it cannot penetrate their lipid membrane. Studies have also demonstrated that teicoplanin is less nephrotoxic compared to vancomycin, even in the case of close association with aminoglycosides.[12]

Prior to development of antibiotics with new modes of mechanism, vancomycin became the most widely used control drug for the treatment of body-related infections caused by methicillin-resistant *Staphylococcus aureus* (MRSA). However, its limited tissue distribution, as well as the emergence of isolates with reduced susceptibility has led to development of alternative therapies that target MRSA.[13, 14]

Vancomycin's mode of action involves inhibition of peptidoglycan cell wall synthesis by binding to the D-alanyl-D-alanine terminus of a pentapeptide. The binding inhibits addition of late precursors through a transglycosylation process by the transglycosylase enzyme thereby preventing peptidoglycan elongation and cross-linking. [15] It has also been observed that vancomycin appears to have specific activity on RNA synthesis and on the permeability of the cytoplasmic membrane in *S. aureus*. However, this mode of action is faced by non-specific binding to glycopeptides that occurs within the already mature peptidoglycan. The non-specific binding affects the action of autolysins involved in the physiological hydrolysis of peptidoglycan. [16]

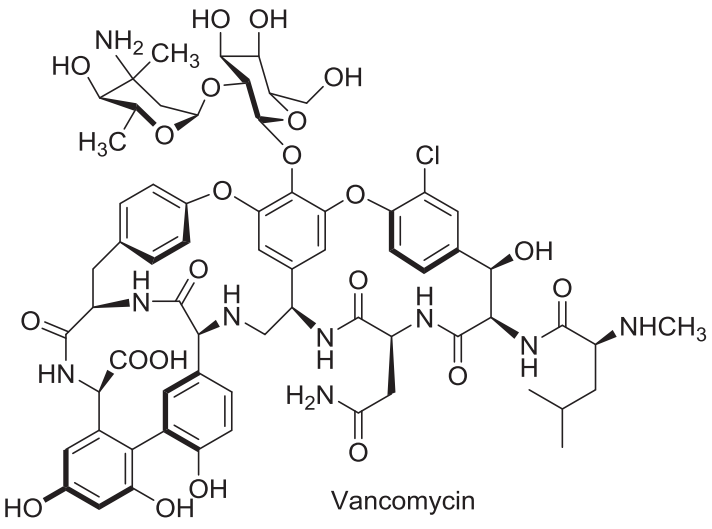


**Figure 2:** Vancomycin as a glycopeptide antibiotic.

## Resistance to Macrolides

Macrolides are antibiotic agents with a lactone ring made up of twelve or more elements. Such compounds portray better tissue penetration and good antimicrobial activity against Gram-positive bacteria. Their main mechanism of action is based upon protein synthesis inhibition by binding to the *50S* ribosomal sub-unit. Their role in treatment of MRSA infections is quite limited since they retain efficacy only against a small proportion of MRSA strains.[17]

## Resistance to Quinolones

Quinolones are a heterogeneous group of potent synthetic bactericidal antibiotics. Originally derived from nalidixic acid (**Figure 3**), modern quinolones have evolved to compounds with improved activity preferentially against Gram-negative bacteria (ciprofloxacin, Figure 3, and ofloxacin) or against Gram-positive bacteria (levofloxacin, Figure 3, gatifloxacin and moxifloxacin). The best known mechanism is the rapid inhibition of bacterial DNA synthesis and replication, by binding to the DNA-gyrase or topoisomerase IV.[18]

Levofloxacin and newer compounds such as gatifloxacin and moxifloxacin have markedly improved activity against Gram-positive pathogens. Despite this observation, the use of these agents for the treatment of MRSA is still under intense debate. Moreover, fluoroquinolone resistance can emerge rapidly after widespread utilization of these molecules. The selectivity of fluoroquinolones towards MRSA from among heterogeneous MRSA has been linked to the increased risk of hospital acquisition of MRSA, and not of MSSA (methicillin-sensitive *Staphylococcus aureus*).[19]

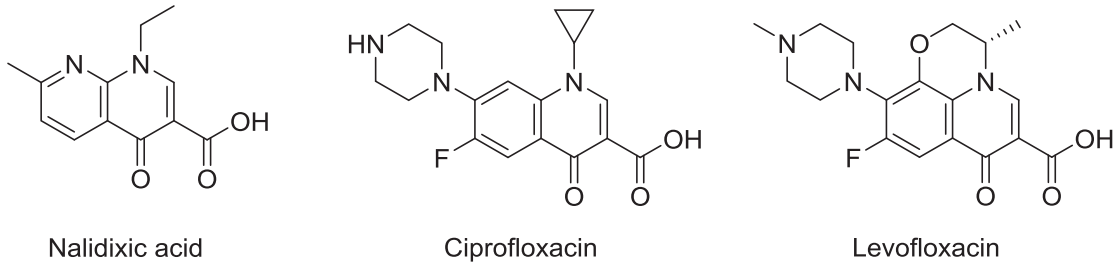


**Figure 3:** Quinolone antibiotic derivatives.

### Resistance to Tetracyclines

Tetracyclines are bacteriostatic and act by binding to the *30S* sub-units. This prevents the linking of the aminoacyl-tRNA and the microorganism ribosomes, consequently inhibiting protein synthesis. The extended use of tetracyclines in clinical practice and emergence of efflux genes and ribosomal protection proteins has led to widespread resistance against most Gram-positive and Gram-negative strains. Therefore, their role in the treatment of *staphylococcal* infections is nowadays quite limited.[20]

### Resistance to Trimethoprim/Sulfametoxazole

Trimethoprim/sulfametoxazole or Co-trimoxazole (**Figure 4**) belongs to the antibiotic group of folate inhibitors that is derived from the fixed combination of trimethoprim and sulfamethoxazole. Sulfametoxazole inhibits the production of dihydrofolic acid while trimethoprim inhibits the production of tetrahydrofolic acid. Dihydrofolic acid and tetrahydrofolic acid are forms of folic acid that *S aureus* utilizes for nucleotides and amino acids synthesis. Trimethoprim inhibits production of tetrahydrofolic acid by inhibiting tetrahydrofolate synthase, an enzyme responsible for making tetrahydrofolic acid from dihydrofolic acid. By combining both drugs, the two important steps required in the synthesis of bacterial proteins are inhibited. Resistance to

Co-trimoxazole by MRSA has been linked to the involvement of plasmids that carry altered genes. Such genes facilitate amino acid substitution in the Co-trimoxazole drug complex rendering it less effective.[21]

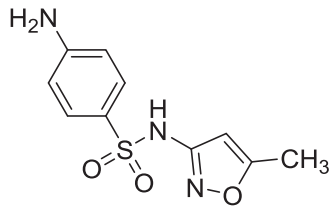


Co-trimoxazole

**Figure 4:** Structure of Co-trimoxazole.

## Development of new anti-microbial drugs for the treatment of Methicillin-Resistant *Staphylococcus aureus* infections

Generation of new antibiotic drugs has significantly decreased in the past 10 to 15 years and this can be attributed to the following two major reasons. Firstly, there is the constant evolution of new defense mechanisms by MRSA and VRSA that to a larger extent results from the over usage and inappropriate dosage of antibiotics. Secondly, many challenges met in developing new antibiotic agents with new mechanisms of action have led to the pull out of many funding agencies. However, the continuous vigorous search for new agents by scientists has paved the way for the emergence of the following twenty first century anti-infective drugs proven by FDA for the treatment of MRSA based on controlled clinical trials.[22]

## Oxazolidinones

Oxazolidinones are a new class of synthetic antibacterial agents, which have a new mechanism of action that involves early inhibition of bacterial protein synthesis. Linezolid and tedizolid (**Figure 5**) are the first molecules of the class of the oxazolidinones, and exert their bacteriostatic action by binding to the *50S* ribosome, thus inhibiting it from complexing with the *30S* sub-units, mRNA, tRNA and initiation factors. The overall goal is to disrupt the assembly of functional initiation complex of protein synthesis hence preventing translation of the mRNA.[23] In most instances; other protein synthesis inhibitors are only involved in disruption of peptide elongation while allowing for the translation of mRNA to take place at the initial stages.

With the new mode of action, oxazolidinone derivatives have been considered effective in preventing the synthesis of both staphylococcal and streptococcal virulence factors. Secondly, these agents have specific targets that do not coincide with those of existing protein synthesis inhibitors hence their activity is maintained irrespective of resistance to the other drugs. Thirdly, their activity is unaffected by the rRNA methyl-ases that modify the *23S* rRNA.[24]

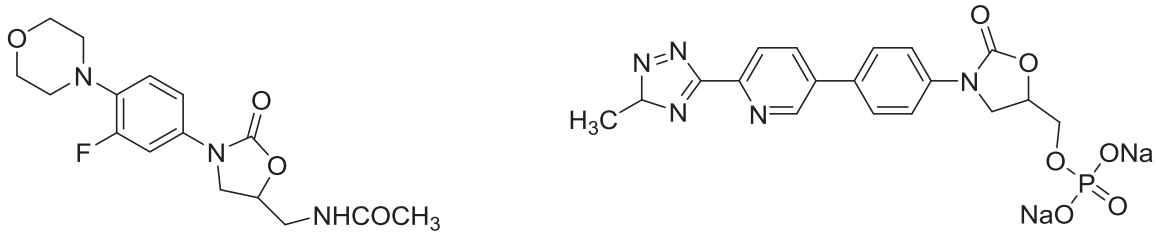


**Figure 5:** Oxazolidinone antibiotic derivatives.

## Daptomycin and Telavancin

Daptomycin is a cyclic lipopeptide and its mode of action against Gram-positive bacteria involves insertion of its lipophilic tail into the bacterial cell membrane. This results in rapid depolarization of the bacteria cell membrane and potassium ion efflux that eventually inhibits protein synthesis, DNA, and RNA. Such actions finally lead to bacterial cell lysis.[25]As a lipoglycopeptide antibiotic agent, telavancin is considered a derivative of vancomycin with a hydrophobic side chain attached to the vancosamine sugar. Studies have shown that telavancin activity is caused by the combined action on the cell wall synthesis and disruption of bacterial cell membrane. Furthermore, it has also been demonstrated that telavancin's role in inhibiting cell wall synthesis resembles that of vancomycin whereby the glycopeptide core binds to the terminal acyl-D-alanyl-D-alanine chains of the cell wall through hydrogen bonding and hydrophobic packing interaction. Such interactions prevent peptide chain elongation and cross-linking of the cell wall precursors. [26]

## Quinupristin-Dalfopristin

Quinupristin/dalfopristin is the first streptogramin that has been licensed for antibiotic therapy. This drug is available as a fixed combination of the two compounds quinupristin and dalfopristin, with appropriate ratios and has a wide range of activity against Gram-positive bacteria including inhibition of mRNA translation. In order to carry out its antibacterial activity, the action of both dalfopristin and quinupristin must be involved. That is, dalfopristin inhibits protein synthesis and peptide chain elongation by binding to the *50S* sub-units during the initial stages while quinupristin binds to the *50S*

ribosome subunits at the later stages thereby preventing peptide elongation and release of incomplete chains.[27]

## Tigecycline

As a glycylcycline derivative, tigecycline is made up of minocycline with an *N*-alkyl-glycylamido group substituted at the 9 position. These structural properties define its broad spectrum of activity and protection from resistance. As a protein synthesis inhibitor, tigecycline binds to the *30S* ribosomal subunit of bacteria and blocks the entry of amino-acyl transfer RNA into the A site of the ribosome. Studies have also indicated that steric hindrance due to a large substituent at position 9 enhances the drug activity. [28]

## Ceftobiprole and Ceftaroline

An increase in prescription of cephalosporin derivatives against MRSA has been attributed to their wide spectrum activity and acceptable levels of safety profile. Studies have shown that ceftobiprole's strong affinity for the PBP 2a results in the formation of a stable inhibitory acyl-enzyme complex that retards protein synthesis. This drug is currently under phase III clinical trials in the USA though it has been approved in some parts of the world. Ceftaroline as an antimicrobial agent is derived from the modification of the fourth-generation cephalosporin cefozopran structure. Both *in vivo* and *in vitro* assessments have shown that ceftaroline possesses a wide spectrum of activity against Gram-positive MRSA and its mechanism of action also involves binding to the penicillin-binding protein (PBP). The effective binding disrupts the mRNA translation and peptide chain elongation.[29, 30]

**Structure of Capsular Polysaccharide of *Staphylococcus aureus***

*S. aureus* produces many components that affect its virulence, including extracellular capsular polysaccharides (CPs) which enhance resistance against phagocytic uptake by human polymorphonuclear leukocytes. Capsular polysaccharides are polymeric carbohydrates attached to the outer surface of *S. aureus* and have been categorized into 12 serotypes. However, type 5 and 8 comprise the majority of clinical isolates, and thereby represent an important target for the development of a conjugate vaccine. Type 5 and 8 capsular polysaccharides (**Figure 6**) are structurally very similar to each other (each polysaccharide contains repeating units of D-FucNAc, L-FucNAc, and D-MaNAcA), but differ only in the linkages between the sugars and in the sites of *O*-acetylation.[31]

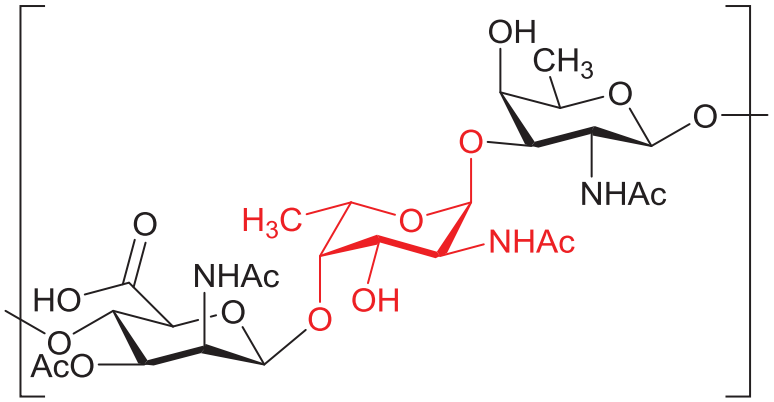


Serotype 5

**Type 5**: →4)-β-D-ManNAcA-(1→4)-α-L-FucNAc(3OAc)-(1→3)-β-D-FucNAc-(1→

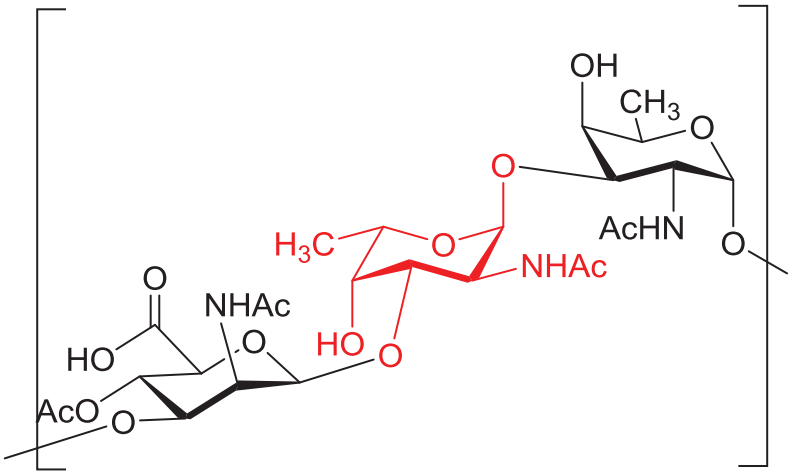


Serotype 8

**Type 8**: →3)-β-D-ManNAcA(4OAc)-(1→3)-α-L-FucNAc-(1→3)-α-D-FucNAc-(1→

**Figure 6:** Capsular polysaccharides of serotypes 5 and 8.

### Biosynthesis of UDP-L-FucNAc in *S. aureus*

*CapF* is an essential enzyme for the synthesis of UDP-L-FucNAc (UDP-*N*-acetyl-L-fucosamine), a monosaccharide derivative that is a component of CP5 and CP8. The pathway for the synthesis of UDP-L-FucNAc from UDP-D-GlcNAc (UDP-2-acetamido-2,6-dideoxy-D-galactose) has been characterized extensively. This pathway (**Figure 7**) involves three enzymes: *CapE*, *CapF* and *CapG* (Figure7). As a bifunctional enzyme, *CapE* catalyzes C-4, C-6 dehydration and C-5 epimerization of UDP-D-GlcNAc. *CapF* catalyzes the C-3 epimerization and C-4 reduction of UDP-2-acetamido-2,6-dideoxy-L-*xylo*-4-hexulose to UDP-2-acetoamido-2,6-dideoxy-L-talose, which is the second reaction in the pathway. UDP-2-acetoamido-2,6-dideoxy-L-talose is epimerized at C-2 by *CapG* to give UDP-L-FucNAc which is incorporated into the capsule polysaccharide by glycosyl transferase through condensation.[32]

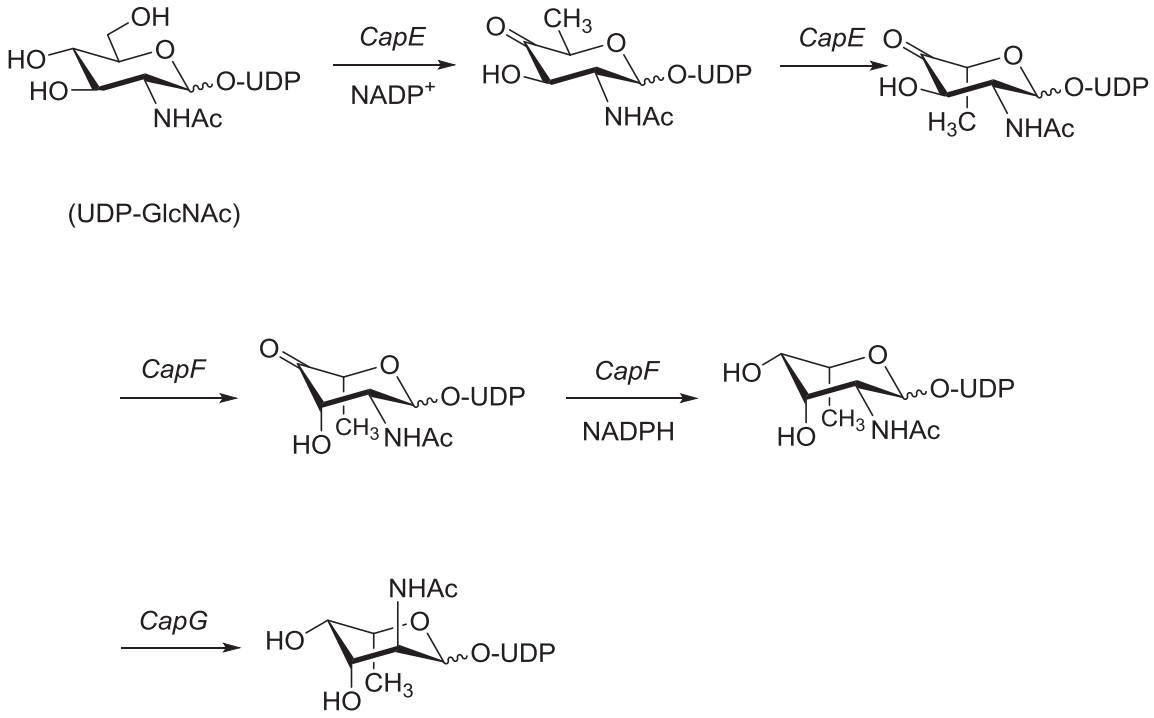


**Figure 7:** Biosynthesis of UDP-L-FucNAc in *S. aureus.*

## Azide-Phosphine Chemistry

The azide functionality serves as a reactive functional group both as an electrophile and nucleophile. Its wide application in biological systems in peptide synthesis is attributed to its unique characteristics such as absence in all naturally occurring compounds (i.e. it is *bioorthogonal*), it participates in chemoselective reactions with a limited number of other functional groups and it's smaller size that allows it to be introduced in biological systems without much alteration. Chemoselective reaction between an azide and a phosphine has greatly been utilized in tagging of molecules in biological systems.[33]

There are many well-documented reactions of azides to afford amides, for example the Huisgen 1,3 dipolar cycloadditions and the related click chemistry. The most noticeable reaction is the metal-catalyzed reduction of the glycosyl azide to the corresponding amine followed by subsequent acylation to yield the glycosyl amide. This method suffers from poor anomeric control and potential hydrolysis of the anomeric amine. Many of the so called Staudinger-type methods have also generated oxide by-products which in most cases are very hard to separate.[34]

The Staudinger ligation is a well-known technique for synthesizing a variety of glycosyl amides, including complex glycopeptides, from a reaction between an azide and phosphine. This reaction results in an iminophosphorane which in the presence of water hydrolyzes spontaneously into a primary amine and the corresponding phosphine oxide. The intermediate can also react with an acylating agent to form an amide product with controlled stereochemistry and the by-product is easily removed during the work up.[35]

We intend to utilize such properties of this particular reaction in constructing L-FucNAc analogues.

**Scheme1** shows the accepted mechanism of the Staudinger reaction in which a nucleophilic addition of the phosphine at the terminal nitrogen of the azide forms a phosphoazide, which in turn loses di-nitrogen ($N_2$) via the 4-membered-ring transition state to generate an iminophosphorane, which undergoes hydrolysis in the presence of water to form an amine or reacts with an acyl chloride to form an amide compound and phosphine oxide.[36]

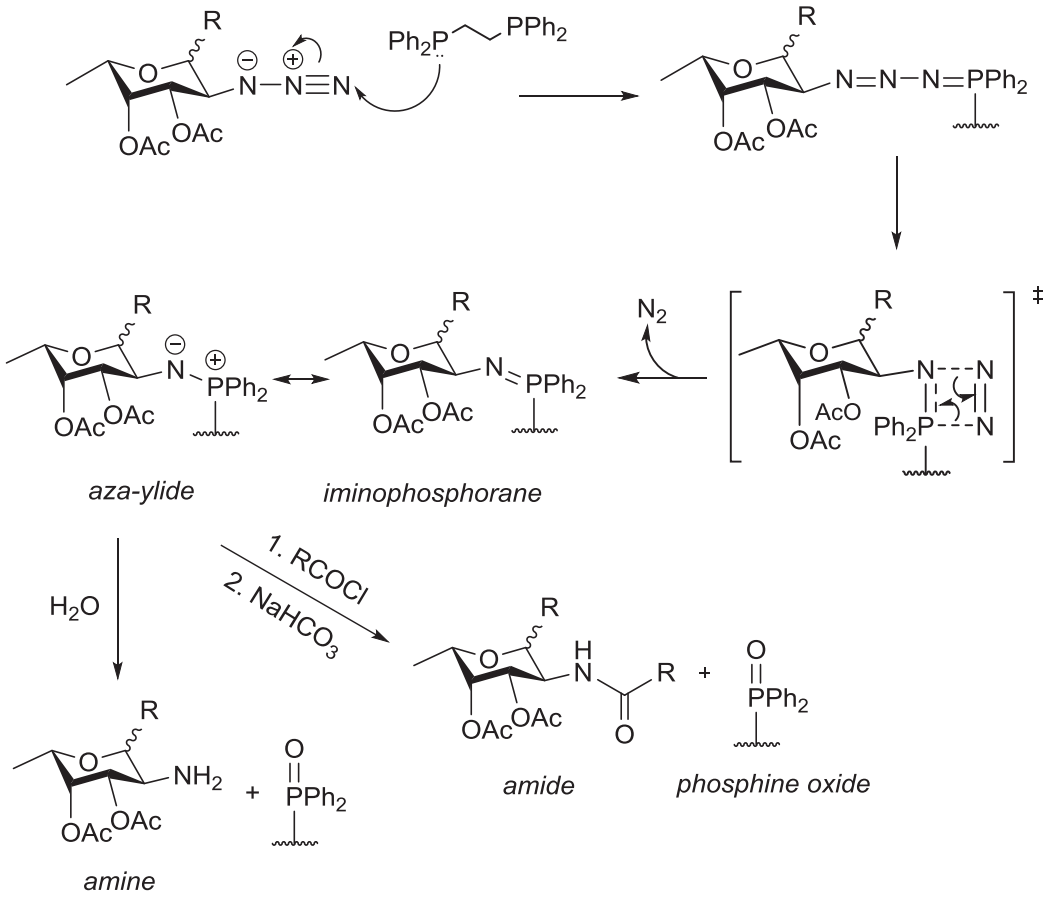


**Scheme 1:** Staudinger ligation reaction between an azide and phosphine.

## Statement of the Problem

*Staphylococcus aureus* is a leading cause of nocosomial infections in hospitals worldwide and it has become increasingly difficult to treat due to its prevalent resistance to antibiotics. Sereotypes 5 and 8 of *Staphylococcus aureus* are the most virulent strains of bacteria in the *staphylococcal* species due to the formation of polysaccharide capsules, which serve as a protective barrier in preventing phagocytosis, thereby enabling these invasive pathogens to exist in the bloodstream multiplying and destroying host cells. MRSA has wider economic effects that involve indirect costs to the patient and to society. In addition, there is some evidence suggesting that MRSA infections increase morbidity and the risk of mortality.

We intend to utilize Staudinger ligation chemistry to construct novel mimics of UDP-*N*-acetyl-L-fucosamine as potential inhibitors for bacterial glycosyltransfares. Ongoing efforts also involve attempts at incorporation of oxazolidinone structures into the L-fucosamine structure and if successful we hope to carry out bioassay studies on the target bacteria.

## Results and Discussions

### 1.0 Retrosynthetic analysis

*S. aureus* produces capsular polysaccharides which enhance resistance against phagocytic uptake by human polymorphonuclear leukocytes. L-FucNAc is considered to be part of the capsular polysaccharide. The objective of this project was to develop synthetic monosaccharide analogues of this structure by introducing different substituents at C-2 and C-1 of the fucose unit using both known and new synthetic methods.

### 1.1 Synthesis of 1-bromo-2,3,4-tri-*O*-acetyl-α-L-fucose (3)

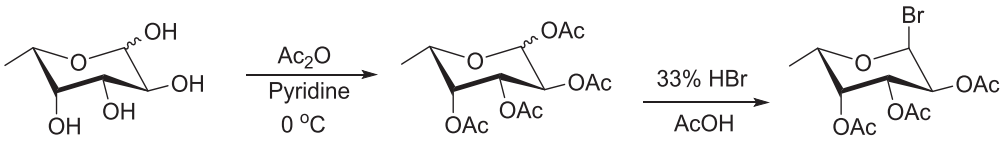


1 2 3

**Scheme 2:** Synthesis of 2,3,4-tri-*O*-acetyl-α-L-fucosyl bromide **(3)** from L-fucose (**1**).

Synthesis of fucosyl bromide **3** (**Scheme 2**) involved a two-step process from L-fucose (**1**) as the main precursor. The commercially available L-fucose was dissolved in pyridine and cooled to 0 $^{o}$C followed by a dropwise addition of acetic anhydride. The reaction was stirred overnight and its completion monitored by TLC (1:1, hexane: ethyl acetate) which confirmed the formation of compound **2** with the product $R_f$ value of 0.38. Analysis of the $^{1}$H NMR spectrum of compound **2** revealed that the resonance observed as a doublet at 6.34 ppm, with a coupling constant of 2.72 Hz, corresponded to the alpha anomeric proton, while the distinct doublet observed upfield at 5.69 ppm, with a coupling constant of 8.28 Hz corresponded to the beta anomeric proton. Integration of the ratios (α:β, 10:1) confirmed that compound **2** had an alpha configuration formed in large amounts. Analysis of the $^{13}$C NMR showed 4 distinct peaks at 169.09-170.49 ppm which

corresponded to the carbonyl groups of the acetate protecting groups while the peak at 92.96 ppm corresponded to the anomeric carbon.

Fucosyl bromide **3** was synthesized via treatment of compound **2** with 33% hydrobromic acid (HBr) in glacial acetic acid (AcOH) that resulted in the substitution of the anomeric acetate with bromide through an $S_N1$ reaction mechanism. Analysis of the $^1H$ NMR spectrum of compound **3** revealed that the resonance observed as a doublet at 6.70 ppm with a coupling constant of 3.92 Hz, corresponded to the anomeric proton confirming that compound **3** had an alpha configuration.

The alpha configuration of bromide **3** is considered to arise from the fact that the electronegative group at the anomeric position was thermodynamically favored in the axial orientation alignment which allowed for an overlap of the anti-bonding orbital with the lone pair of electrons on the oxygen ring. Using the Karplus model curve, the previous works[34] showed that the dihedral angle between H**1** and H**2** is $60^o$ as illustrated in the Newman projection of compound **3** (**Figure 8**).

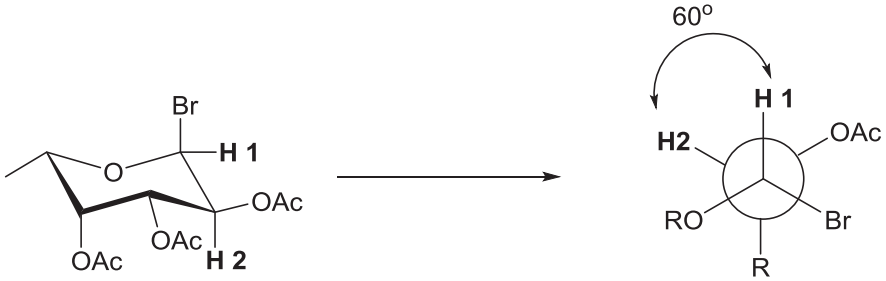


**3**

**Figure 8:** Dihedral angle between **H1** and **H2** of compound **3**.

The $^{13}C$ NMR spectrum of bromide **2** confirmed loss of one of the acetyl protecting groups as there were only 3 signals observed at 169.79-170.25 ppm while the peak at 89.32 ppm corresponded to the anomeric carbon.

### 1.2 Synthesis of 1,3,4-tri-*O*-acetyl-2-azidodeoxy-α,β-L-fucose (6)

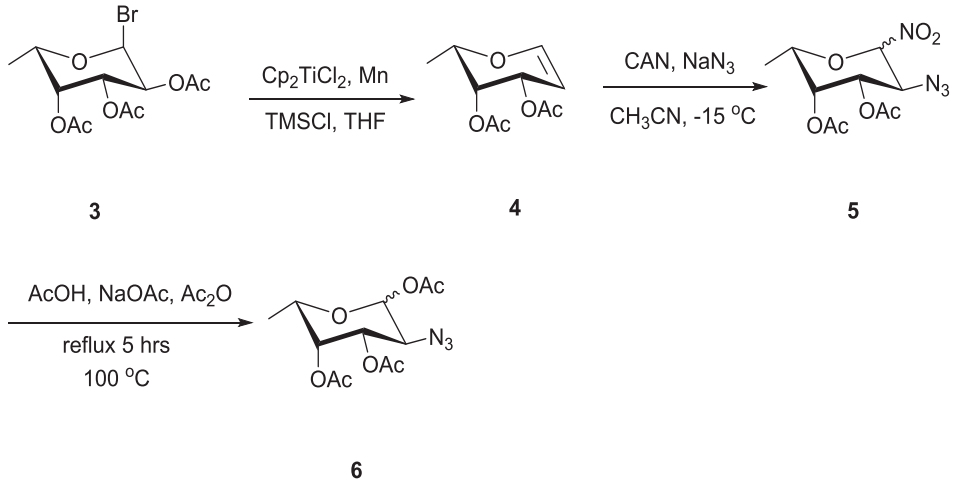


**Scheme 3:** Synthesis of 1,3,4-tri-*O*-acetyl-2-azidodeoxy-α,β-L-fucose **(6)**.

Glycals (e.g. **4**, **Scheme 3**) are well known synthesis intermediates for the preparation of oligosaccharides, *O*- or *C*-glycosides and non-carbohydrate-based natural products. They can be easily transformed into 2-amino-2-deoxy sugars which are not easily obtained by other means. Schwartz and coworkers reported on a mild and efficient means for reduction of glycosyl bromides using the dimeric titanium (III) reagent in.[37] THF promotes a fast electron transfer to the bromide to give an anomeric radical species which is reduced by another $Cp_2TiCl$ to give glycosyl titanium(IV) complex which then eliminates $Cp_2TiCl(OAc)$ (**Scheme 4**).

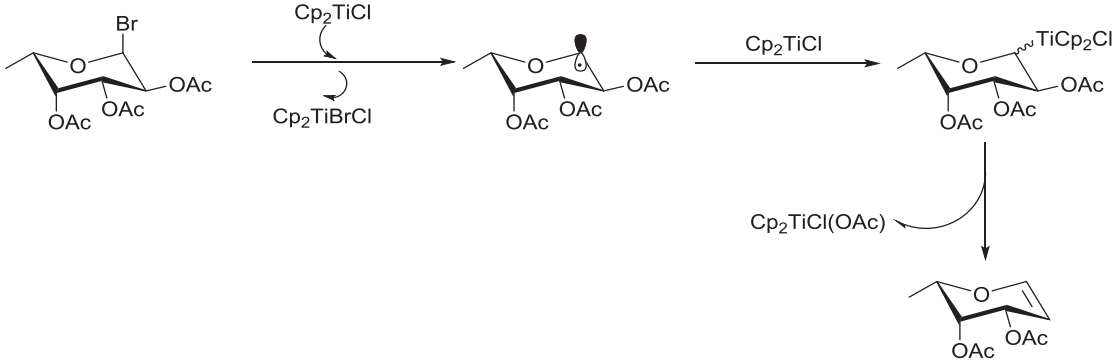


**Scheme 4:** Mechanism for the reduction of fucosyl bromide to fucal with $(Cp_2TiCl)_2$.

Compound **4** was synthesized by dissolving $(Cp_2TiCl)_2$ and Mn in THF followed by addition of a catalytic amount of TMSCl. Fucosyl bromide **3** in THF was then added in a dropwise fashion to the mixture and reaction mixture was vigorously stirred overnight. Completion of reaction was confirmed by TLC (3:1, hexane: ethyl acetate) with a product Rf value 0.30 which was lower than that of compound **3**. Analysis of the $^{1}H$ NMR spectrum of compound **4** revealed that the resonance observed as a doublet of doublets at 6.46 ppm with coupling constants of 1.88 Hz and 6.34 Hz, corresponded to the two vinyl hydrogens. Analysis of the $^{13}C$ NMR spectrum showed two distinct peaks at 170.39 and 170.68 ppm which corresponded to the carbonyl groups of the acetate protecting groups, an indication of loss of one acetate protecting group.

**1.3 Azidonitration of glycals**

The presence of 2-aminosugars in nearly every class of glycoconjugates and a number of natural products has inspired the development of synthetic methods for the construction of 2-aminoglycosides. The use of glycals as precursors for the synthesis of 2-amino sugars was pioneered by Lemieux, who introduced the azidonitration process, where glycals are transformed to 2-aminopyranosyl derivatives.[38]In a typical example, treatment of fucal **4** with CAN and sodium azide in acetonitrile gave 2-azido-deoxyfucose **5** which was further functionalised to provide fucosyl acetate **6**.

Though the mechanism of the azidonitration is not still clear, studies done by Trahanovsky *et a1*on oxidation of organic compounds with cerium(IV) to form azido-nitrate-alkanes from olefins, showed that the regioselectivity of the reaction presumably involves addition of an azide radical to form a radical intermediate containing the azide

group. The azide radical can be generated according to the reaction shown in **equation (1)**. The azide radical is then trapped by the olefins in preference to forming nitrogen gas.

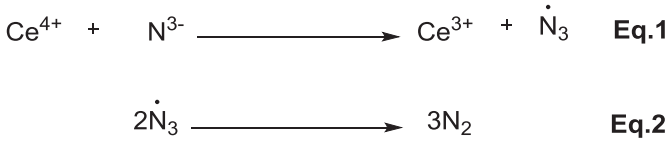


**Equation 1:** Generation of azide radical.

The overall reaction then proceeds as shown in **Scheme 5** where the resulting anomeric radical 2-azido-deoxyfucosyl is oxidized by cerium (IV) to form the oxocarbenium ion which can then react with the nucleophilic nitrate ion on either face depending probably on the orientation of the C-2 azide and the anomeric effect.[39]

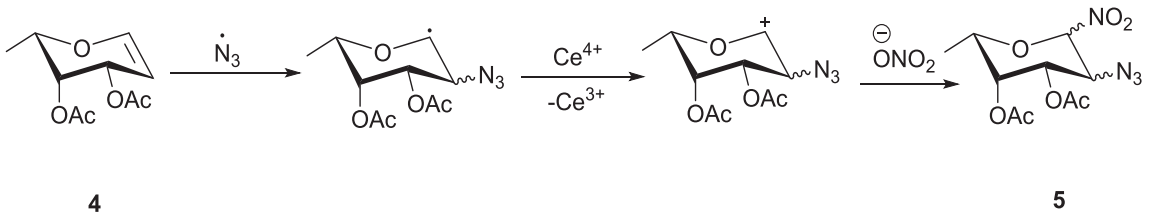


**Scheme 5:** Proposed mechanism for azidonitration reaction.

In order to prepare compound **5** a mixture of sodium azide and ceric ammonium nitrate was cooled to -15 $^{o}$C in an acetone dry-ice bath. A pre-cooled solution of L-fucal **4** in anhydrous acetonitrile was then added slowly into the reaction flask and the resulting mixture was stirred vigorously at -15 $^{o}$C for 5 hours under inert conditions. Completion of reaction was confirmed by TLC (3:1 pet. ether: ethyl acetate) with the product $R_f$ value of 0.36. The resulting product was used in the next step without further purification. Analysis by the $^{1}$H NMR spectrum confirmed the formation of compound **5** whereby the peak observed downfield at 6.31 ppm (d, $J$ = 4.16 Hz) was identified as proton adjacent to the nitrate group (C<u>H</u>-$NO_2$). Further analysis showed that the peak observed upfield at

4.08 ppm (dd, $J$ = 4.18 Hz, 11.30 Hz) corresponded to the proton adjacent to the azide group (C<u>H</u>-$N_3$). The $^{13}$C NMR spectrum revealed two peaks at 169.46 and 170.04 ppm which corresponded to the carbonyl of acetate group while the peak at 97.86 ppm was identified to belong to the C-$NO_2$ carbon and 55.89 ppm corresponded to the C-$N_3$ carbon. The IR spectrum showed strong band peaks at 2114.58 $cm^{-1}$ and 1686.05 $cm^{-1}$ confirming that azide and nitrate groups were present in the sugar compound.

**1.4 Azidochlorination of Glycals**

Protected glycals have a long history of use as building blocks in carbohydrate chemistry, particularly because of their effectiveness as glycosyl donors. Azidochlorination as a method for preparation of 2-amino sugars involves treatment of protected glycals with ferric chloride, sodium azide, and catalytic amount of hydrogen peroxide in acetonitrile to yield 2-azido galactosyl chlorides. These compounds are good intermediates for synthesis of 2-*N*-acetamido-2-deoxygalactosides that are components of naturally occurring glycoconjugates and oligosaccharides.[40]

However, this particular reaction resulted in lower yield for compound **19** (**Equation 2**) and only traces for compound **20** (**Equation 3**) which could not be purified through column chromatography for the next reaction step.

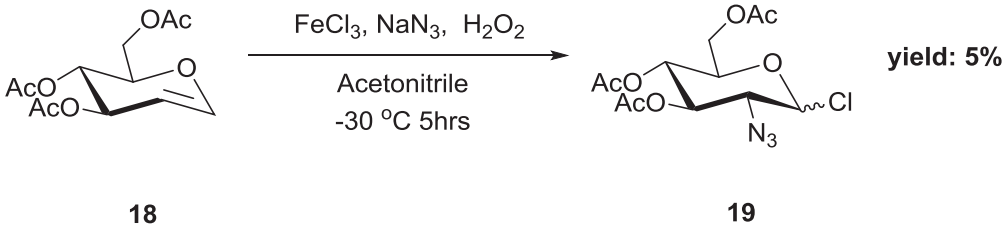


**18** **19**

**Equation 2:** Synthesis of 3,4,6-tri-*O*-acetyl-2-azidodeoxy-1-chloro-α,β-D-glucose **(19)**.

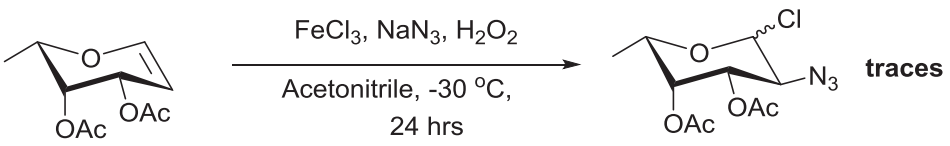


**4** **20**

**Equation 3:** Attempted synthesis of 3,4-di-*O*-acetyl-2-azidodeoxy-1-chloro-α,β-L-fucose **(20)**.

Compound **19** was prepared by cooling a mixture of compound **18**, sodium azide, and iron (III) chloride in dry acetonitrile at -30 $^{o}$C followed by dropwise addition of hydrogen peroxide resulting in 5% yield (**Equation 2**). The $^{1}$H NMR spectrum of compound **19** revealed a peak downfield at 6.35 ppm (d, $J$ = 5.92 Hz). The downfield shift of C-Cl was due to the deshielding effect of chloride as a good electron-withdrawing group. A peak observed upfield at 3.62 ppm (dd, $J$ = 3.76, 10.56 Hz) further confirmed that azide was coupled onto the C-2 carbon. Characterization by the $^{13}$C NMR spectrum revealed three peaks at 169.67-170.68 ppm which corresponded to the carbonyls of acetate groups while the peak at 96.50 ppm was identified to belong to the C-Cl carbon and 53.38 ppm corresponded to the C-$N_3$ carbon.

**1.5 Conversion of azido nitrates to azido acetates**

Preparation of compound **6** involved treatment of compound **5** with acetic acid, sodium acetate, and a catalytic amount of acetic anhydride. The mixture was refluxed for 5 hours and completion of reaction confirmed by TLC (6:4, hexane: ethyl acetate). The proton NMR spectrum confirmed that the product consisted of two anomers and was used for the next step without isolation of the two products. Analysis of the $^{1}$H NMR spectrum of compound **6** revealed that the resonance observed downfield at 6.29 ppm (d, $J$ = 3.64 Hz) corresponded to the β-anomeric proton while the upfield peak at 5.53 ppm

(d, $J$ = 8.48 Hz), corresponded to the α-anomeric proton. The substitution of the nitrate group with the acyl group was further confirmed by the $^{13}C$ NMR spectrum from the three peaks observed at 169.65-170.29 ppm, and at 20.59-20.96 ppm. These peaks corresponded to the carbonyl and methyl groups on the acetates respectively.

### 1.6 Synthesis of amides from azides via non-traceless Staudinger reaction

*N*-Glycosyl amide functionality has been utilized in the synthesis of various carbohydrate derivatives as well as their utilization in glycosylation reactions. Therefore, an extensive exploration into simple and safe methodologies for their synthesis has been given much attention in the recent past.

The Staudinger reaction as a tool of chemo-selective conjugation has been utilized to form stable amide bonds by trapping a nucleophilic intermediate formed from the reaction of a phosphine and an azide using acyl chloride (**Scheme 6**). Utilization of DPPE in the Staudinger reactions generates a phosphine oxide by-product that is readily removed allowing for rapid and simple purification of the reaction mixture.

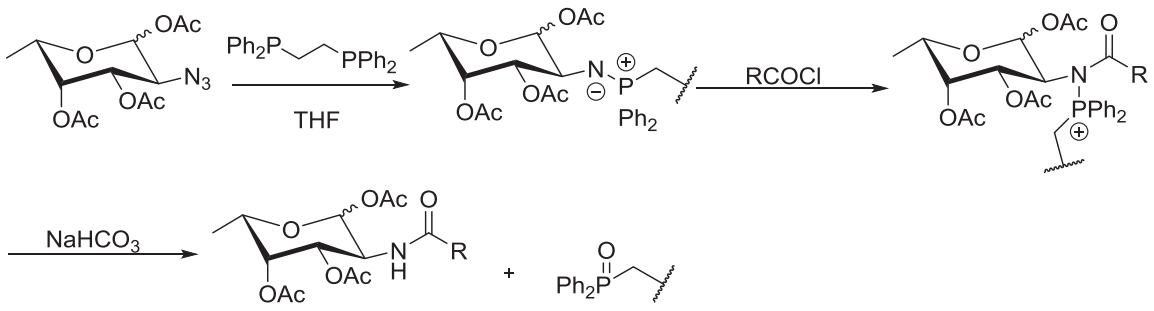


**Scheme 6:** Modified non-traceless Staudinger reaction.

**Table1.** Synthesis of L-FucNAc derivatives from acyl chlorides

| Starting material | Acyl chloride | Product | Yield (%) |
|---|---|---|---|
| **6** | Phenyl acetyl chloride | **7** | **51** |
| | Benzyl chloroformate | **8** | **30** |
| **13** | Benzyl chloroformate | **9** | **28** |
| **6** | 4-methoxy benzoyl chloride | **10** | **47** |
| | 4-chloro benzoyl chloride | **11** | **54** |
| | 2-chloro benzoyl chloride | **12** | **50** |
| **15** | 4-methoxybenzoyl chloride | **13** | **57** |

**Table2.** Structures of L-FucNAc Synthons

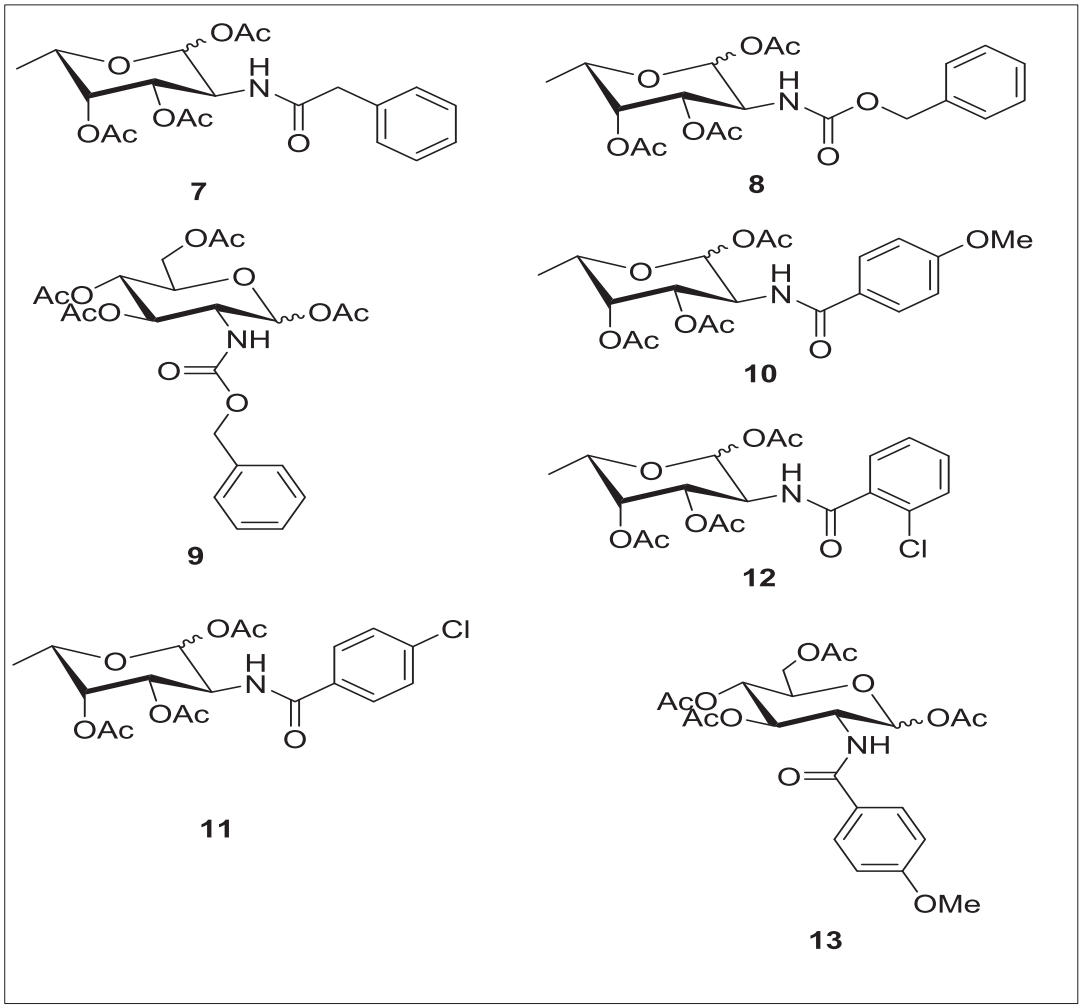

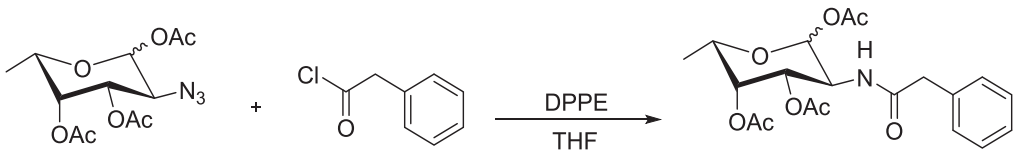


**6** **7**

**Equation 4:** Synthesis of 1,3,4-tri-*O*-acetyl-2-*N*-(phenylacetamido)-α,β-L-fucose **(7)**.

Amide **7** was obtained from a one-step synthetic protocol with 51% overall yield (**Equation 4**). In more details, azide **6** was treated with phenyl acetyl chloride and DPPE (1,2-bis (diphenylphosphine )ethane) in THF and the formation of amide **7** confirmed by TLC (2:1, hexane:ethyl acetate) with the product $R_f$ value of 0.36. Characterization by the proton NMR indicated little to no anomerization at the anomeric position with azide **6** having coupling constant of 3.64 Hz while the amide **7** had a coupling constant of 4.16 Hz. Further analysis of the proton spectrum revealed a peak downfield at 8.04 ppm (d, *J* = 8.20 Hz). This peak was assigned to the proton adjacent to the nitrogen, and the multiplicity of doublets of doublets indicated that the proton was coupled to two protons with different electronic environments. The observed downfield shift was attributed to the deshielding effect of the amide nitrogen. The $^{13}C$ NMR spectrum revealed three peaks at 169.50-170.08 ppm which corresponded to the carbonyls of acetate groups while the peak at 55.93 ppm was identified to belong to the $C_2$-N carbon and 159.63 ppm corresponded to the amide carbonyl. The IR spectrum showed strong bands at 1640.90 $cm^{-1}$, 1755.44 $cm^{-1}$, and 3156.06 $cm^{-1}$ which were assigned to the amide carbonyl, acetate carbonyl and NH respectively.

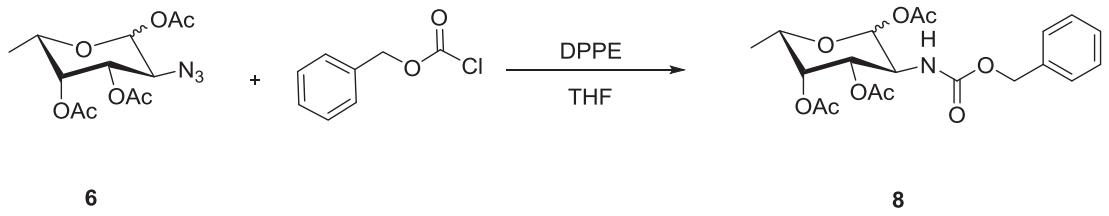


**6** **8**

**Equation 5:** Synthesis of 1,3,4-tri-*O*-acetyl-2-*N*-(benzyloxyacetamido)-α,β-L-fucose **(8)**.

Staudinger reaction protocol was utilized in the reduction of azide **6** eventually resulting in the formation of compound **8** in 30% yield (**Equation 5**). A reaction between an azide and benzyl ester in the presence of a reducing agent has extensively been utilized in formation of the key intermediate in this case; amide **8** which undergoes addition reactions to generate oxazolidinone derivative (**Scheme 7**).

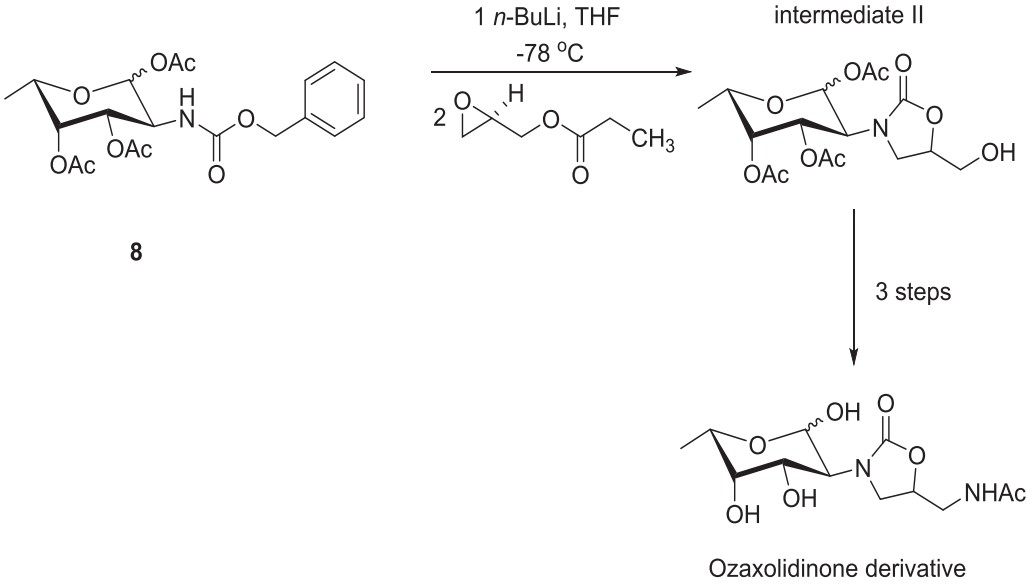


**8**

**Scheme 7:** Schematic representation of Oxazolidinone derivative synthesis from **8**.

Analysis by the proton NMR confirmed the formation of compound **8** whereby the distinct peak observed at 5.69 ppm (d, $J$ = 2.36 Hz) was assigned the anomeric proton while the peak observed further downfield at 6.34 ppm (d, $J$ = 8.28 Hz) was assigned to the proton adjacent to the nitrogen. Further characterization by the $^{13}C$ NMR spectrum revealed three peaks at 169.94-170.57 ppm which were assigned to the carbonyls of acetate groups while the peak at 55.69 ppm was identified to belong to the carbon adjacent to the nitrogen. In addition to that, the peak at 46.36 ppm was assigned the ($CH_2$) carbon and a significant peak at 156.72 ppm confirmed the reduction of an azide to an amide. The IR spectrum also proved that the reduction process had taken place as was shown by the shift of the azide band from 2114.58 $cm^{-1}$ to amide carbonyl band at 1649.76 $cm^{-1}$. Other significant band was at 1746.66 $cm^{-1}$ and it was assigned to the acetate carbonyls.

Our main goal was to transform compound **8** into intermediate II (**Scheme 7**) which would then undergo nucleophilic additions to generate Oxazolidinone derivative as a potential antibacterial drug with new mechanism of action. However, treatment of compound **6** with benzyl chloroformate and DPPE in THF resulted in formation of compound **8** and compound **14** (**Figure 9**). Formation of **14** in larger amounts compared to **8** affected our next synthetic step because the amount of starting material was of great importance in this case. The 1H NMR spectrum of compound 14 showed a peak at 3.65 ppm (d, 2H, J = 13.76Hz) indicating a methylene group coupled to the phosphorous. 13C NMR revealed a peak at 38.18 ppm (d, C-P, J = 66.55 Hz) confirming the methylene carbon was coupled to the phosphorous and 31P NMR also showed a peak at 29.31 ppm.

We noted that addition of benzyl chloroformate prior or after the formation of aza-ylide (**Scheme1**) still led to the formation of compound **14,** therefore, mechanistic aspects of the reaction outcome are yet to be fully understood.

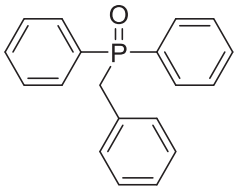

**14**

**Figure 9:** Compound formed in the presence of DPPE and benzyl chloroformate.

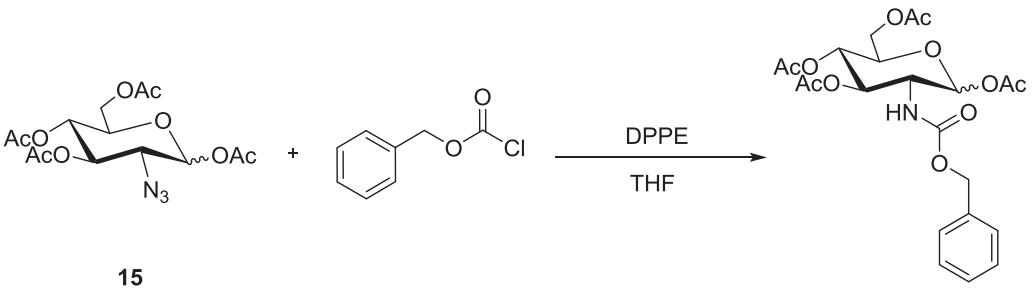


**Equation 6:** Synthesis of 1,3,4,6-tetra-*O*-acetyl-2-*N*-(benzyloxyacetamido)-α,β-L-glucose **(9)**.

The protocol utilized in synthesis of compound **9** was similar to that of compound **8** resulting in 28% yield (**Equation 6**). Characterization by the $^{1}$H NMR spectrum on compound **9** showed a peak at 5.65 ppm (d, $J$ = 2.31 Hz) which was assigned to the anomeric proton. Observance of a peak at 6.43 ppm (d, $J$ = 8.03 Hz) further affirmed the presence of a proton adjacent to the nitrogen in the compound. The $^{13}$C NMR spectrum revealed four peaks at 168.49-170.51 ppm that indicated the presence of carbonyls of

acetate groups while the peak at 55.61 ppm was identified to belong to the sugar carbon attached to the nitrogen. The presence of methylene group was affirmed by the peak at 46.23 ppm and a significant peak at 156.58 ppm confirmed formation of an amide compound. The IR spectrum showed strong bands at 1647.73 $cm^{-1}$, 1751.56 $cm^{-1}$, and 3156.37 $cm^{-1}$ which were assigned to the amide carbonyl, acetate carbonyl, and NH, respectively.

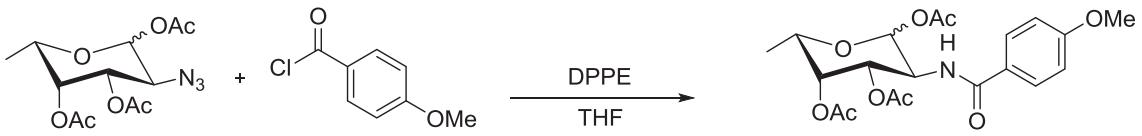


**6** **10**

**Equation 7:** Synthesis of 1,3,4-tri-*O*-acetyl-2-*N*-(4-methoxybenzamido)-α,β-L-fucose **(10)**.

Compound **10** was synthesized from a reaction of azide **6** with 4-methoxybenzoyl chloride resulting in 47% yield (**Equation 7**) and completion of reaction confirmed by TLC (2:1, hexane:ethyl acetate) with an $R_f$ value of 0.29 for the product. The $^1$H NMR spectrum showed a peak at 6.31 ppm (d, $J$ = 3.44 Hz) which was assigned as the anomeric proton and the smaller differences noted in coupling constants for the anomeric proton of **6** and **10** indicated little anomerization at the anomeric position. A downfield peak at 8.09 ppm (d, $J$ = 8.11 Hz) corresponded to the nitrogen proton and the multiplicity of doublet of doublets was an indication that the proton was coupled to two protons in different environments. The presence of the methoxy protons was also affirmed by the signal observed upfield at 3.87 ppm (s, 3H) and the multiplicity observed as a singlet in this case showed that the three protons were not coupled to any proton.

Presence of carbonyls of acetate protecting groups was confirmed by the $^{13}C$ NMR spectrum by the three peaks observed at 168.51-170.57 ppm while the peak at 55.65 ppm resulted from the attachment of the nitrogen to the second carbon of the sugar derivative. The peak at 158.99 ppm confirmed the presence of amide carbonyl. IR spectrum was utilized to further confirm the reduction of an azide to amide as was shown by the band peak at 1605.31 $cm^{-1}$ which corresponded to the amide carbonyl. The band at 1755.44 $cm^{-1}$ was assigned to the acetate carbonyl groups.

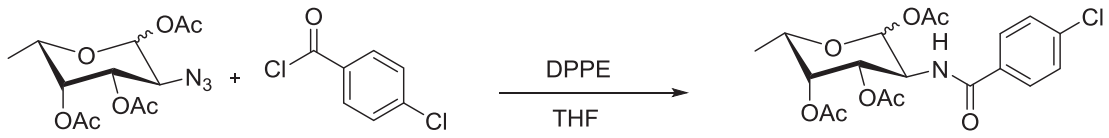


**6** **11**

**Equation 8:** Synthesis of 1,3,4-tri-*O*-acetyl-2-*N*-(4-chlorobenzamido)-α,β-L-fucose **(11)**.

In order to prepare compound **11,** azide **6** was treated with two equivalence of 4-chlorobenzoyl chloride resulting in 54% yield (**Equation 8**). Formation of **11** was confirmed by the $^{1}H$ NMR spectrum whereby the peak observed at 6.47 ppm (d, 1H, H-1, $J$ = 4.84 Hz) was assigned to the anomeric proton. A significant shift of the azide peak (3.81 ppm) to an amide peak at 8.03 ppm (d, $J$ = 8.60 Hz) confirmed the reduction of the azide to amide. The $^{13}C$ NMR spectrum revealed three peaks at 169.92-170.62 ppm which corresponded to the carbonyls of acetate groups while the distinct peak at 160.20 ppm corresponded to the amide carbonyl. IR spectrum showed bands at 1645.13 cm-1, 1747.80 cm-1, and 3156.01 cm-1 which were assigned to the amide carbonyl, acetate carbonyls, and NH, respectively.

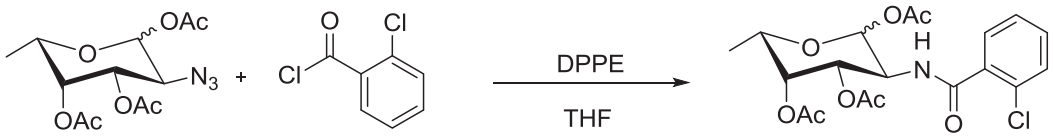


**6** **12**

**Equation 9:** Synthesis of 1,3,4-tri-*O*-acetyl-2-*N*-(2-chlorobenzamido)-α,β-L-fucose **(12)**.

Nucleophilic addition of the phosphine (DPPE) at the terminal nitrogen of the azide **6** in the presence of 2-chlorobenzoyl chloride led to the formation of compound **12** in 50% yield (**Equation 9**) with the product $R_f$ value of 0.30 by TLC (2:1, hexane:ethyl acetate). Characterization by $^1$H NMR spectroscopy revealed a peak at 5.69 ppm (d, $J$ = 2.84 Hz) that was assigned the anomeric proton while the peak observed at 8.02 ppm (d, $J$ = 8.80 Hz) was assigned to the nitrogen proton. The larger coupling constant of the amide proton compared to the azide coupling constant (4.15 Hz) affirmed that we had indeed formed compound **12**. Peaks observed between 169.90-170.80 ppm in the $^{13}$C NMR spectrum revealed the presence of carbonyls of acetate groups while the peak at 60.30 ppm was identified to belong to the C2-N carbon. A significant peak at 160.42 ppm confirmed the presence of amide carbonyl in the carbohydrate derivative **12**. IR spectrum further confirmed the conversion of azide **6** to amide **12** by the strong band peak at 1651.02 cm-1 that was assigned the amide carbonyl while the band peak at 1747.81 cm-1 was assigned the acetate carbonyls.

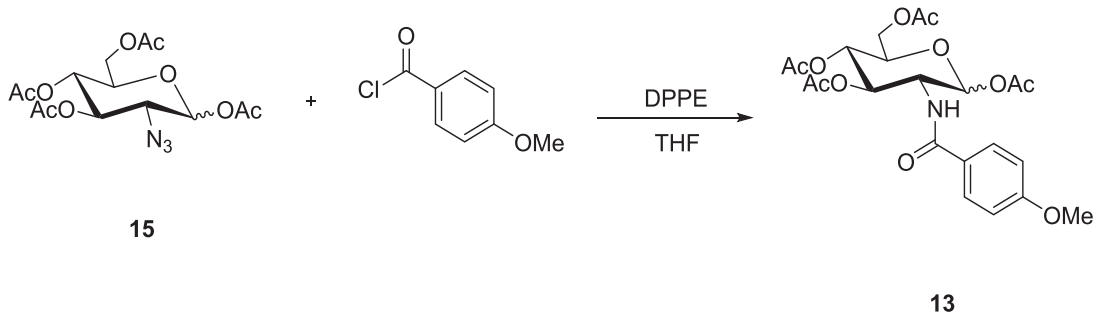


**Equation 10:** Synthesis of 1,3,4,6-tetra-*O*-acetyl-2-*N*-(4-methoxybenzamido)-α,β-D-glucose **(13)**.

Compound **13** was synthesized by employing the Staudinger reaction protocol for compound **10** resulting in 57% yield (**Equation 10**). Appearance of a purple spot with an $R_f$ value of 0.37 on TLC plate upon staining and heating on a hot plate was an indication of the formation of compound **13**. Analysis by the $^1$H NMR spectrum showed a peak at 6.34 ppm (d, $J$ = 3.40Hz) which corresponded to the anomeric proton while the peak at 8.06 ppm (d, $J$ = 8.13 Hz) was assigned the nitrogen proton. The presence of the methoxy protons was also affirmed by the signal observed upfield at 3.87 ppm (s, 3H). Further analysis done by $^{13}$C NMR spectrum revealed four peaks at 168.50-170.54 ppm which corresponded to the carbonyls of acetate groups while the peaks at 29.70 ppm and 55.72 ppm were identified to belong to the methoxy carbon and the $C_2$-N carbon respectively. Formation of an amide was proven by the peak at 159.00 ppm that was assigned the amide carbonyl. IR spectrum showed strong bands at 1605.31 cm$^{-1}$, 1755.44 cm$^{-1}$, and 3156.62 cm$^{-1}$ which were assigned to the amide carbonyl, acetate carbonyl, and NH, respectively.

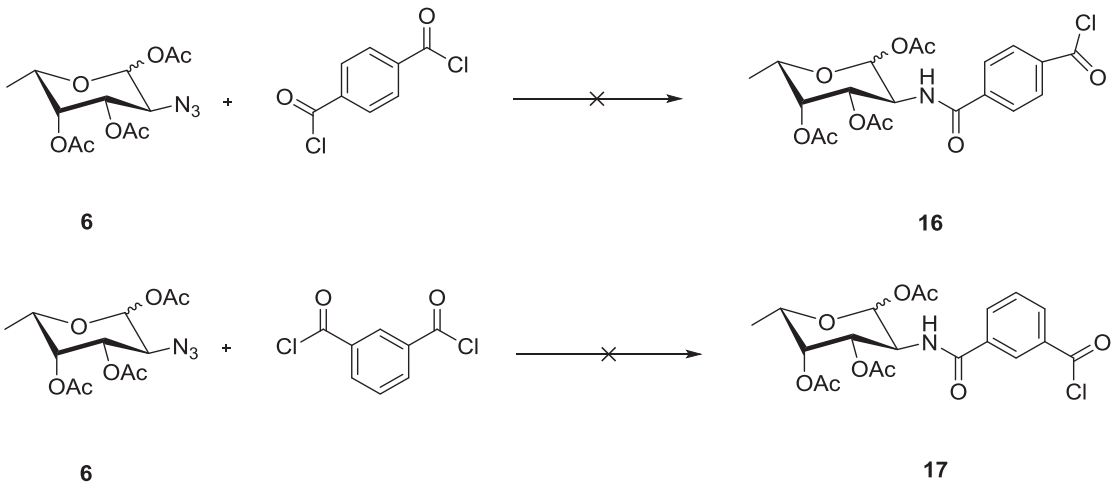


**Equation 11**: Attempted synthesis of compounds **16** and **17** from di-substituted acyl chlorides.

Treatment of **6** with either terephthaloyl chloride or isophthaloyl chloride and DPPE in THF neither led to the formation of **16** nor **17,** respectively (**Equation 11**). The azide orientation or steric effects are thought to have had great influence in the observed outcome. It is also suggested that attachment of the azide onto the sugar molecule also makes it difficult to have acyl substitution at both sides of the electrophilic carbonyl of the two acyl chlorides.

## Conclusion

Throughout this project we have succeeded in synthesizing various L-FucNAc analogs through the utilization of non-traceless modified Staudinger reaction as a feasible, safe and efficient method. We hope that optimization of our reaction conditions could result in optimum yields which could be tested and evaluated against *Staphylococcus aureus* bacteria.

The impracticability of azidochlorination method was also demonstrated, establishing that this approach was not a feasible route to 3,4-di-*O*-acetyl-2-azido-deoxyfucose derivative **20** and 3,4,6-tri-*O*-acetyl-2-azido-2-deoxyglucose derivative **19** which are good intermediates for synthesis of 2-N-acetomido deoxysugar derivatives that are components of naturally occurring glycoconjugates and oligosaccharides.

In the future, we would also want to study the feasibility of converting fucose unit **6** to an amine derivative to avoid the formation of side product **14** in the presence of DPPE and benzyl chloroformate. This will then allow us to easily introduce our oxazolidinone structure onto the fucose unit and if successful evaluate their activity against *Staphylococcus aureus* bacteria.

## GENERAL EXPERIMENTAL PROCEDURES

All reagents used were purchased from commercial sources and used without further purification. All reactions were done in oven-dried glassware fitted with rubber septum and magnetic stir bar. The reactions were monitored by thin layer chromatography whereby the spots made on the TLC plates (Aluminum- backed plates coated with silica gel) were detected upon dipping in 5% Sulfuric acid- 95% ethanol solution and heating on hot plate. A Bruker Avance III 400 NMR system was used to obtain $^{1}H$, $^{13}C$ and COSY spectrum at frequencies of 400 MHz and 100 MHz using $CDCl_3$ as solvent. Chemical shifts were measured in parts per million (ppm) and the coupling constants measured in Hertz (Hz).

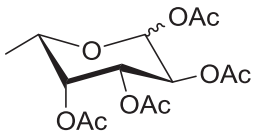


**2**

**1,2,3,4-Tetra-*O*-acetyl-α,β-L-fucose** (**2**). L-Fucose (5.0 g, 30 mmol) was dissolved in pyridine (20 mL, 248 mmol) under nitrogen atmosphere and the mixture cooled in an ice-water bath at 0 $^{o}$C. Acetic anhydride (50 mL, 529 mmol ) was then added dropwise and the reaction allowed to stir for 4 hrs during which the target product showed an $R_f$ value of 0.38 by TLC (1:1, hexane-ethyl acetate) confirming completion of the reaction. The crude mixture was then transferred to a 250 mL Erlenmeyer flask containing 40 mL ice-water and was gently stirred till all the ice melted. Organic product was extracted with methylene chloride (30 mL) and washed with 5% $H_2SO_4$ (3 × 20 mL) followed by *DI* $H_2O$ (2 × 50 mL). The Organic layer was dried over anhydrous magnesium sulfate. Evaporation *in vacuo* afforded compound **2** as a colorless syrup (8.5 g, 28 mmol, 93.33%).

**α – Anomer**

$^1$H NMR ($CDCl_3$) $\delta$ 1.16 (d, 3H, $J$ = 6.52 Hz), 2.00, 2.01, 2.14, 2.18 (s, 12H), 4.12 (dq, 1H, H-5, $J$ = 7.13 Hz), 4.27 (dd, 1H, H-4, $J$ = 6.42, 12.94 Hz), 5.08 (dd, 1H, H-3, $J$ = 3.48, 10.38 Hz), 5.27 (dd, 1H, H-2, $J$ = 0.87, 3.39 Hz), 6.34 (d, 1H, H-1, $J$ = 2.75 Hz ).

**β – Anomer**

$^1$H NMR ($CDCl_3$) $\delta$ 1.16 (d, 3H, $J$ = 6.52 Hz), 2.00, 2.01, 2.14, 2.18 (s, 12H), 4.12 (dq, 1H, H-5, $J$ = 7.13 Hz), 4.27 (dd, 1H, H-4, $J$ = 6.42, 12.94 Hz), 5.08 (dd,

1H, H-3, $J$ = 3.48, 10.38 Hz), 5.27 (dd, 1H, H-2, $J$ = 0.87, 3.39 Hz), 5.69 (d, 1H, H-1, $J$ = 8.29 Hz ).

$^{13}$C NMR ($CDCl_3$) $\delta$ 15.04, 20.53, 20.57, 20.63, 20.88, 66.51, 67.29, 67.85, 70.61, 90.00, 169.09, 169.90, 170.14, 170.49.

$R_f$ = 0.38 (1:1 hexane: ethyl acetate). M.P ($^oC$) = N/A syrup

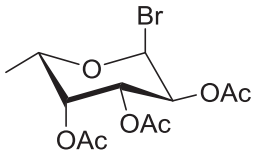


**3**

**2,3,4-Tri-*O*-acetyl-1-bromo-α-L-fucose** (**3**). L-fucosyl tetraacetate (**2**, 8.50 g, 28 mmol) was dissolved in 33% HBr in glacial acetic acid (70 mL) and the resulting brown solution mixture allowed to stir for three hours during which the target product showed an $R_f$ value of 0.39 by TLC (1:1, hexane-ethyl acetate) confirming completion of the reaction. The reaction mixture was then diluted with methylene chloride (25 mL), cooled to 0 $^oC$ and thereafter neutralized with 10% aqueous sodium hydroxide (50 mL) and saturated sodium hydrogen carbonate (5 mL). The mixture was then extracted with methylene chloride (3 × 25 mL), washed with DI H2O (3 × 25 mL), and dried over anhydrous magnesium sulfate. Evaporation in vacuo afforded compound 3 as a brown syrup. (7.24 g, 20.5 mmol, 73 %).

$^{1}$H NMR ($CDCl_3$) $\delta$ 1.22 (d, 3H, $J$ = 6.52 Hz), 2.01, 2.11, 2.17 ( s, 9H ), 4.41 (q, 1H, H-5, $J$ = 6.54 Hz), 5.03 (dd, 1H, H-4, $J$ = 3.92, 10.56 Hz ), 5.36 (dd, 1H, H-2, $J$ = 1.24, 3.32 Hz ), 5.40 ( dd, 1H, H-3, $J$ = 3.28, 10.60 Hz), 6.70 (d, 1H, H-1, $J$ = 3.92 Hz).

$^{13}$C NMR ($CDCl_3$) $\delta$ 15.57, 20.55, 20.61, 20.77, 67.91, 68.47, 69.86, 70.06, 89.32, 169.79, 170.13, 170.25.

$R_f$ = 0.39 (1:1 hexane: ethyl acetate). M.P ($^{o}$C) = N/A syrup

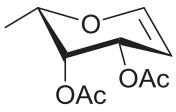


**4**

**3,4-Di-*O*-acetyl-L-fucal** (**4**). $Cp_2TiCl_2$ (3.62 g, 14.5 mmol), and Mn granules (1.81 g, 32.9 mmol) were added to THF (15 mL). A catalytic amount of TMSCl (0.51 mL) was then added and the mixture allowed to stir for 20 min. A solution of L-fucosyl bromide **3** (7.24 g, 20.5 mmol) in THF (15 mL) was added dropwise into the reaction flask then stirred vigorously and the reaction monitored by TLC (3:1 hexane: ethyl acetate). Change of color from red to green-blue was an indication of reaction going to completion with the product $R_f$ value of 0.30 that was lower than the starting material. The mixture was diluted with $CH_2Cl_2$ (30 mL) and the inorganic material filtered off through a short vaccum column. The filtrate was then concentrated *in vacuo* to afford a brown syrup

which was purified *via* flash column chromatography (3:1, hexane: ethyl acetate) yielding compound **4** as a light green oil. (3.62 g, 16.9 mmol, 82%).

$^{1}$H NMR ($CDCl_3$) $\delta$ 1.28 (d, 3H, $J$ = 6.64 Hz), 2.02, 2.16 (s, 6H ), 4.22 (dd, 1H, H-2, $J$ = 6.54, 13.21 Hz), 4.64 (dq, 1H, H-5, $J$ = 6.34 Hz ), 5.29 (dd, 1H, H-4, $J$ = 1.35, 4.62 Hz ), 5.58 (dd, 1H, H-3, $J$ = 1.06, 4.66 Hz), 6.46 (dd, 1H, H-1, $J$ = 1.88, 6.32 Hz).

$^{13}$C NMR ($CDCl_3$) $\delta$ 16.52, 20.69, 20.85, 65.07, 66.33, 71.55, 98.29, 146.13, 170. 39, 170.68.

$R_f$ = 0.30 (3:1 hexane: ethyl acetate). M.P ($^{o}$C) = N/A oil

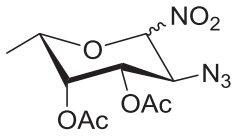


**5**

**3,4-Di-*O*-acetyl-2-azidodeoxy-1-nitro-α,β-L-fucose** (**5**). A mixture of sodium azide (1.65 g, 16.6 mmol) and ceric ammonium nitrate (27.80 g, 33.3 mmol) was cooled to -15 $^{o}$C in an acetone dry- ice bath. A pre-cooled solution of L-fucal **4** (3.6 g, 16.9 mmol) in anhydrous acetonitrile (20 mL) was slowly added into the reaction flask and the resulting mixture was stirred vigorously at -15 $^{o}$C for 5 hrs under inert conditions. Completion of reaction was confirmed by TLC (3:1 Pet. Ether: ethyl acetate) with the product Rf value of 0.36. The resulting yellow mixture was diluted with $CH_2Cl_2$ (30 mL) and washed with *DI* $H_2O$ (4 × 20 mL). The Organic layer was dried over anhydrous $MgSO_4$, filtered, and evaporated *in vacuo* to afford compound **5** as a yellow syrup (2.90 g, 9.6 mmol, 57 %).

**α – Anomer**

$^{1}$H NMR ($CDCl_3$) $\delta$ 1.18 (d, 3H, $J$ = 6.52 Hz), 2.07, 2.19 (s, 6H ), 4.08 (dd, 1H, H-2, $J$ = 4.18, 11.30 Hz), 4.30 (dq, 1H, H-5, $J$ = 6.48 Hz ), 5.25 (dd, 1H, H-4, $J$ = 3.16, 11.28 Hz ), 5.35 (dd, 1H, H-3, $J$ = 1.20, 3.20 Hz), 6.31 (d, 1H, H-1, $J$ = 4.16 Hz).

**β – Anomer**

$^{1}$H NMR ($CDCl_3$) $\delta$ 1.18 (d, 3H, $J$ = 6.52 Hz), 2.07, 2.19 (s, 6H ), 4.08 (dd, 1H, H-2, $J$ = 4.18, 11.30 Hz), 4.30 (dq, 1H, H-5, $J$ = 6.48 Hz ), 5.25 (dd, 1H, H-4, $J$ = 3.16, 11.28 Hz ), 5.35 (dd, 1H, H-3, $J$ = 1.20, 3.20 Hz), 5.56 (d, 1H, H-1, $J$ = 8.84 Hz).

$^{13}$C NMR ($CDCl_3$) δ 15.85, 20.50, 20.53, 55.89, 68.08, 68.96, 69.72, 97.86, 169.46, 170.04.

IR ($CDCl_3$) 2115.63 $cm^{-1}$ ($N_3$), 1751.27 $cm^{-1}$ (acetate carbonyls), 1674.28 $cm^{-1}$ (nitrate).

$R_f$ = 0.30 (3:1 Pet. Ether: ethyl acetate). M.P ($^{o}$C) = N/A syrup

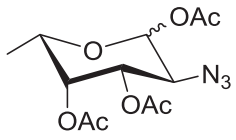


**6**

**1,3,4-Tri-*O*-acetyl-2-azidodeoxy-α,β-L-fucose** (**6**). Compound **5** (2.90 g, 9.6 mmol) and sodium acetate (3.65 g, 44.5 mmol) were dissolved in glacial acetic acid (85 mL). Acetic anhydride (4.5 mL) was then added and the resulting mixture was refluxed for 5 hrs. Crude mixture was extracted with $CH_2Cl_2$ (25 mL) and transferred into a 250 mL Erlenmeyer flask containing ice-water. The Organic layer was washed with $NaHCO_3$ (2 × 30 mL) followed by 10% NaCl (2 × 20 mL), dried over anhydrous $MgSO_4$, filtered, and evaporated *in vacuo* to afford compound **6** as a light brown syrup. **(**1.61 g, 5.1 mmol, 53%).

**α - Anomer**

$^1$H NMR ($CDCl_3$) $\delta$ 1.22 (d, 3H, $J$ = 6.44 Hz), 2.18, 2.19, 2.22 (s, 9H ), 3.81 (dd, 1H, H-2, $J$ = 8.52, 10.80 Hz), 3.90 (dq, 1H, H-5, $J$ = 6.44 Hz ), 4.89 (dd, 1H, H-4, $J$ = 3.36, 10.80 Hz ), 5.23 (dd, 1H, H-3, $J$ = 0.90, 3.32 Hz), 6.29 (d, 1H, H-1, $J$ = 3.64 Hz).

$^{13}$C NMR ($CDCl_3$) $\delta$ 15.97, 20.67, 20.91, 20.96, 67.25, 69.37, 71.74, 92.96, 169.65, 169.89, 170.29.

IR ($CDCl_3$) 2114.61 cm$^{-1}$ ($N_3$), 1751.27 cm$^{-1}$ (acetate carbonyl).

**β -anomer**

$^{1}$H NMR ($CDCl_3$) $\delta$ 1.22 (d, 3H, $J$ = 6.44 Hz), 2.18, 2.19, 2.22 (s, 9H ), 3.81 (dd, 1H, H-2, $J$ = 8.52, 10.80 Hz), 3.90 (dq, 1H, H-5, $J$ = 6.44 Hz ), 4.89 (dd, 1H, H-4, $J$ = 3.36, 10.80 Hz ), 5.23 (dd, 1H, H-3, $J$ = 0.90, 3.32 Hz), 5.53 (d, 1H, H-1, $J$ = 8.48 Hz).

$^{13}$C NMR ($CDCl_3$) $\delta$ 15.97, 20.67, 20.91, 20.96, 67.25, 69.37, 71.74, 92.96, 169.65, 169.89, 170.29.

$R_f$ = 0.34 (6:4 hexane: ethyl acetate). M.P ($^{o}$C) = N/A syrup

**General procedure for conversion of Azides to Amides via modified Staudinger reaction**

One equivalent of fucosyl azide and two equivalents of acylating agent were dissolved in anhydrous THF (0.1 g/mL). A solution of DPPE (0.65 mmol equiv.) in anhydrous THF was added dropwise to the mixture which was allowed to stir for 2 hrs at rt under inert conditions. Saturated solution of $NaHCO_3$ was added to the mixture after TLC (2:1, hexane: ethyl acetate) showed consumption of aza-ylide intermediate. The reaction mixture was then stirred vigorously for 3 hrs after which the organic solvent was removed under reduced pressure and the resulting mixture extracted with $CH_2Cl_2$ and water. Organic layer was dried over anhydrous magnesium sulfate and evaporated *in vacuo* to afford a solid mixture which was purified by flash column chromatography using appropriate solvent system.

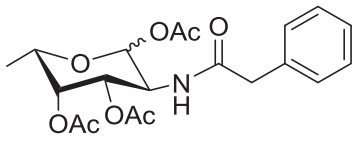


**7**

**1,3,4-Tri-*O*-acetyl-2-*N*-(phenylacetamido)-α,β-L-fucose** (**7**). Synthesized from compound **6** (98 mg, 0.31 mmol), phenyl acetyl chloride (0.08 mL, 0.62 mmol), and DPPE (0.65 mmol equiv) in THF according to the general procedure described above. Purification by flash column chromatography (2:1, hexane: ethyl acetate) yielded compound **7** as a colorless syrup (65 mg, 0.16 mmol, 51%).

$^{1}$H NMR ($CDCl_3$) $\delta$ 1.22 (d, 3H, $J$ = 6.44 Hz), 2.07, 2.15, 2.19 (s, 9H), 3.49 (s, 2H), 3.98 (dq, 1H, H-5, $J$ = 6.42 Hz), 4.20 (ddd, 1H, H-2, $J$ = 2.58, 6.22, 12.44 Hz), 5.08 (dd, 1H, H-4, $J$ = 3.34, 10.94 Hz), 5.24 (dd, 1H, H-3, $J$ = 0.94, 3.34 Hz), 6.31 (d, 1H, H-1, $J$ = 4.16 Hz), 7.26-7.32 (m aryl group), 8.04 (d, 1H, NH, $J$ = 8.20 Hz).

$^{13}$C NMR ($CDCl_3$) $\delta$ 15.89, 20.42, 20.53, 20.56, 29.71, 55.93, 68.11, 69.00, 69.76, 71.21, 97.48, 125.32, 128.24, 129.05, 159.63, 169.50, 169.50, 170.08.

IR ($CDCl_3$) 3156.47 cm$^{-1}$ (NH), 1755.44 cm$^{-1}$ (acetate carbonyls), 1640.90 cm$^{-1}$ (NHCO).

$R_f$ = 0.36 (2:1 hexane: ethyl acetate). M.P ($^{o}$C) = N/A syrup

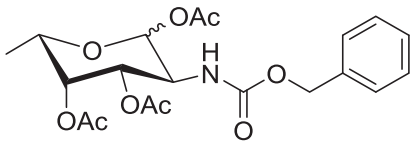


**8**

**1,3,4-Tri-*O*-acetyl-2-*N*-(benxyloxyacetamido)-α,β-L-fucose** (**8**). Synthesized from compound **6** (100 mg, 0.32 mmol), benzyl chloroformate (0.10 mL, 0.64 mmol), and DPPE (0.65 mmol equiv) in THF according to the general procedure described above. Purification by flash column chromatography (2:1, hexane: ethyl acetate) yielded compound **8** as a colorless syrup (40 mg, 0.095 mmol, 30 %).

$^{1}$H NMR ($CDCl_3$) $\delta$ 1.15 (d, 3H, $J$ = 6.44 Hz), 2.00, 2.02, 2.15 (s, 9H), 3.93 (dq, 1H, H-5, $J$ = 6.40 Hz), 4.12 (ddd, 1H, H-2, $J$ = 2.58, 5.56, 11.08 Hz), 5.04 (dd, 1H, H-4, $J$ = 3.44, 10.24 Hz), 5.09 (s, 2H), 5.27 (dd, 1H, H-3, $J$ = 1.02, 3.40 Hz), 5.69 (d, 1H, H-1, $J$ = 2.36 Hz), 6.34 (d, 1H, NH, $J$ = 8.28Hz), 7.29-7.32 (m, Aryl).

$^{13}$C NMR ($CDCl_3$) $\delta$ 16.38, 20.58, 20.65, 20.73, 46.36, 67.07, 70.84, 72.02, 92.19, 128.50, 128.54, 128.69, 137.50, 156.72, 169.94, 169.97, 170.16, 170.57.

IR ($CDCl_3$) 3156.47 cm$^{-1}$ (NH), 1746.66 cm$^{-1}$ (acetate carbonyls), 1649.76 cm$^{-1}$ (NHCO).

$R_f$ = 0.31 (2:1 hexane: ethyl acetate) . M.P ($^{o}$C) = N/A syrup

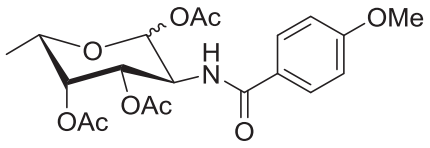


**10**

**1,3,4-Tri-*O*-acetyl-2-*N*-(4-methoxybezamido)-α,β-L-fucose** (**10**). Synthesized from compound **6** (0.17 g, 0.54 mmol), 4-methoxy benzoyl chloride (0.15 mL, 1.08 mmol), and DPPE (0.65 mmol equiv) in THF according to the general procedure described above. Purification by flash column chromatography (2:1, hexane: ethyl acetate) yielded compound **10** as a colorless syrup (0.107 g, 0.25 mmol, 47%).

$^{1}$H NMR ($CDCl_3$) $\delta$ 1.17 (d, 3H, $J$ = 6.24 Hz), 2.07, 2.09, 2.16 (s, 9H ), 3.71 (dq, 1H, H-5, $J$ = 6.42 Hz), 3.87 (s, 3H ), 4.13 (ddd, 1H, H-2, $J$ = 2.58, 5.56, 11.08 Hz), 5.04 (dd, 1H, H-4, $J$ = 3.42, 10.22 Hz), 5.28 (dd, 1H, H-3, $J$ = 0.88, 3.44 Hz), 6.31 (d, 1H, H-1, $J$ = 3.44 Hz), 8.09 (d, 1H, NH, $J$ = 8.11 Hz), 7.01-7.12 (m, Aryl).

$^{13}$C NMR ($CDCl_3$) $\delta$ 16.40, 20.46, 20.63, 20.69, 55.50, 66.78, 67.07, 70.84, 72.02, 73.40, 90.37, 126.91, 132.50, 133.01, 137.73, 158.99, 168.51, 170.23, 170.57.

IR ($CDCl_3$) 3156.62 cm$^{-1}$ (NH), 1755.44 cm$^{-1}$ (acetate carbonyls), 1605.31 cm$^{-1}$ (NHCO).

$R_f$ = 0.29 (2:1 hexane: ethyl acetate). M.P ($^{o}$C) = N/A syrup

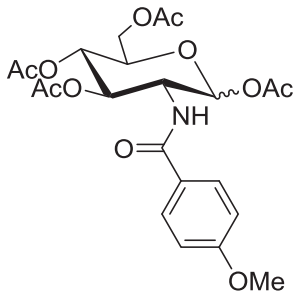


**13**

**1,3,4,6-Tetra-*O*-acetyl-2-*N*-(4-methoxybenzamido)-α,β-D-glucose** (**13**). Synthesized from compound **15** (0.107 g, 0.29 mmol), 4-methoxy benzoyl chloride (0.08 mL, 0.58 mmol), and DPPE (0.65 mmol equiv) in THF according to the general procedure described above. Purification by flash column chromatography (2:1, hexane: ethyl acetate) yielded compound **13** as a colorless syrup (0.078 g, 0.16 mmol, 57%).

$^{1}$H NMR ($CDCl_3$) $\delta$ 2.09, 2.011, 2.16 (s, 12H), 3.89 (s, 3H ), 4.09 (dd, 1H, H-6, $J$ = 4.80, 14.25 Hz), 4.29 (ddd, 1H, H-5, $J$ = 2.58, 3.96, 12.45 Hz ), 5.09 (ddd, 1H, H-2, $J$ = 9.76, 19.57 Hz), 5.46 (dd, 1H, H-4, $J$ = 10.00, 20.00 Hz), 5.62 (dd, 1H, H-3, $J$ = 3.44, 7.86 Hz), 6.34 (d, 1H, H-1, $J$ = 3.40 Hz), 6.79-7.25 (m, aryl group), 8.06 (d, 1H, NH, $J$ = 8.13 Hz).

$^{13}$C NMR ($CDCl_3$) $\delta$ 20.38, 20.53, 20.57, 20.66, 55.72, 59.55, 67.85, 68.51, 69.88, 71.93, 90.38, 113.78, 114.16, 126.91, 132.42, 132.85, 137.72, 159.00, 168.50, 169.42, 169.98, 170.54.

IR ($CDCl_3$) 3156.62 cm$^{-1}$ (NH), 1755.44 cm$^{-1}$ (acetate carbonyl), 1605.31 cm$^{-1}$ (NHCO).

$R_f$ = 0.37 (2:1 hexane: ethyl acetate). M.P ($^{o}$C) = N/A syrup

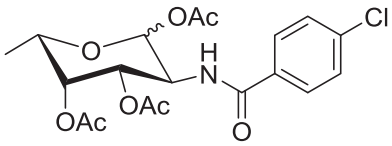


**11**

**1,3,4-Tri-*O*-acetyl-2-*N*-(4-chlorobenzamido)-α,β-L-fucose** (**11**). Synthesized from compound **6** (0.124 g, 0.39 mmol), 2-chlorobenzoyl chloride (0.10 mL, 0.78 mmol), and DPPE (0.65 mmol equiv) in THF according to the general procedure described above. Purification by flash column chromatography (2:1, hexane: ethyl acetate) yielded compound **11** as a pale green syrup (0.090 g, 0.21 mmol, 54 %).

$^{1}$H NMR ($CDCl_3$) $\delta$ 1.17 (d, 3H, $J$= 6.24 Hz), 2.03, 2.15, 2.17 (s, 9H ), 3.71 (dq, 1H, H-5, $J$ = 6.42 Hz), 4.13 (ddd, 1H, H-2, $J$ = 2.58, 5.56, 11.08 Hz), 5.04 (dd, 1H, H-4, $J$ = 3.42, 10.22 Hz), 5.28 (dd, 1H, H-3, $J$ = 0.88, 3.44 Hz), 6.47 (d, 1H, H-1, $J$ = 4.84 Hz), 7.26-7.52 (m, Aryl), 8.03 (d, 1H, NH, $J$ = 8.60Hz).

$^{13}$C NMR ($CDCl_3$) $\delta$ 16.40, 20.46, 20.63, 20.69, 66.78, 67.07, 70.84, 72.02, 73.40, 90.00, 126.88, 128.87, 129.36, 131.86, 140.26, 160.20, 169.92, 170.02, 170.23, 170.62.

IR ($CDCl_3$) 3156.01 cm$^{-1}$ (NH), 1747.80 cm$^{-1}$ (acetate carbonyl), 1645.13 cm$^{-1}$ (NHCO).

$R_f$ = 0.35 (2:1 hexane: ethyl acetate) . M.P ($^{o}$C) = N/A syrup

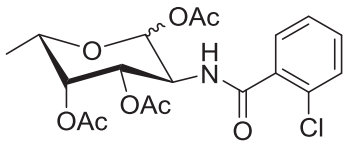


**12**

**1,3,4-Tri-*O*-acetyl-2-*N*-(2-chlorobezamido)-α,β-L-fucose** (**12**). Synthesized from compound **6** (0.102 g, 0.32 mmol), 2-chlorobenzoyl chloride (0.08 mL, 0.64 mmol), and DPPE (0.65 mmol equiv) in THF according to the general procedure described above. Purification by flash column chromatography (2:1, hexane: ethyl acetate) yielded compound **12** as a colorless syrup (0.069 g, 0.16 mmol, 50 %).

$^{1}$H NMR ($CDCl_3$) $\delta$ 1.15 (d, 3H, $J$= 6.44 Hz), 2.05, 2.15, 2.17 (s, 9H ), 3.70 (dq, 1H, H-5, $J$ = 6.42 Hz), 4.12 (ddd, 1H, H-2, $J$ = 2.58, 5.56, 11.08 Hz), 5.07 (dd, 1H, H-4, $J$ = 3.24, 6.48 Hz), 5.56 (dd, 1H, H-3, $J$ = 1.10, 3.02 Hz), 5.69 (d, 1H, H-1, $J$ = 2.84 Hz), 8.02 (d, 1H, NH, $J$ = 8.80Hz), 7.45-7.53 (m, Aryl).

$^{13}$C NMR ($CDCl_3$) $\delta$ 16.39, 20.58, 20.65, 20.69, 66.78, 67.07, 70.84, 72.02, 73.40, 92.22, 126.67, 128.56, 129.20, 130.70, 131.45, 132.40, 133.44, 134.68, 160.42, 169.9, 170.11, 170.42, 170.80.

IR ($CDCl_3$) 3156.44 cm$^{-1}$ (NH), 1747.81 cm$^{-1}$ (acetate carbonyl), 1651.02 cm$^{-1}$ (NHCO).

$R_f$ = 0.30 (2:1 hexane: ethyl acetate). M.P ($^{o}$C) = N/A syrup.

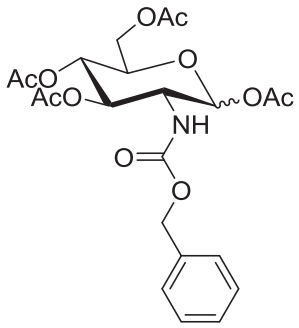


**9**

**1,3,4,6-Tetra-*O*-acetyl-2-*N*-(benzyloxyacetamido)-α,β-D-glucose** (**9**). Synthesized from compound **15** (0.261 g, 0.70 mmol), benzyl chloroformate (0.20 mL, 1.4 mmol), and DPPE (0.65 mmol equiv) in THF according to the general procedure described above. Purification by flash column chromatography (2:1, hexane: ethyl acetate) yielded compound **7** as colorless syrup (0.026 g, 0.05 mmol, 28 %).

$^{1}$H NMR ($CDCl_3$) $\delta$ 2.04, 2.07, 2.08, 2.16 (s, 12H), 3.89 (s, 3H), 4.09 (dd, 1H, H-6, $J$ = 4.80, 14.25 Hz), 4.29 (ddd, 1H, H-5, $J$ = 2.58, 3.96, 12.45 Hz), 5.09 (ddd, 1H, H-2, $J$ = 9.76, 19.57 Hz), 5.10 (s, 2H), 5.46 (dd, 1H, H-4, $J$ = 10.00, 20.00 Hz), 5.62 (dd, 1H, H-3, $J$ = 3.44, 7.86 Hz), 5.65 (d, 1H, H-1, $J$ = 3.52 Hz), 6.79-7.25 (m, aryl group), 6.43 (d, 1H, NH, $J$ = 8.03 Hz).

$^{13}$C NMR ($CDCl_3$) $\delta$ 20.50, 20.55, 20.64, 20.66, 46.24, 55.69, 66.94 68.48, 69.85, 71.89, 88.79, 90.36, 126.96, 128.12, 128.22, 128.38, 128.55, 128.72, 136.26, 137.49, 156.58, 168.49, 169.39, 169.94, 170.51.

IR ($CDCl_3$) 3156.37 cm$^{-1}$ (NH), 1751.56 cm$^{-1}$ (acetate carbonyl), 1647.73 cm$^{-1}$ (NHCO).

$R_f$ = 0.33 (2:1 hexane: ethyl acetate). M.P ($^{0}$C) = N/A syrup

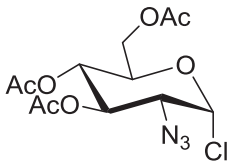


**19**

**3,4,6-Tri-*O*-acetyl-2-azidodeoxy-1-chloro-α-D-glucose** (**19**). Compound **18** (1.0 g, 3.67 mmol), sodium azide (0.48g, 7.33 mmol), and iron (III) chloride (1.79g, 11.02 mmol) were dissolved in anhydrous acetonitrile (30 mL) and the reaction mixture cooled to -30 $^{o}$C in an acetone-dry ice bath. Hydrogen peroxide (0.17 mL, 7.33 mmol) was then added in a dropwise fashion and the reaction was stirred vigorously at -30 $^{o}$C for 5 hrs. Completion of the reaction was confirmed by TLC (3:1, hexane: ethylacetate) with the product $R_f$ value of 0.39 for the product. The brown mixture was then extracted with methylene chloride (20 mL), washed with *DI* $H_2O$ (3 × 20 mL), dried over anhydrous $MgSO_4$, filtered and evaporated *in vacuo* to afford brown syrup which was purified by flash column chromatography (3:1, hexane: ethyl acetate) yielding compound **19** as a light brown syrup. (0.064 g, 0.18 mmol, 5 %).

$^{1}$H NMR ($CDCl_3$) $\delta$ 2.08, 2.10, 2.11, 2.14 (s, 9H), 3.62 ( dd, 1H, H-2, $J$ = 3.76, 10.56 Hz), 4.11 ( ddd, 1H, H-5, $J$ = 2.58, 3.96, 12.45 Hz), 4.36 ( dd, 1H, H-6, $J$ = 3.36,12.36 Hz ), 5.09 ( dd, 1H, H-4, $J$ = 4.36, 10.52 Hz ), 5.78 ( dd, 1H, H-3, $J$ = 4.98, 10.22 Hz), 6.35 ( d, 1H, H-1, $J$ = 5.92 Hz).

$^{13}$C NMR ($CDCl_3$) $\delta$ 20.65, 20.69, 20.87, 53.38, 68.10, 68.90, 70.65, 96.50, 169.67, 170.10, 170.52, 170.68.

IR ($CDCl_3$) 2106.92 $cm^{-1}$ ($N_3$), 1743.29 $cm^{-1}$ (acetate carbonyl). 738.81 $cm^{-1}$ (C-Cl).

$R_f$ = 0.39 (3:1 hexane: ethyl acetate). M.P ($^0C$) = N/A syrup.

## REFERENCES


1. Kathrin, U. J.; Douglas, Q. G.; Ingrid, L. Scully.; Annaliesa, S. A. "*Staphyloccocus aureus* vaccines: Problems and prospects." *Vaccine.* **2013**, *31*, 2723-2730.
2. Edwards, A. M.; Massey, R. C.; Clarke, S. R. "Molecular mechanisms of *Staphylococcus aureus* nasopharyngeal colonization." *Mol. Oral. Microbiol.* **2012**, *27*, 1-10.
3. Peacock, S. J.; Silva, I.; Lowy, F. D. "What determines nasal carriage of *Staphylococcus aureus?*" *Trends. Microbiol.* **2001**, *9*, 605-610.
4. Fournier, B.; Philpott, D. J. "Recognition of *Staphylococcus aureus* by the innate immune system." *Clin. Microbiol. Rev.* **2005**, *18*, 521-540.
5. Krishna, S.; Miller, L. S. "Innate and adaptive immune responses against *Staphylococcus aureus* skin infections." *Semin. Immunopathol.* **2012**, *34*, 261-280.
6. Giuseppe, I.; Sebastiano, L.; Francesco, N. L.; Emanuele, N.; Richard, P. W. "Methicillin-resistant *Staphylococcus aureus*: the superbug." *Int. J. Infect. Dis.* **2010**, S7-S11.
7. Chambers, H. F. "Solving *staphylococcal* resistance to beta-lactams." *Trends. Microbiol.* **2003**, *11*, 145-148.
8. Zhang, H. Z.; Hackbarth, C. J.; Chansky, K. M.; Chambers, H. F. "A proteolytic transmembrane signaling pathway and resistance to beta-lactams in *Staphylococci*." *Science.* **2001**, *291*, 1962-1965.
9. Shrenik, M.; Christopher, S.; Konrad, B. P.; Palas, K. C.; Arundhati, P.; Sarah, R.; Roberto, R. R.; Adriana, E. R. "beta-Lactams increase the antibacterial activity of daptomycin against clinical methicillin-resistant *Staphylococcus aureus* strains and

prevent selection of daptomycin-resistant derivatives." *Int. J. Antimicrob. Agents.* **2012**, *39,* 96-104.

10. Hiramatsu, K.; Hanaki, H.; Ino, T.; Yabuta, K.; Oguri, T.; Tenover, F. C. "Methicillin-resistant *Staphylococcus aureus* clinical strain with reduced vancomycin susceptibility." *J. Antimicrob. Chemother.* **1997**, *40*, 135-136.
11. Denyer, S. P.; Maillard, J. Y. "Cellular impermeability and uptake of biocides and antibiotics in Gram-negative bacteria." *Symp. Ser. Soc. Appl. Microbiol.* **2002**, *31*, 35S-45S.
12. Smith, S. R.; Cheesebrough, J. S. "Teicoplanin administration in patients experiencing reactions to vancomycin." *J. Antimicrob. Chemother.* **1989**, *23*, 810-830.
13. Alexander, M. R. "Review of vancomycin after 15 years of use." *Drug. Intell. Clin. Pharm.* **1974**, *8*, 520-525.
14. Gould, I. M.; David, M. Z.; Esposito, S. "New insights into methicillin resistant *Staphylococcus aureus* pathogenesis, treatment and resistance." *Int. J. Antimicrob. Agents.* **2012**, *39*, 96-104.
15. Schilling, A.; Neuner, E.; Rehm, S. J. "Vancomycin: a 50-something-year-old antibiotic we still don't understand." *Cleve. Clin. J. Med.* **2011**, *78*, 465-471.
16. Mohr, J. F.; Murray, B. E. "Point: vancomycin is not obsolete for the treatment of infection cause by methicillin-resistant *Staphylococcus aureus*." *Clin Infect Dis.* **2007**, *44*, 1536-1542.
17. Weber, J. T. "Community-associated methicillin-resistant *Staphylococcus aureus*." *Clin. Infect. Dis.* **2005**, *41,* S269- S272.

18. Limoncu, M. H.; Ermertcan, S.; Cetin, C. B. “Emergence of phenotypic resistance to ciprofloxacin and levofloxacin in methicillin-resistant and methicillin sensitive *Staphylococcus aureu*s strains.” *Int. J. Antimicrob*. *Agents*. **2003**, *21*, 420-424.

19. Firsov, A. A.; Volstrov, S. N.; Lubenko, Y. “Prevention of the selection of resistant *Staphylococcus aureus* by moxifloxacin plus doxyciclin in an in vitro dynamic model: an additive effect of the combination.” *Int. J. Antimicrob. Agents*. **2004**, *23*, 451-456.

20. Ruhe, J. J.; Menon, A. “Tetracyclines as an oral treatment option for patients with community onset skin and soft tissue infections caused by methicillin-resistant *Staphylococcus aureus*.” *Antimicrob. Agents. Chemother.* **2007**, *51*, 3298-3303.

21. Grim, S. A.; Rapp, R. P. “Trimethoprim-sulfamethoxazole as a viable treatment option for infections caused by methicillin-resistant *Staphylococcus aureus*.” *Pharmacol.* **2005**, *25*, 253-264.

22. Livermore, D. M. “Antibiotic resistance in *Staphylococci*.” *Int. J. Antimicrobial. Agents.* **2000**, *16*, S3-S10.

23. Leach, K. L.; Brickner, S. J.; Noe, M. C.; Miller, P. F. “Linezolid, the first oxazolidinone antibacterial agent.” *Ann*. *NY*. *Acad*. *Sci.* **2011**, *1222*, 49-54.

24. Wunderink, R. G.; Niederman, M. S.; Kollef, M. H. “Linezolid in methicillin-resistant *Staphylococcus aureus* nosocomial pneumonia: a randomized, controlled study.” *Clin. Infect. Dis.* **2012**, *54*, 621-629.

25. Schriever, C. A.; Fernández, C.; Rodvold, K. A.; Danziger, L. H. “Daptomycin, a novel cyclic lipopeptide antimicrobial.” *Am. J. Health-Syst. Pharm.* **2005**, *62*, 1145-1158.

26. Damodaran, S. E.; Madhan, S. “Telavancin: A novel lipoglycopeptide antibiotic.” *J. Pharmacol. Pharmacother.* **2011**, *2*, 135-137.

*27.* Manzella, P. J.; M.D. “Quinupristin-Dalfopristin: A New Antibiotic for Severe Gram-Positive Infections. *Am. Fam. Phy*. **2001**, *64*, 1863-1867.

28. Pankey, A. G. “Tigecycline.” *J. Antimicrob. Chemother.* **2005**, *56,* 470-480.

29. Bogdanovich,T.; Ednie, L. M.; Shapiro, S.; Appelbaum, P. C. “Anti-*staphylococcal* activity of ceftobiprole, a new broad-spectrum cephalosporin.” *Antimicrob*. *Agents*. *Chemother*. ***2*005**, *49*, 4210-4219.

30. File, T. M. Jr.; Wilcox, M. H.; Stein, G. E. “Summary of ceftaroline fosamil clinical trial studies and clinical safety.” *Clin. Infect. Dis.* **2012**, *55*, S173-S180.

31. Takamitsu, M.; Yoshikazu, T.; Makoto, K.; Toshiko, O.; Kouhei, T. “Expression, purification, crystallization and preliminary diffraction analysis of CapF, a capsular polysaccharide-synthesis enzyme from *Staphylococcus aureus*.” *Acta. Cryst.* **2008**, *64*, 512-515.

32. Kneidinger, B.; O’Riordan, K.; Li, J.; Brisson, J. R.; Lee, J. C.; Lam, J. S. “Three highly conserved proteins catalyze the conversion of UDP-N-acetyl-D-glucosamine to precursors for the biosynthesis of O antigen in Pseudomonas aeruginosa O11 and capsule in Staphylococcus aureus type 5. Implications for the UDP-N-acetyl-L-fucosamine biosynthetic pathway.” *J. Biol. Chem.* **2003**, *278*, 3615-3627.

33. Sander, S.; Mark, B.; Jan, C. M. “Staudinger ligation as a method for bioconjugation.” *Angew. Chem. Int. Ed.* **2011**, *50*, 8806-8827.

34. Alhassan, A. B. "Formation of (L-FucNAc) and analogs as potential inhibitors of *Staphylococcus aureus* capsular polysaccharide biosynthesis," MS Thesis, Youngstown State University. **2006**, 13-14.

35. McCutcheon, D. C. "Towards mimics of (UDP-L-FucNAc) as potential inhibitors of *Staphylococcus aureus* capsular polysaccharide biosynthesis," MS Thesis, Youngstown State University. **2008**, 18-20.

36. Breinbauer, M. "The Staudinger ligation-a gift to chemical biology." *Angew. Chem. Int. Ed.* **2004**, 43, 3106-3116.

37. Jeffery, S.; Cullen. L.; Cavallaro. "A rapid synthesis of pyranoid glycals from glycosyl bromides." *J. Org. Chem.* **1995**, *60*, 7055-7057.

38. Lemieux, R. U.; Ratcliffe, R. M. "The azidonitration of tri-*O*-acetyl-D-galactal." *Can. J. Chem.* **1979**, *57*, 1244-1251.

39. Trahanovsky, W. S.; Robbins, M. D. "Oxidation of organic compounds with cerium(1V). XIV. Formation of α-azido-*O*-nitratealkanes from olefins, sodium azide, and ceric ammonium nitrate." *J. Am. Chem. Soc.* **1971**, *93*, 5256-5258.

40. Trahanovsky, W. S.; Cramer, J. "Oxidation of organic compounds with cerium(1V). XII. Oxidative cleavage and ketone formation of alkylphenylcarbinols." *J. Org. Chem.* **1971**, *36*, 1890-1893.

41. Carolin, P.; Michael, H.; Norbert, S. "One-pot azidochlorination of glycals." *Org. Lett.* **2011**, *13*, 545-547.

APPENDIX 1

# $^{1}$H NMR AND $^{13}$C NMR SPECTRA

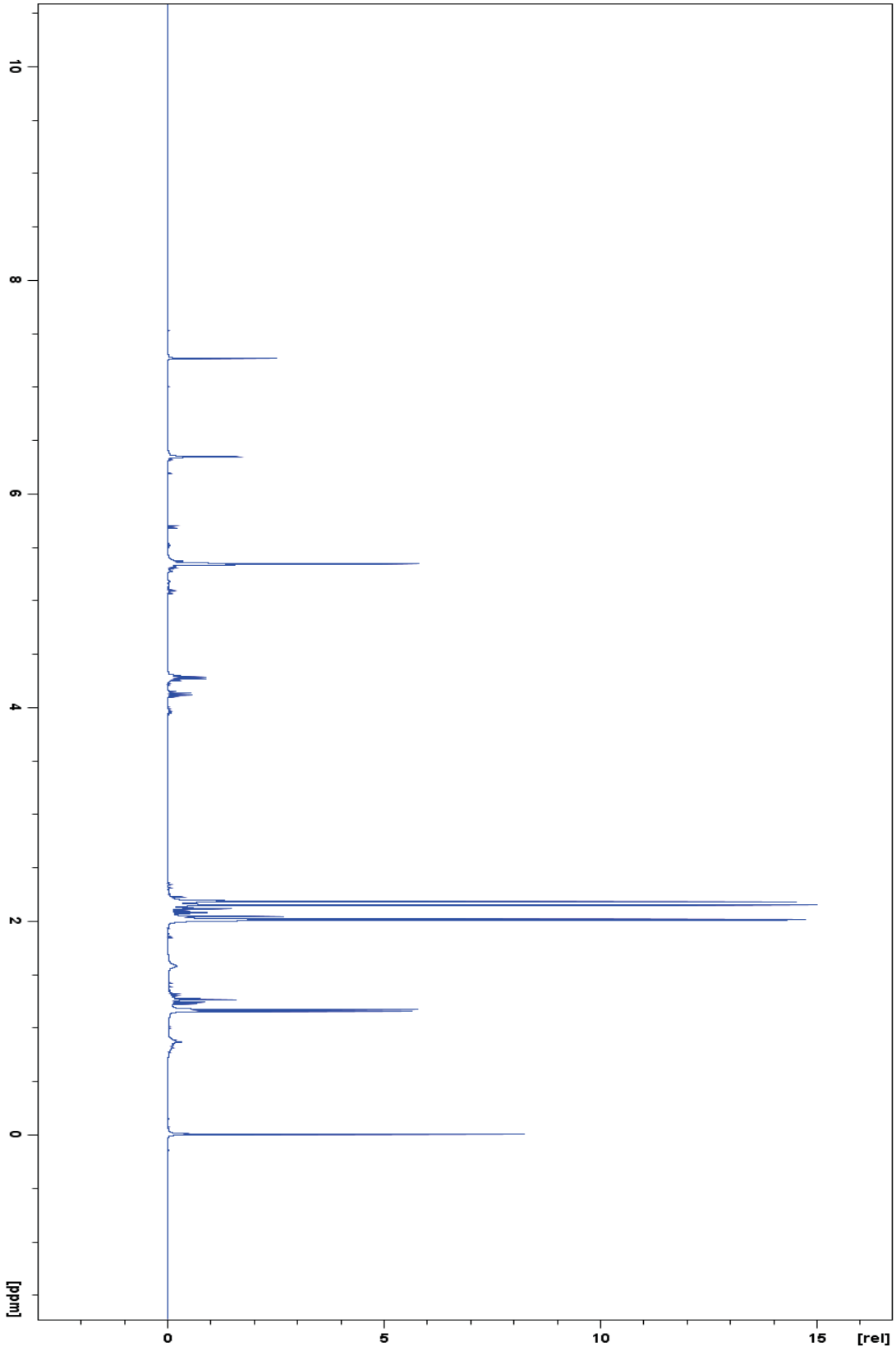


**Figure 10.** $^{1}$H NMR spectrum for 1,2,3,4-tetra-*O*-acetyl-α,β-L-fucose **2**.

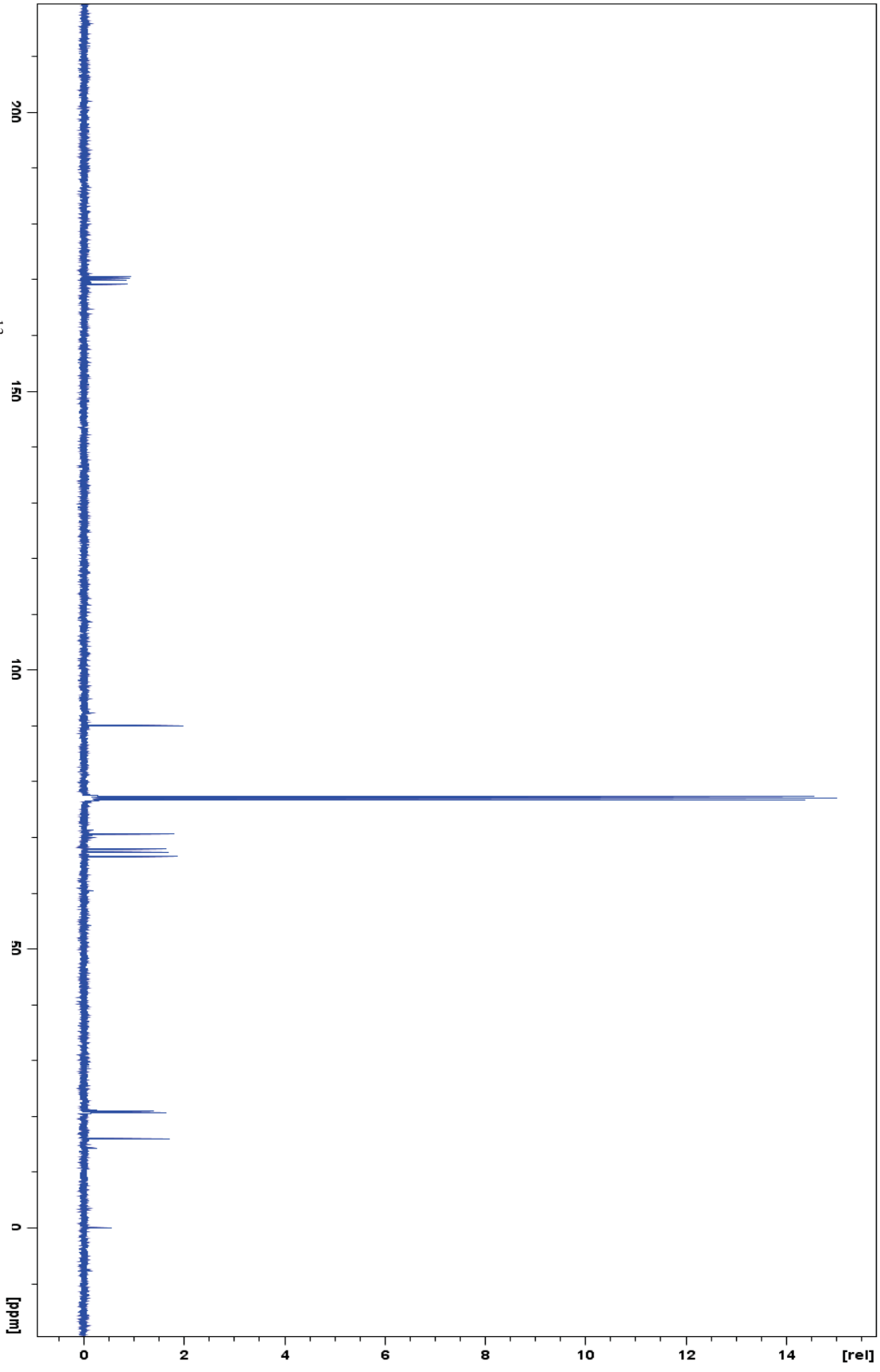


**Figure 11.** $^{13}$C NMR spectrum for 1,2,3,4-tetra-*O*-acetyl-α,β-L-fucose **2**.

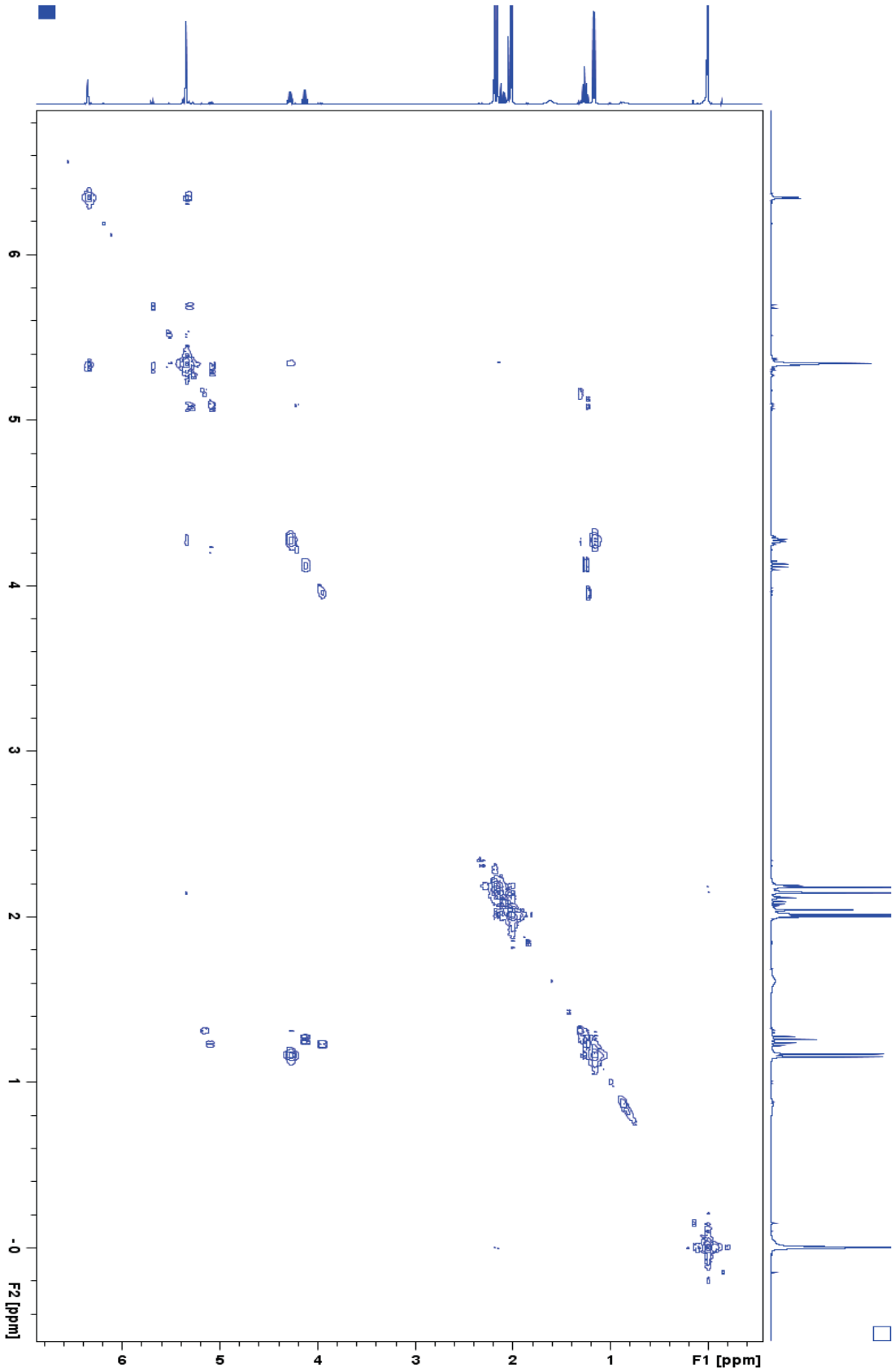


**Figure 12.** COSY spectrum for 1,2,3,4-tetra-*O*-acetyl-α,β-L-fucose **2**.

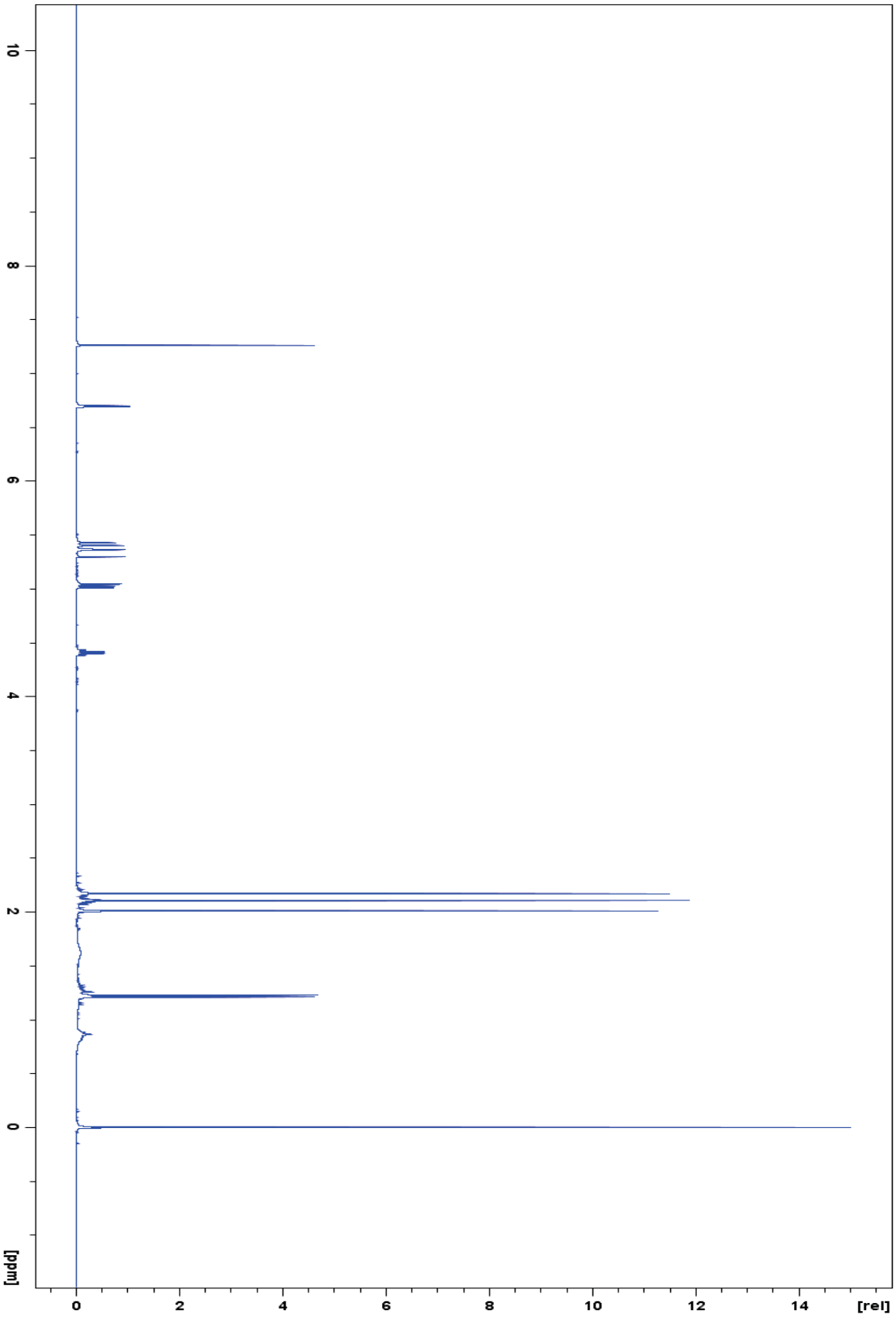


**Figure 13.** $^{1}$H NMR spectrum for 1-bromo-2,3,4-tri-*O*-acetyl-α-L-fucose **3**.

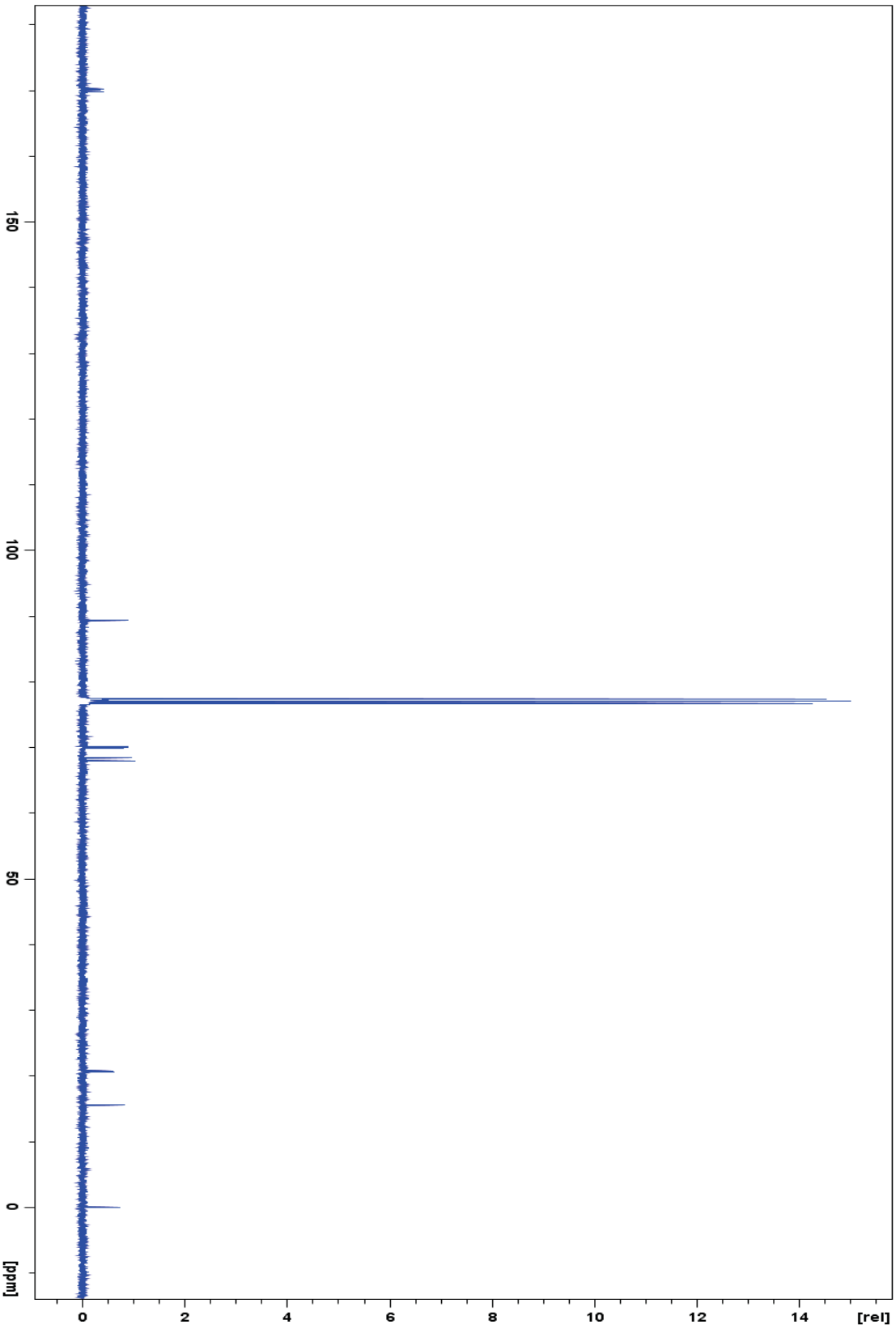


**Figure 14.** $^{13}$C NMR spectrum for 1-bromo-2,3,4-tri-*O*-acetyl-α,β-L-fucose **3**.

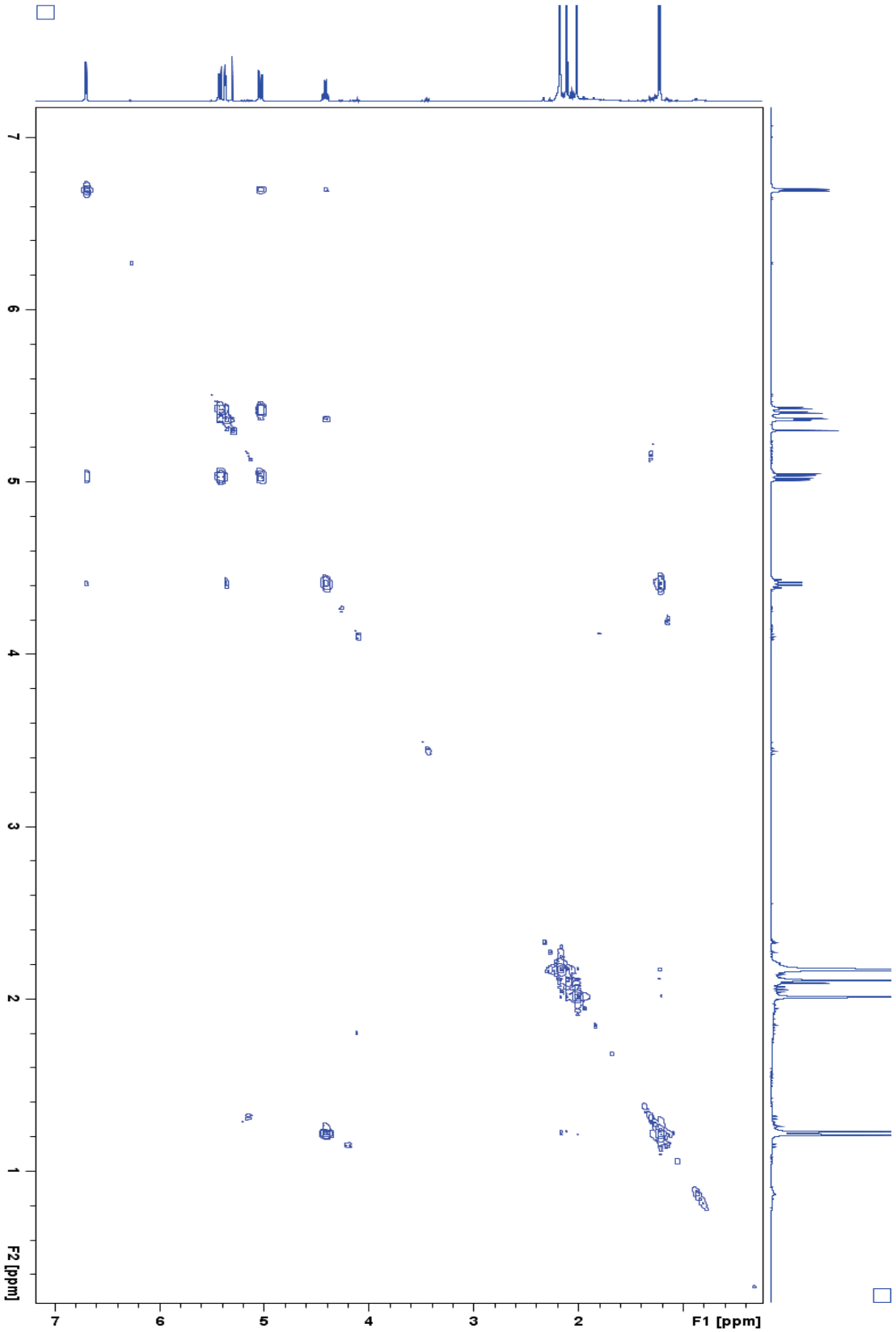


**Figure 15.** COSY spectrum for 1-bromo-2, 3,4-tri-*O*-acetyl-α,β-L-fucose **3**.

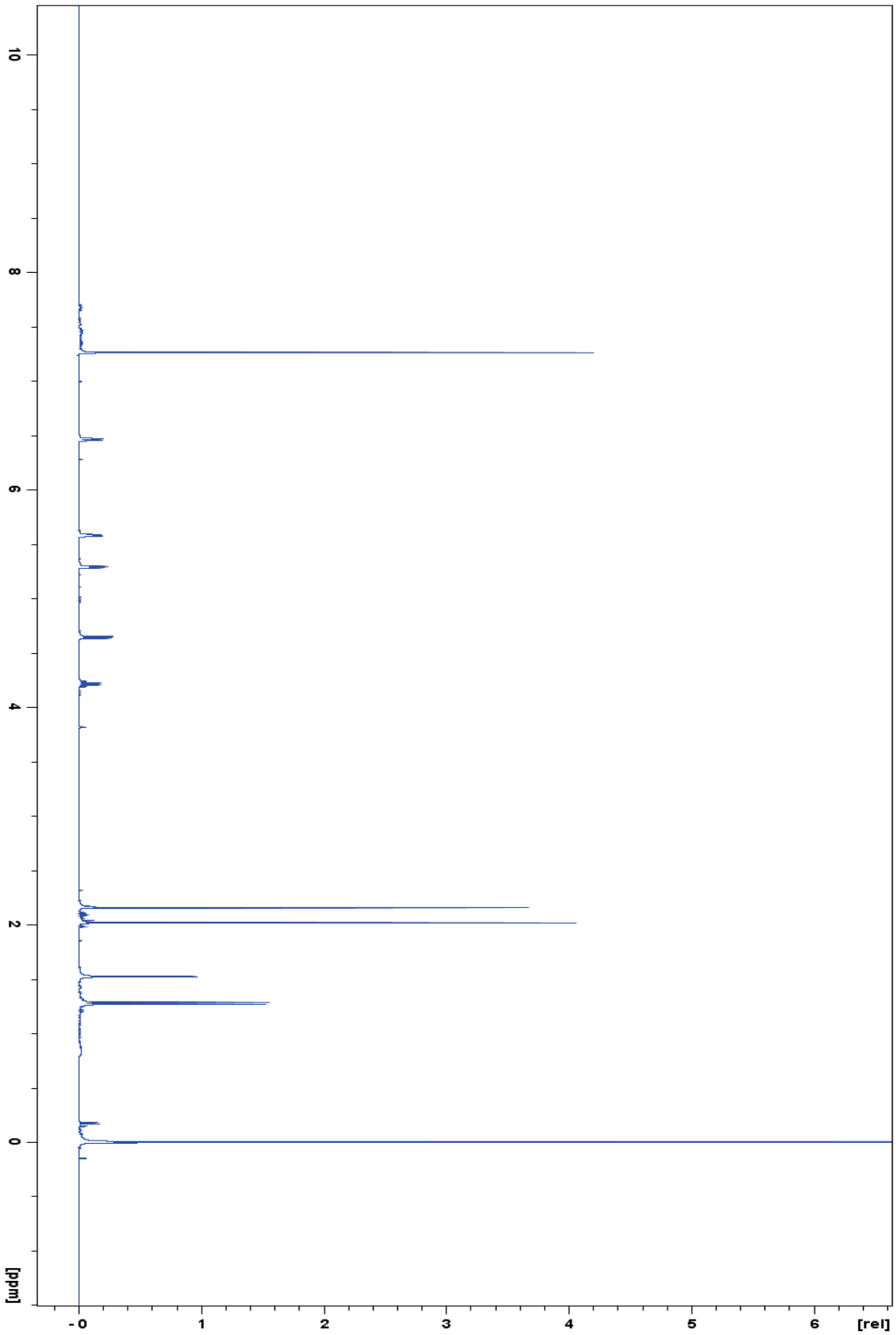


**Figure 16.** $^{1}$H NMR spectrum for 3,4-Di-*O*-acetyl-L-fucal **4**.

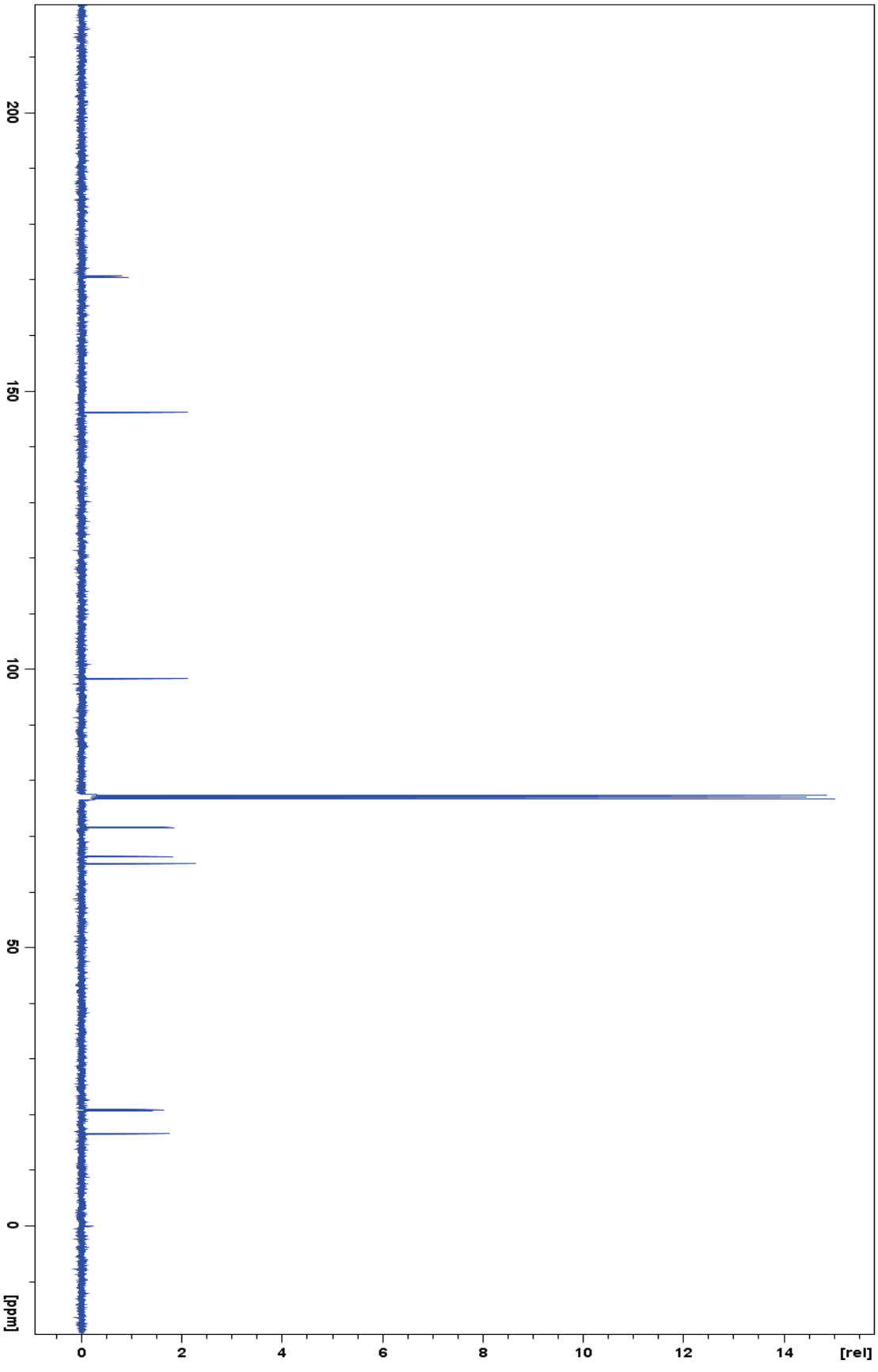


**Figure 17.** $^{13}$C NMR spectrum for 3,4-Di-*O*-acetyl-L-fucal **4**.

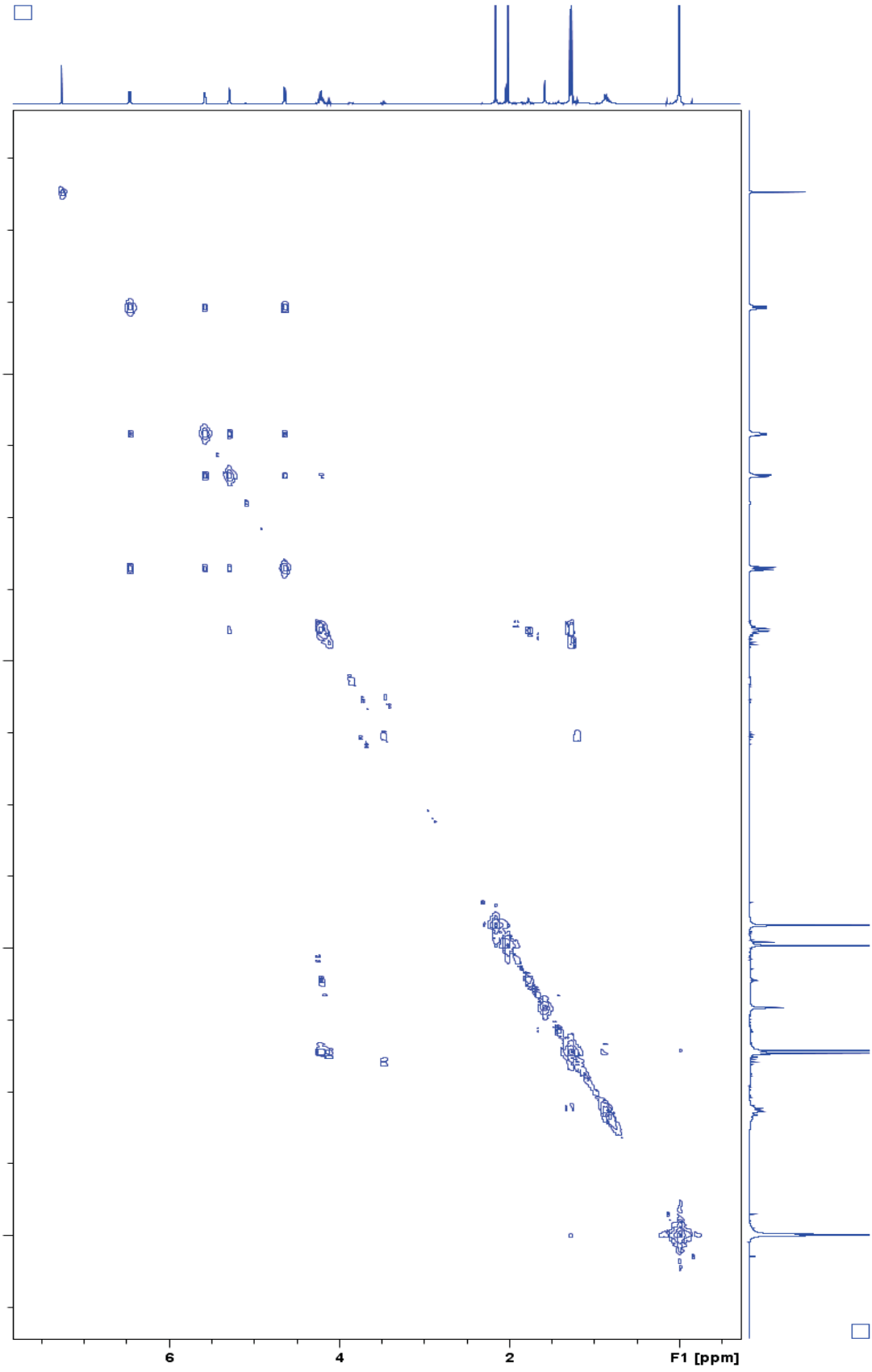


**Figure 18.** COSY spectrum for 3,4-Di-*O*-acetyl-L-fucal **4**.

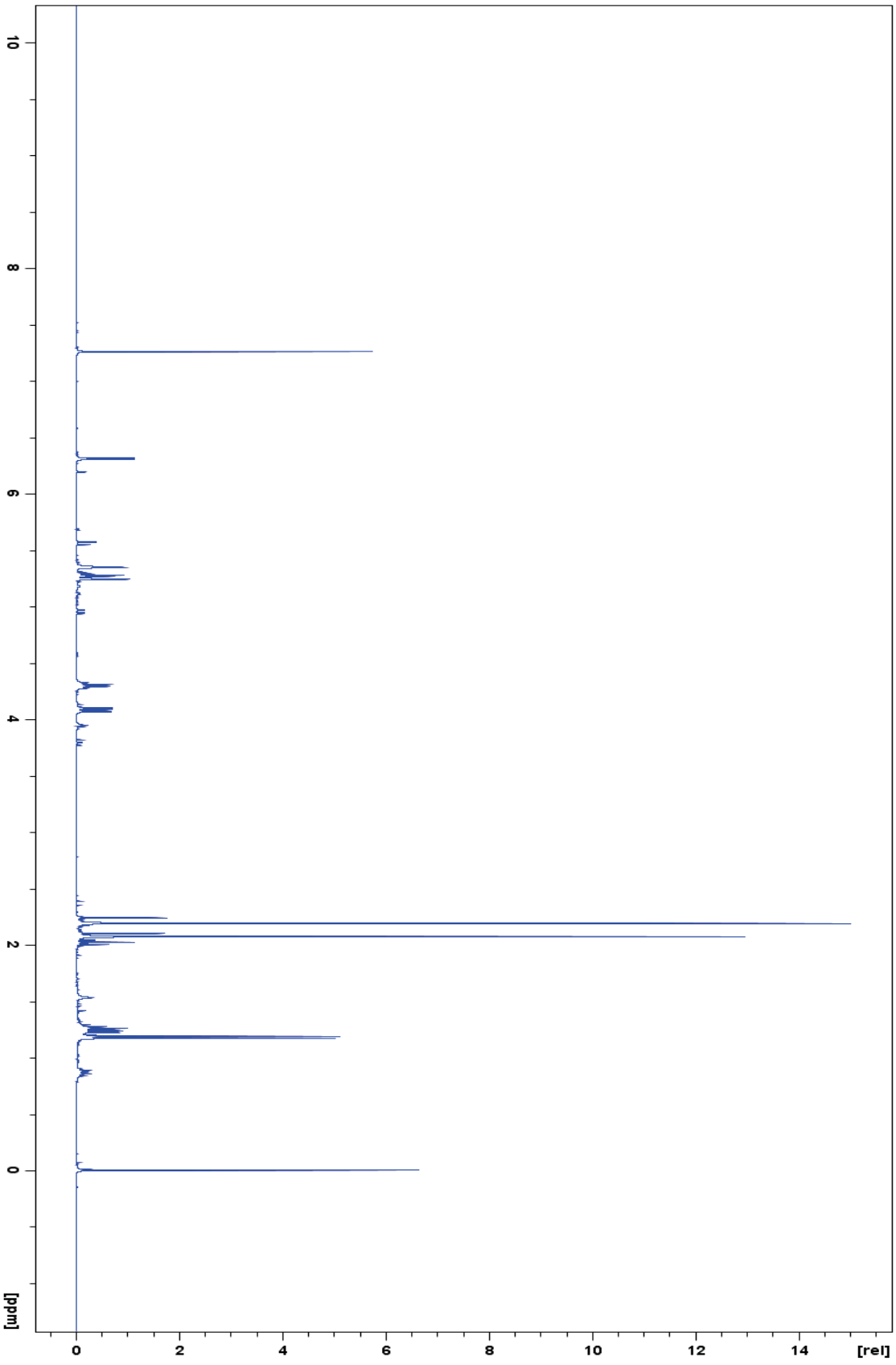


**Figure 19.** $^{1}$H NMR spectrum for 3,4-di-*O*-acetyl-2-azidodeoxy-1-nitro-α,β-L-fucose **5**.

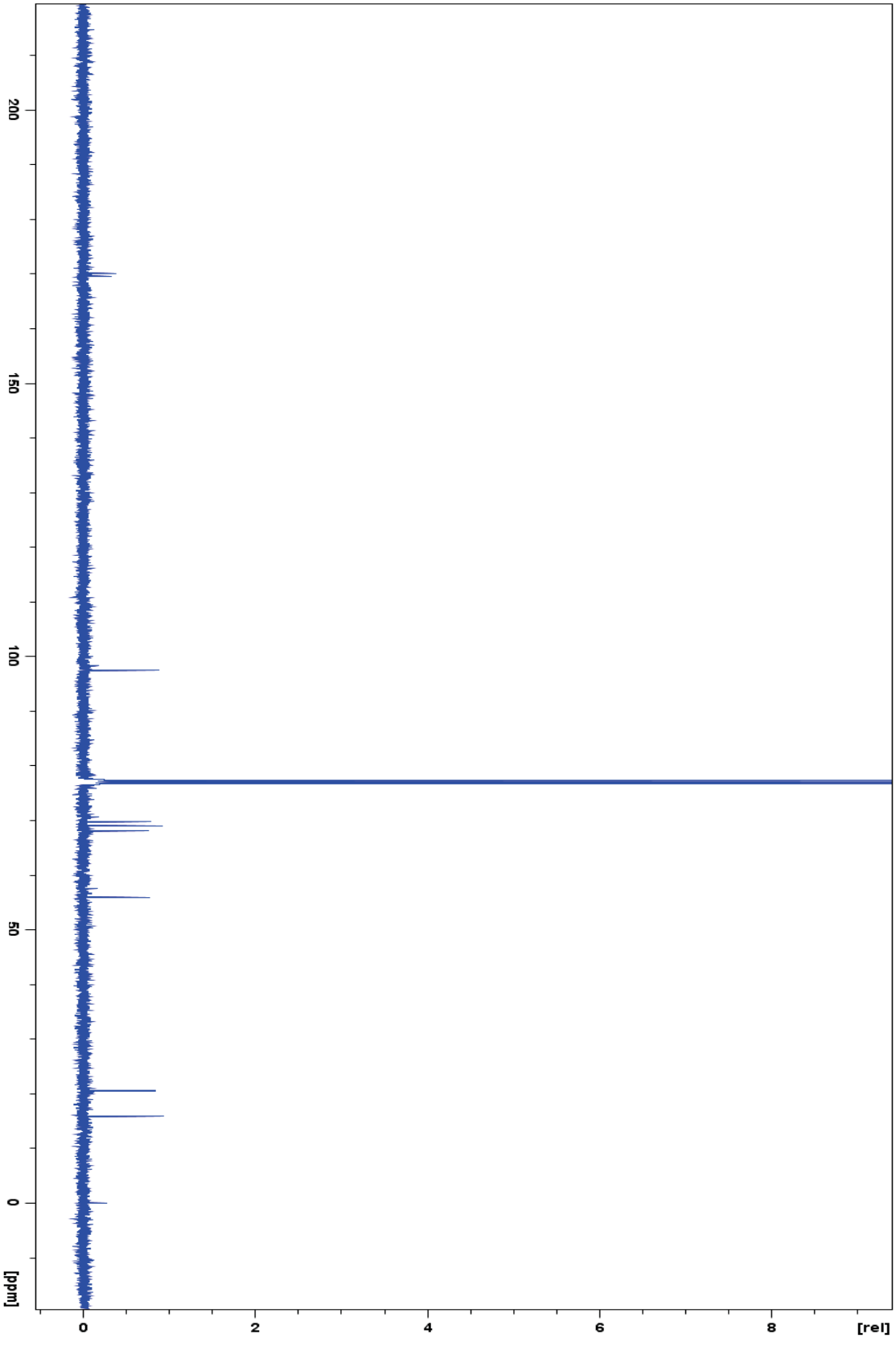


**Figure 20.** $^{13}$C NMR spectrum for 3,4-di-*O*-acetyl-2-azidodeoxy-1-nitro-α,β-L-fucose **5**.

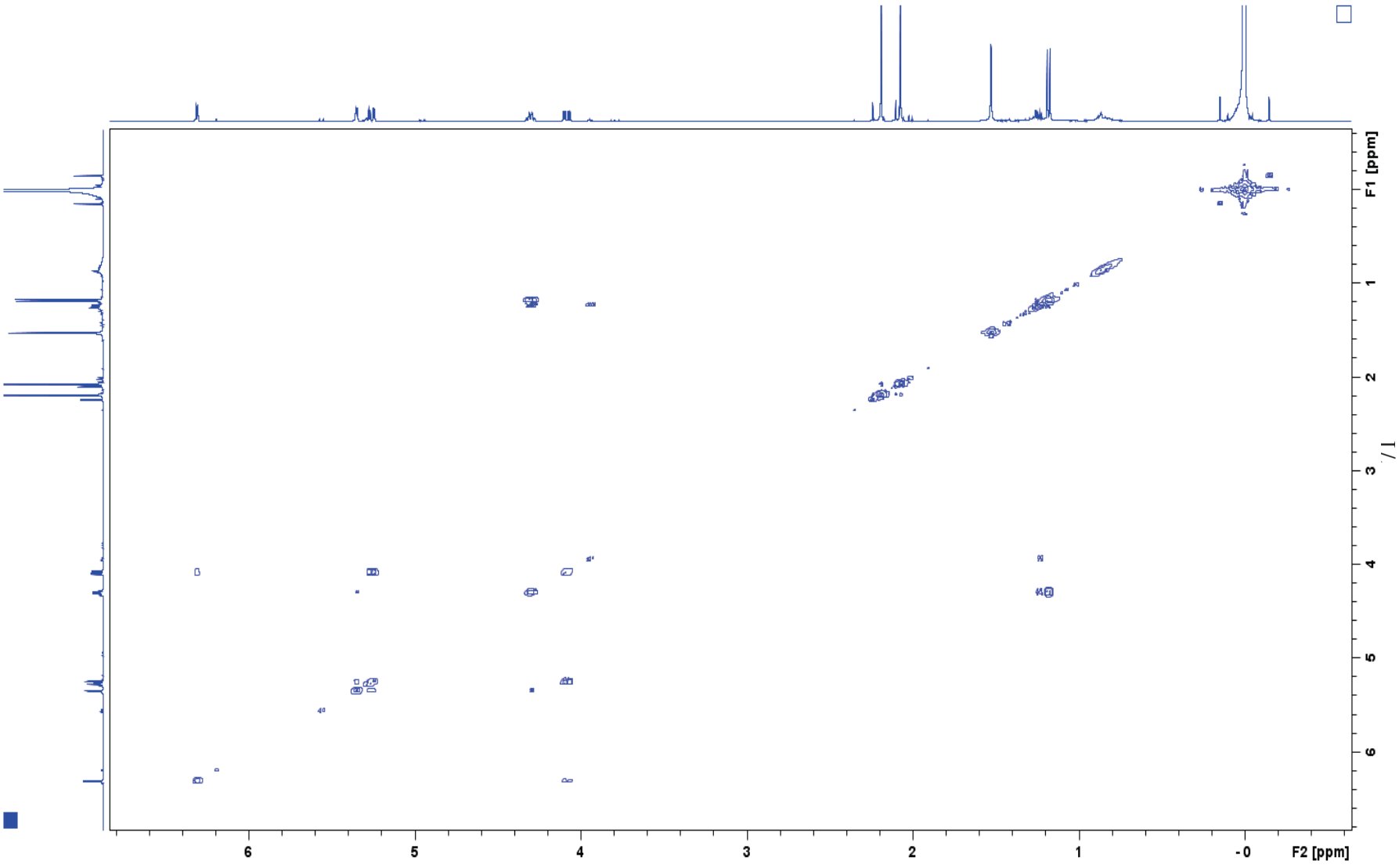


**Figure 21.** COSY spectrum for 3,4-di-*O*-acetyl-2-azidodeoxy-1-nitro-α,β-L-fucose **5**.

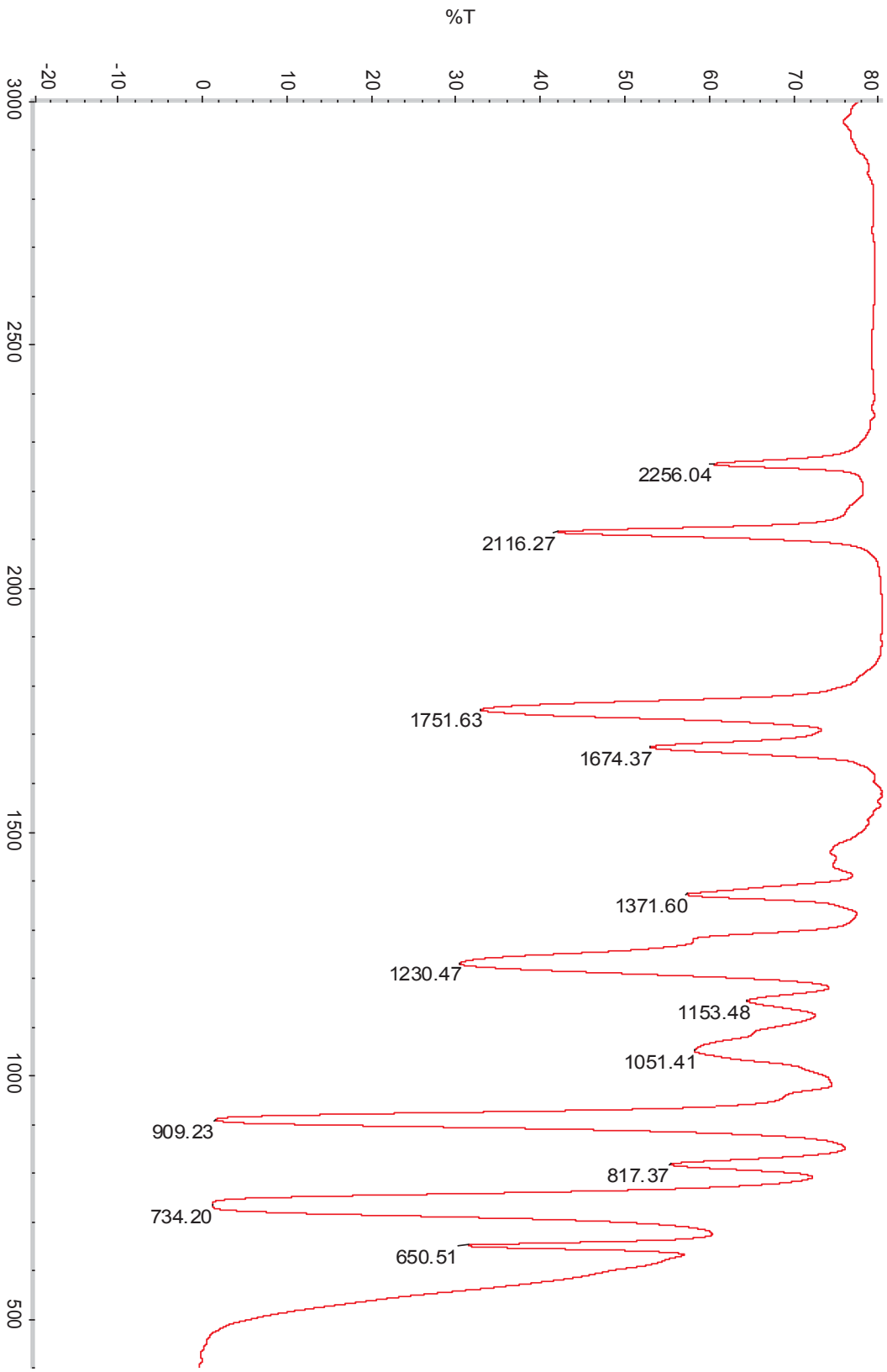


**Figure 22.** IR spectrum for 3,4-di-*O*-acetyl-2-azidodeoxy-1-nitro-α,β-L-fucose **5**.

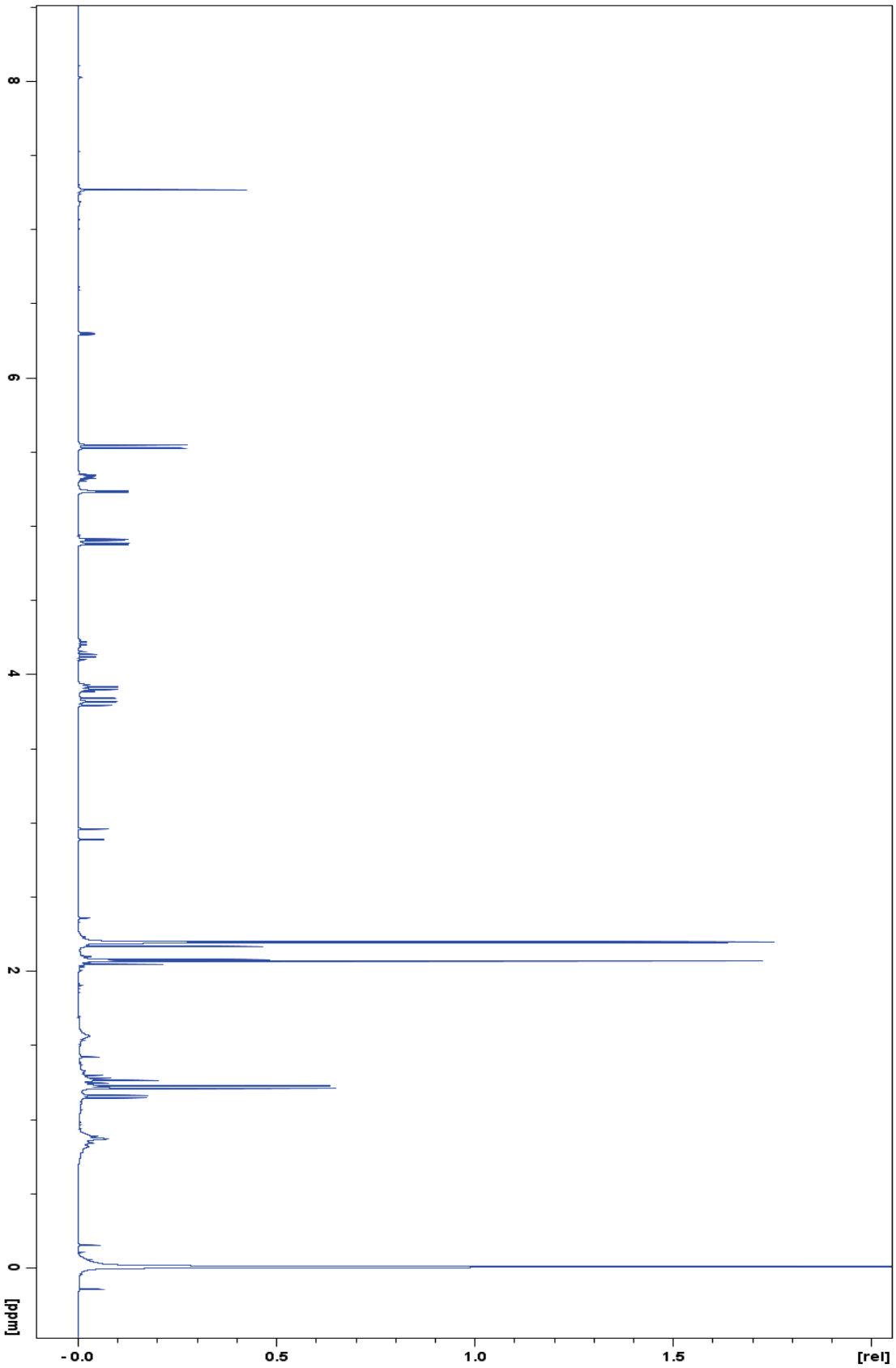


**Figure 23.** $^{1}$H NMR spectrum for 1,3,4-tri-*O*-acetyl-2-azidodeoxy-α,β-L-fucose **6**.

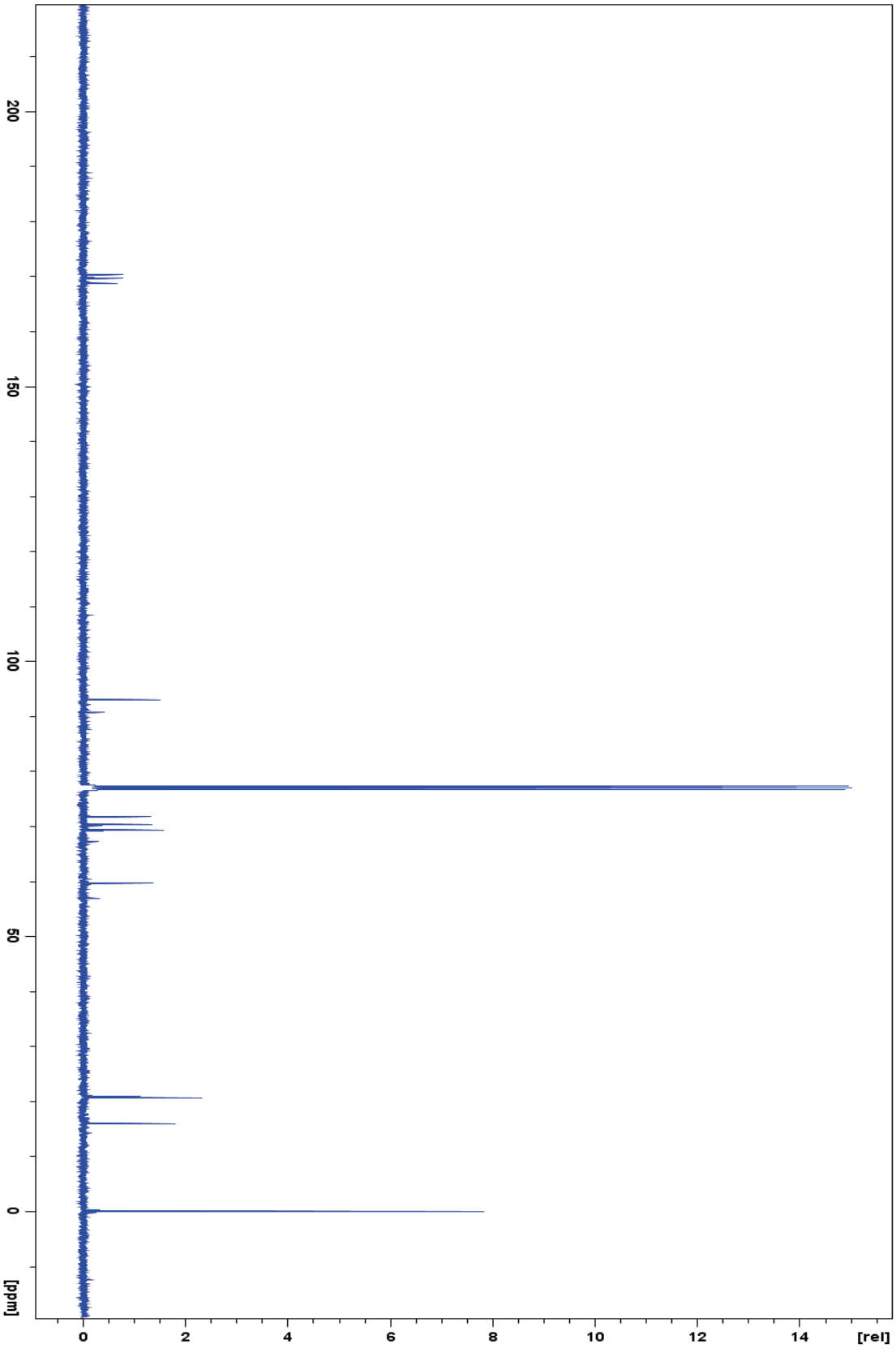


**Figure 24.** $^{13}C$ NMR spectrum for 1,3,4-tri-*O*-acetyl-2-azidodeoxy-α,β-L-fucose **6**.

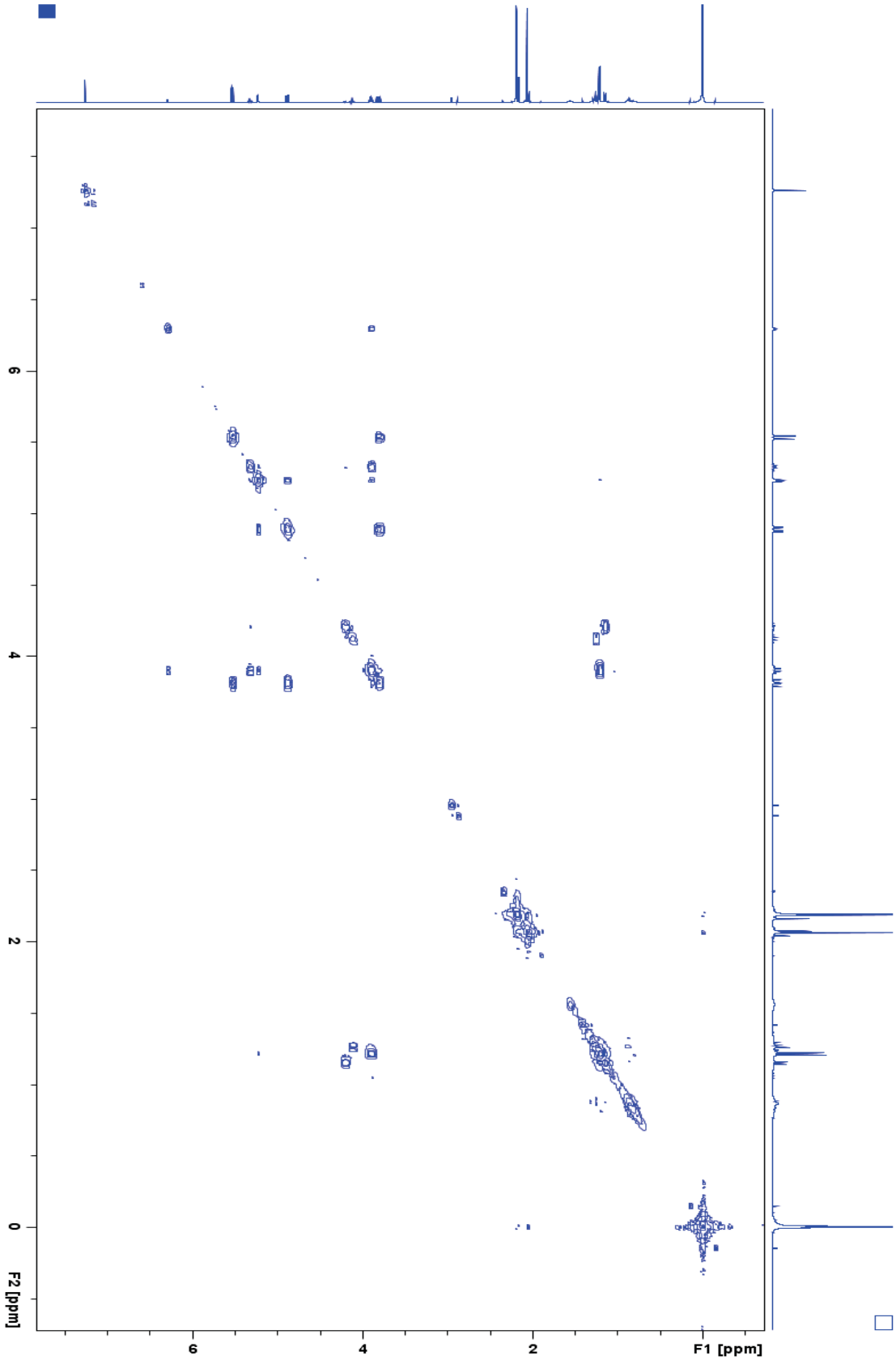


**Figure 25.** COSY spectrum for 1,3,4-tri-*O*-acetyl-2-azidodeoxy-α,β-L-fucose **6**.

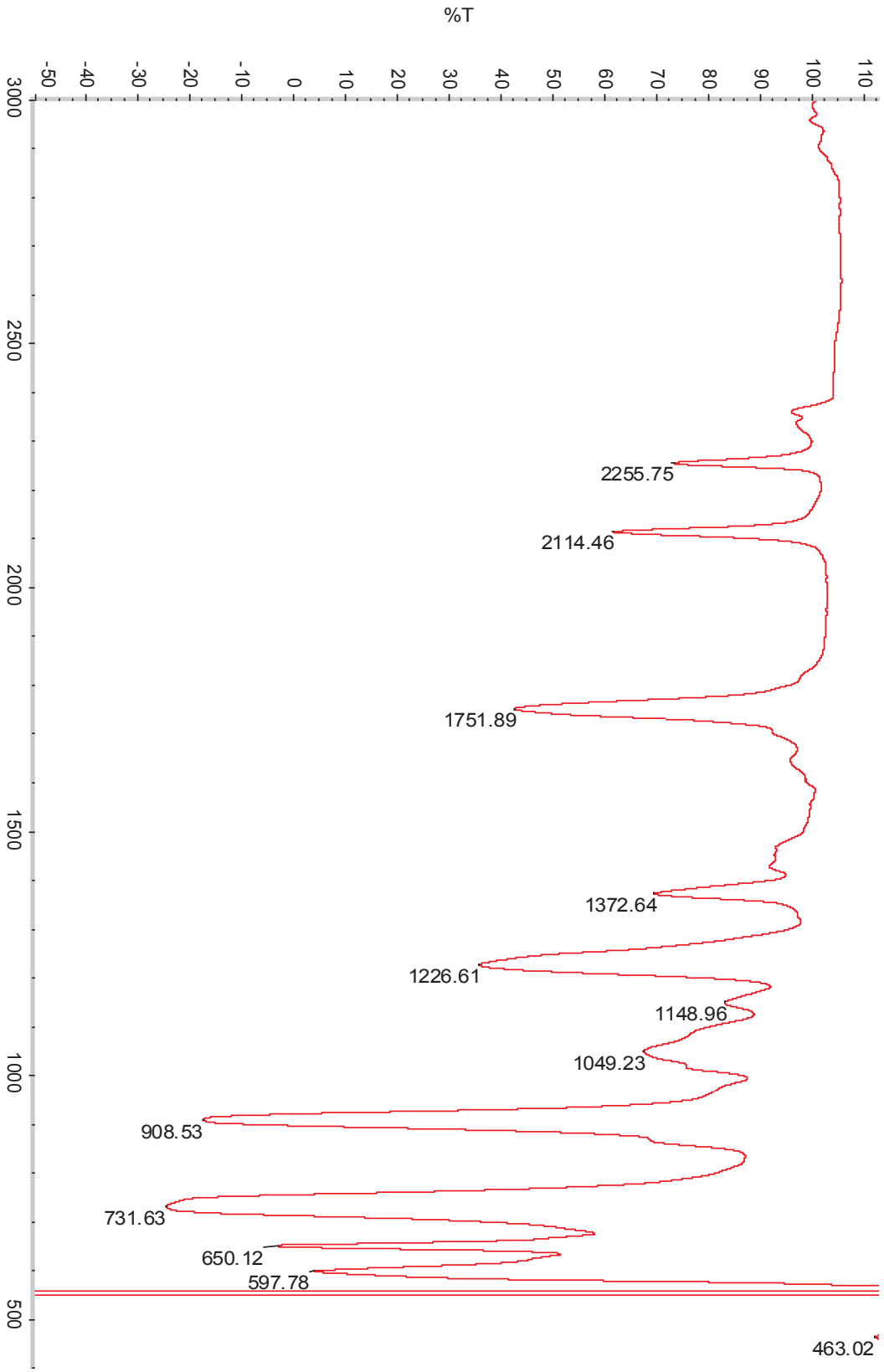


**Figure 26.** IR spectrum for 1,3,4-tri-*O*-acetyl-2-azidodeoxy-α,β-L-fucose **6**.

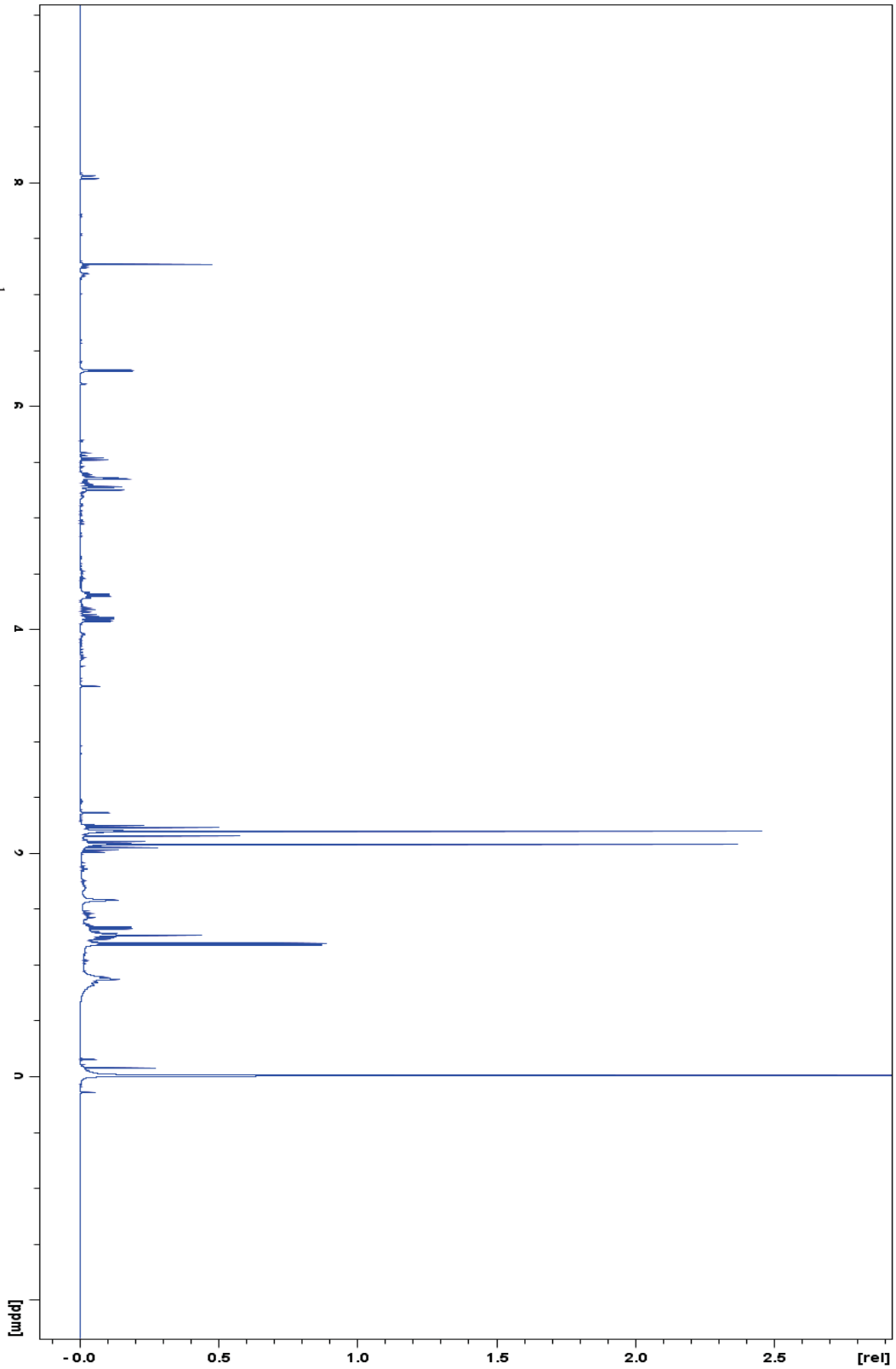


**Figure 27.** $^{1}$H NMR spectrum for 1,3,4-tri-*O*-acetyl-2-*N*-(phenylacetamido)-α,β-L-fucose **7**.

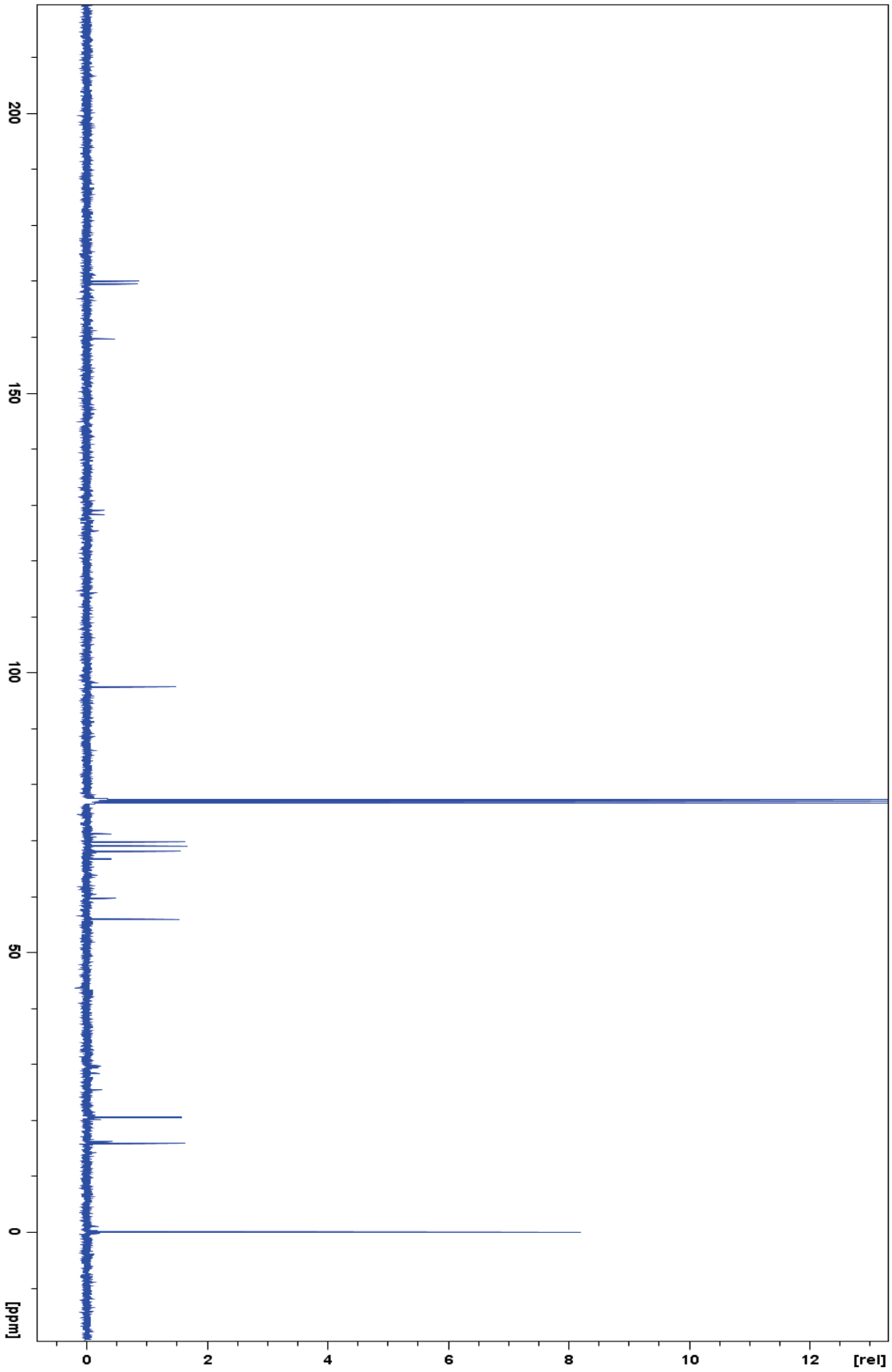


**Figure 28.** $^{13}$C NMR spectrum for 1,3,4-tri-*O*-acetyl-2-N-(phenylacetamido)-α,β-L-fucose **7**.

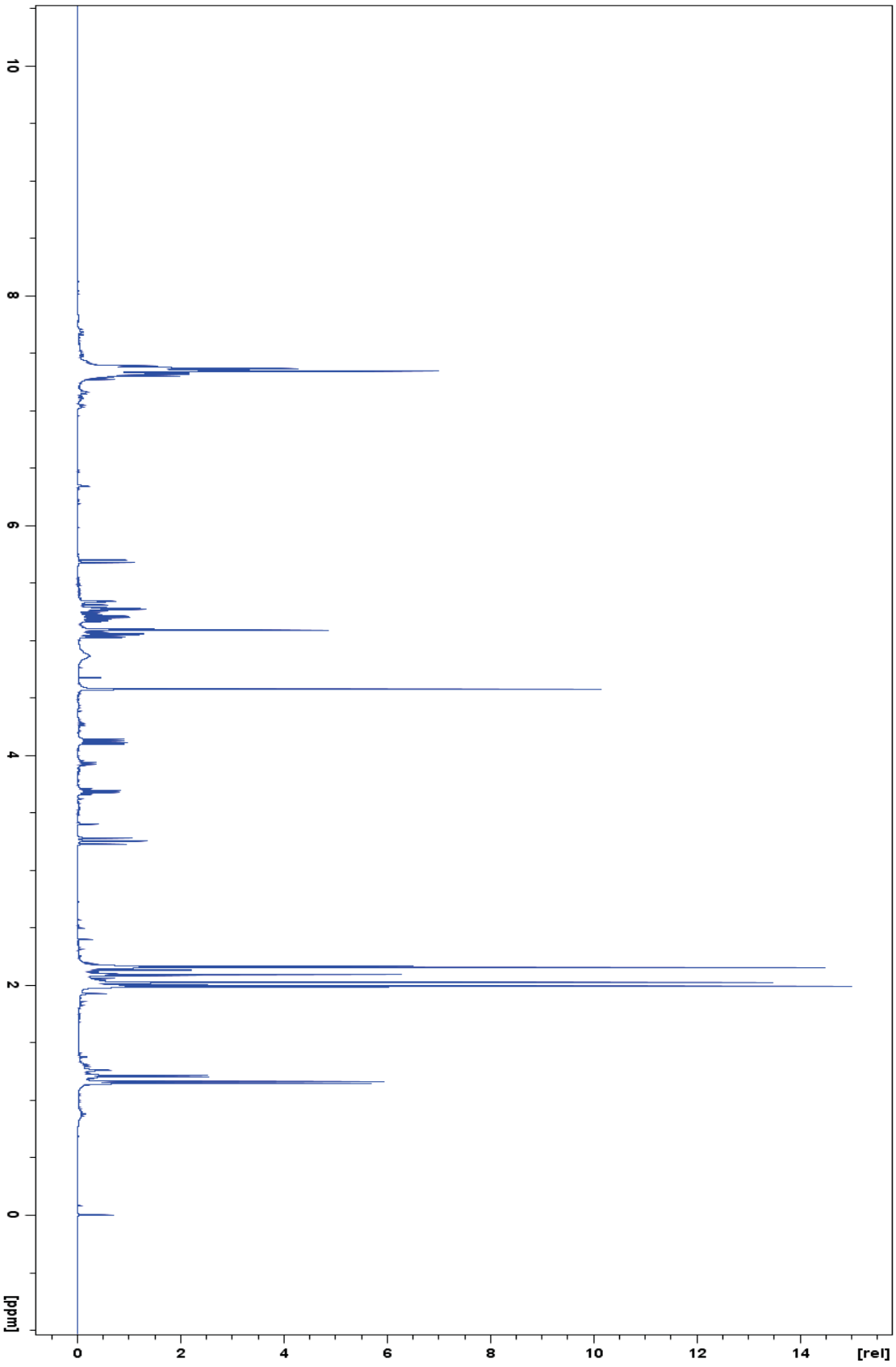


**Figure 29.** $^{1}$H NMR spectrum for 1,3,4-tri-*O*-acetyl-2-*N*-(benzyloxyacetamido)-α,β-L-fucose **8**.

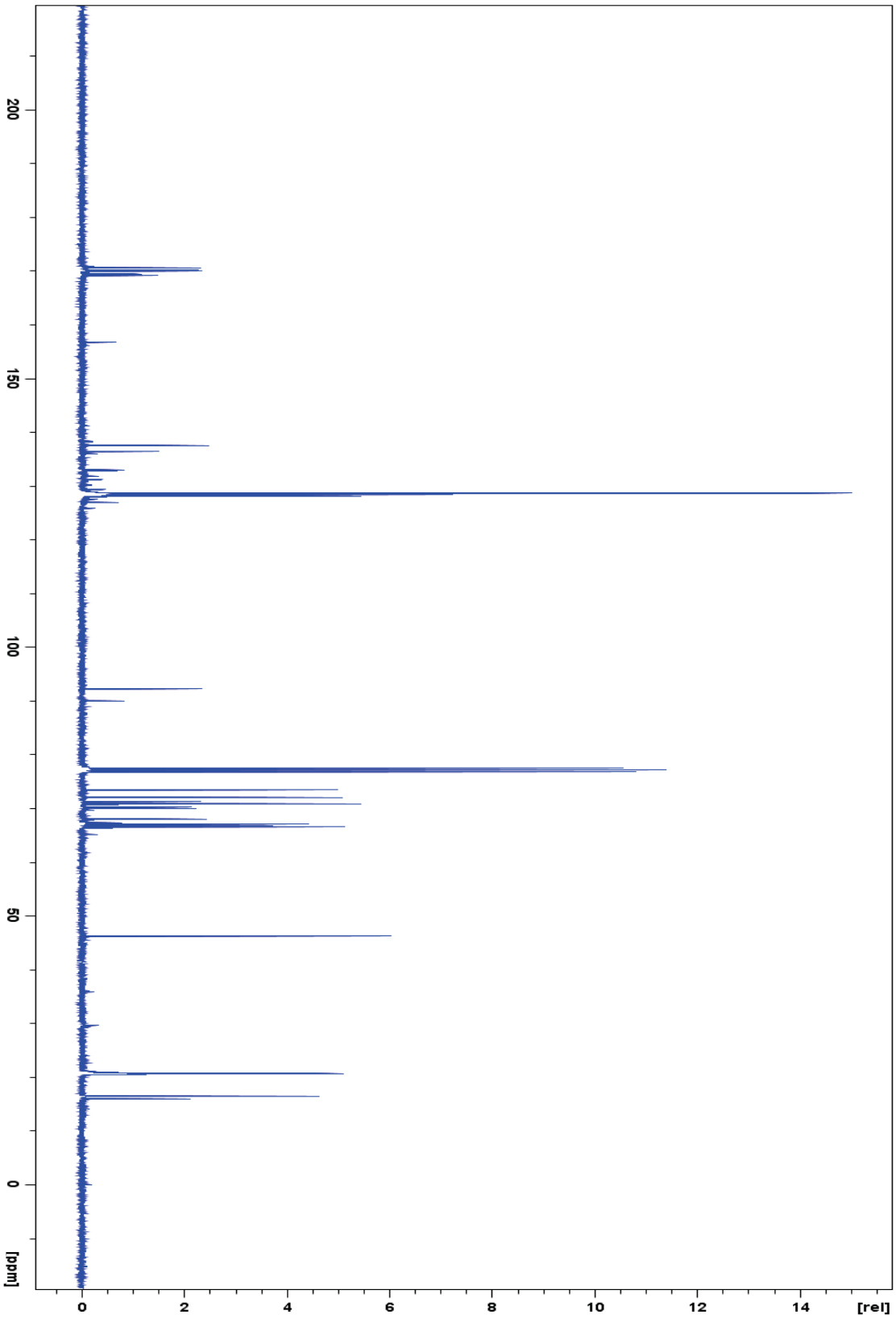


**Figure 30.** $^{13}$C NMR spectrum for 1,3,4-tri-*O*-acetyl-2-*N*-(benzyloxyacetamido)-α,β-L-fucose **8**.

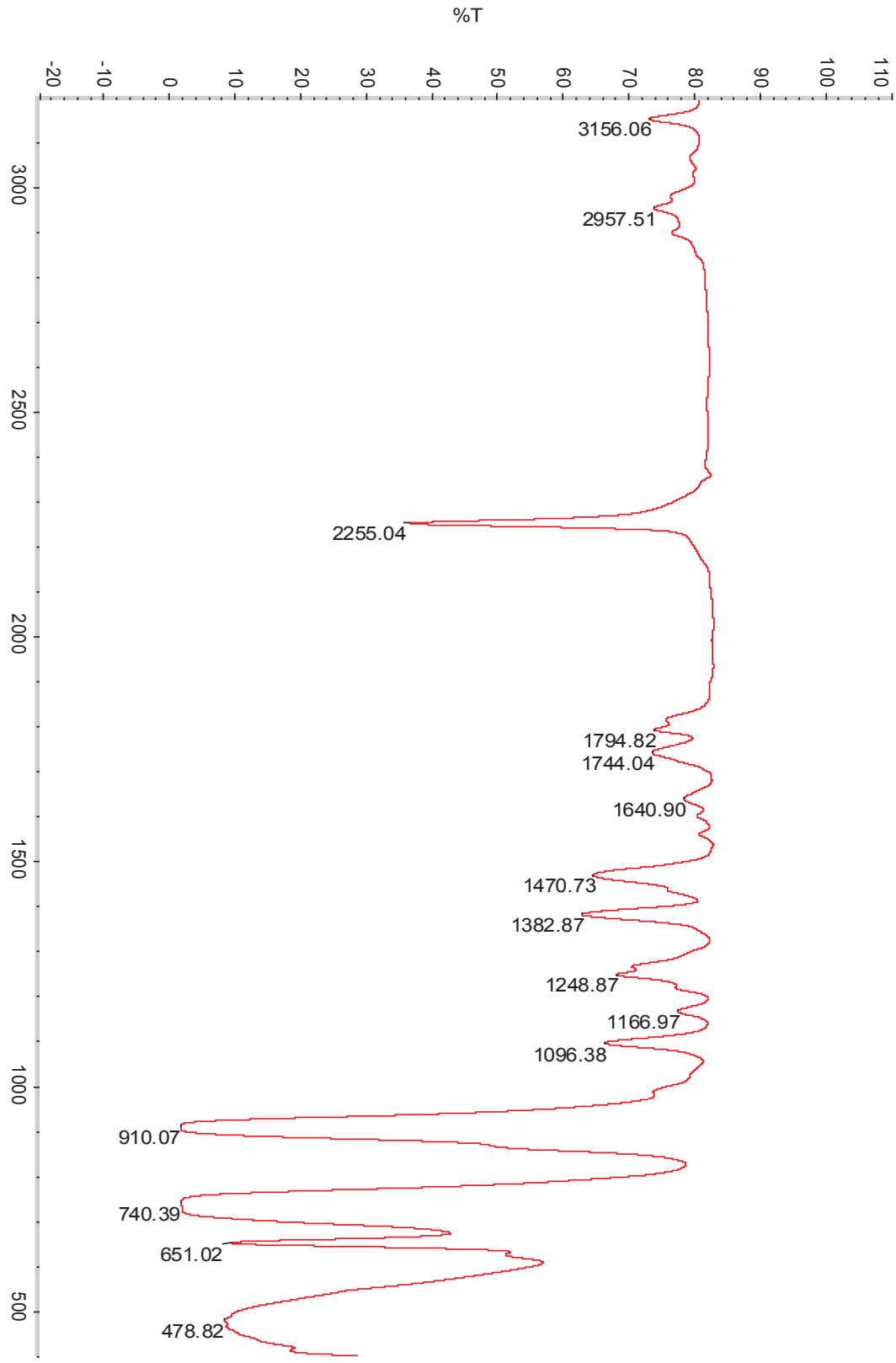


**Figure 31.** IR spectrum for 1,3,4-tri-*O*-acetyl-2-*N*-(benzyloxyacetamido)-α,β-L-fucose **8**.

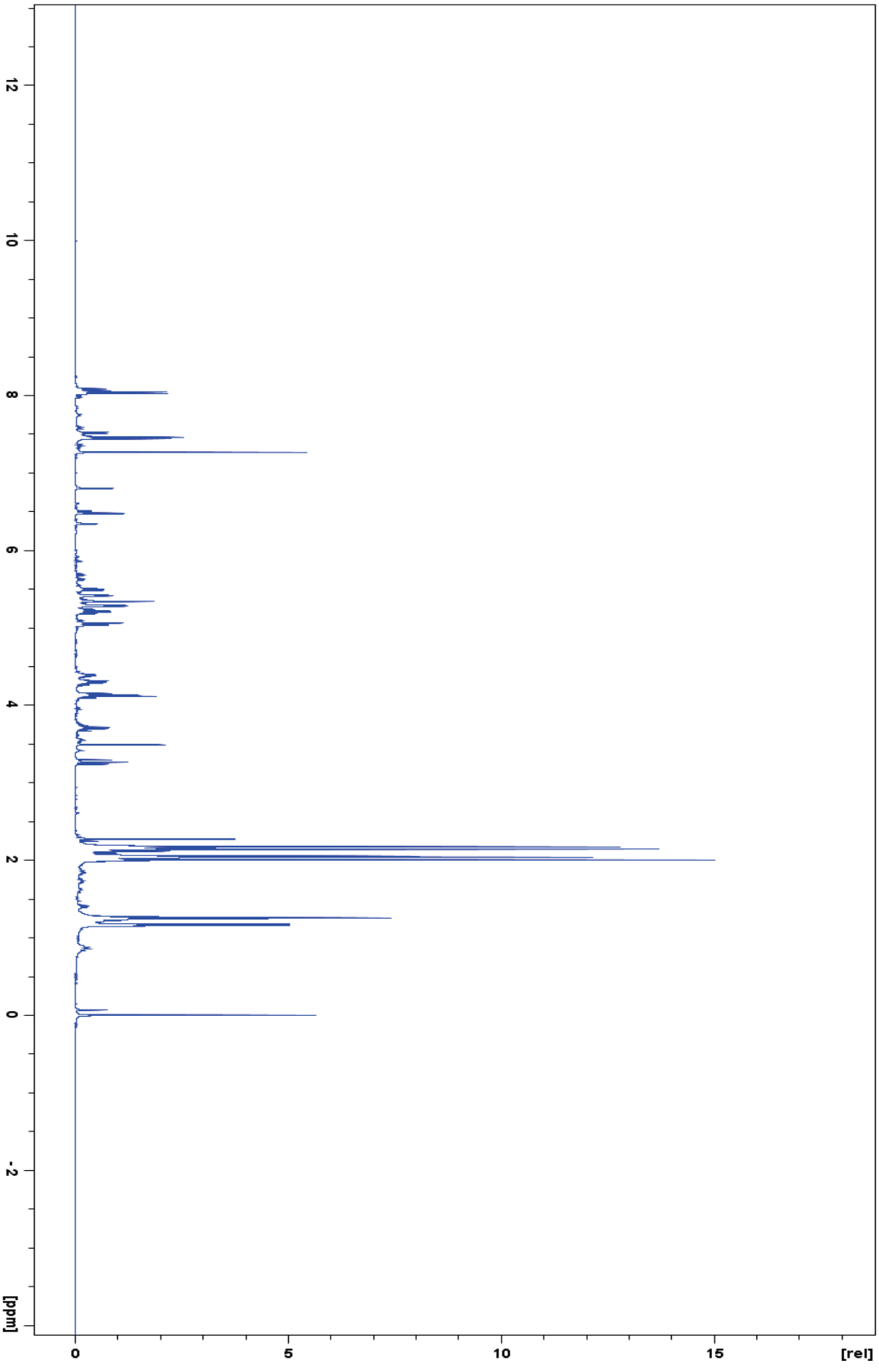


**Figure 32.** $^{1}$H NMR spectrum for 1,3,4-tri-*O*-acetyl-2-*N*-(4-chlorobenzamido)-α,β-L-fucose **11**.

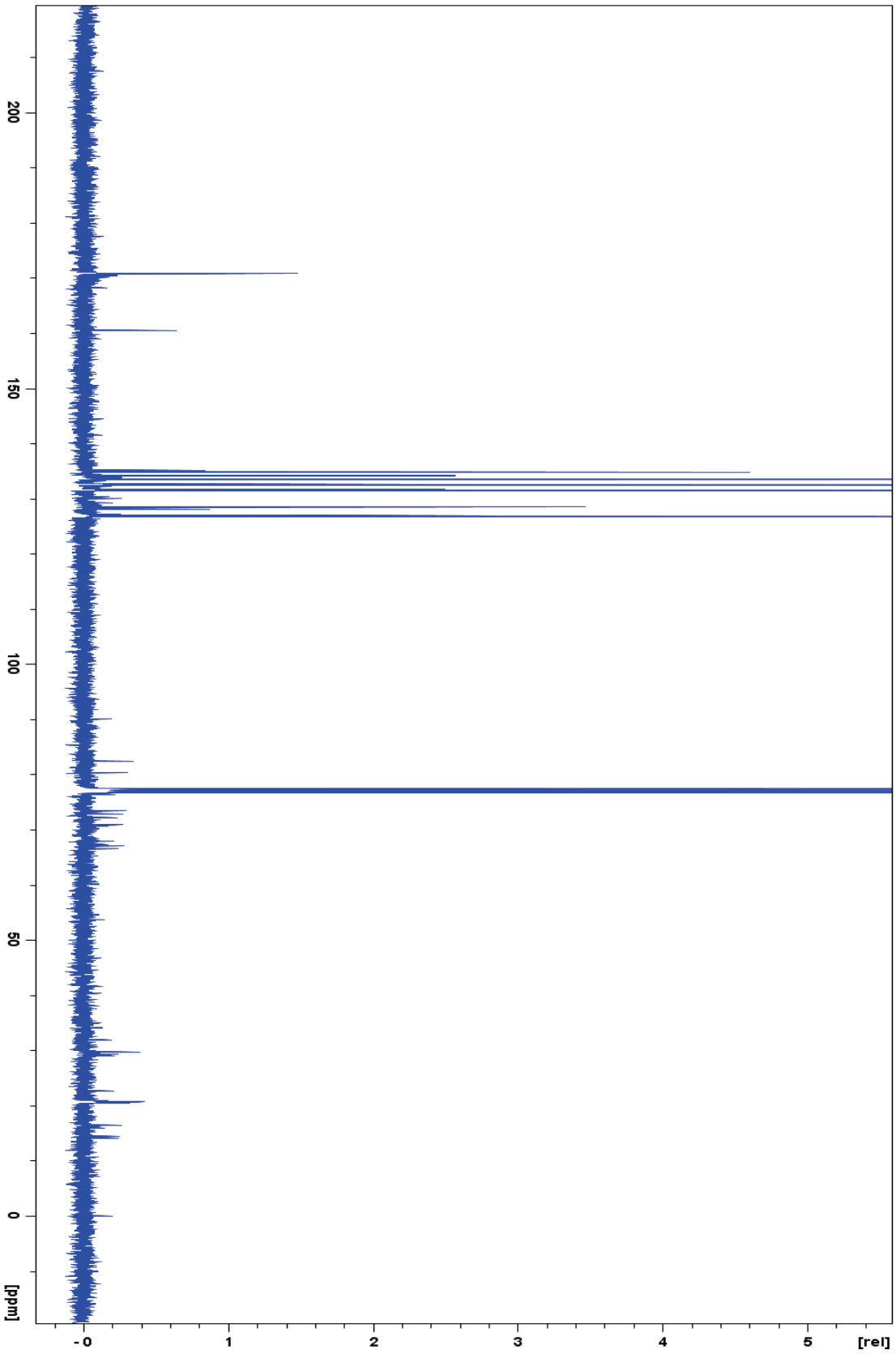


**Figure 33.** $^{13}$C NMR spectrum for 1,3,4-tri-*O*-acetyl-2-*N*-(4-chlorobenzamido)-α,β-L-fucose **11**.

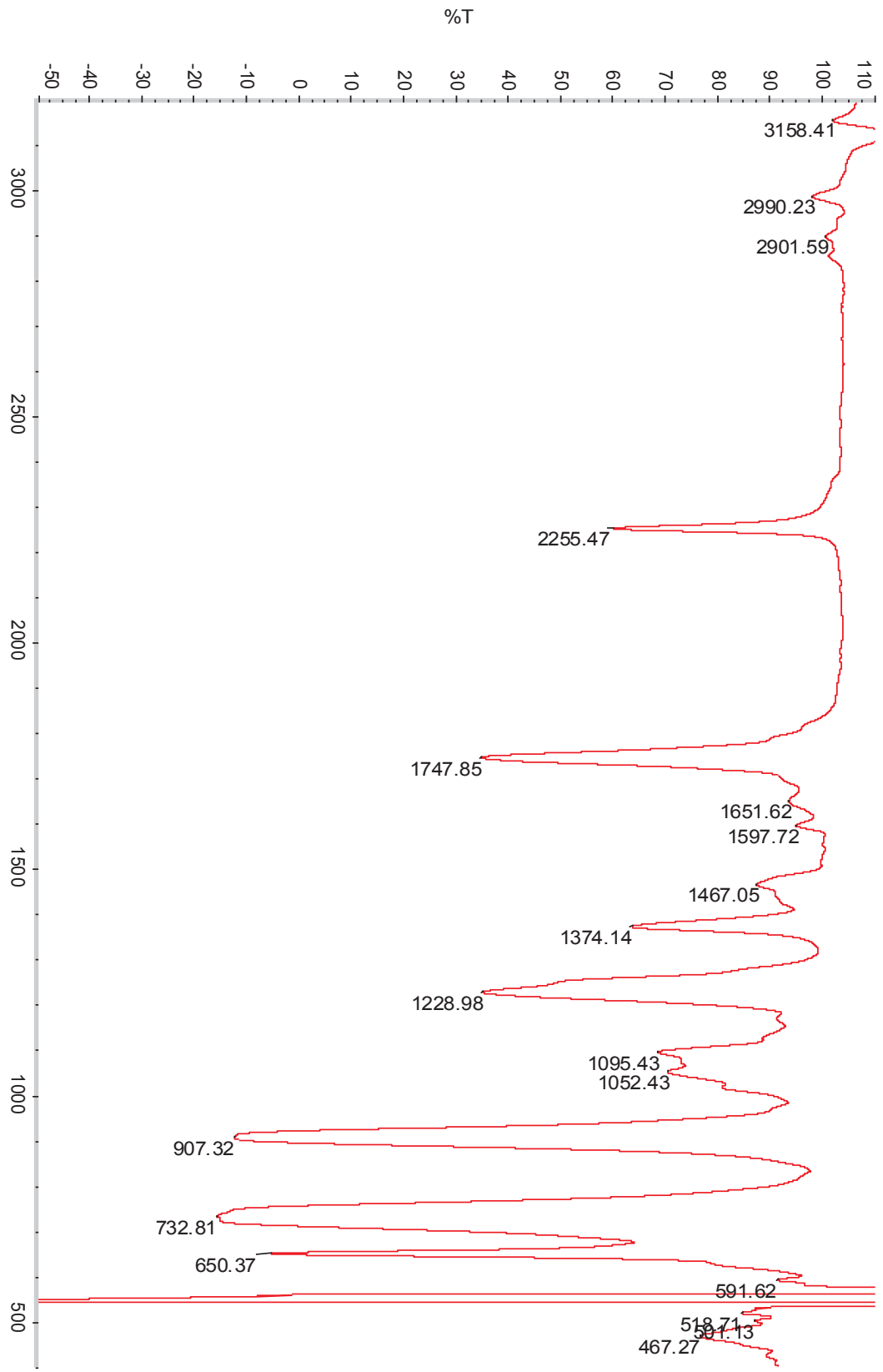


**Figure 34.** IR spectrum for 1,3,4-tri-*O*-acetyl-2-*N*-(4-chlorobenzamido)-α,β-L-fucose **11**.

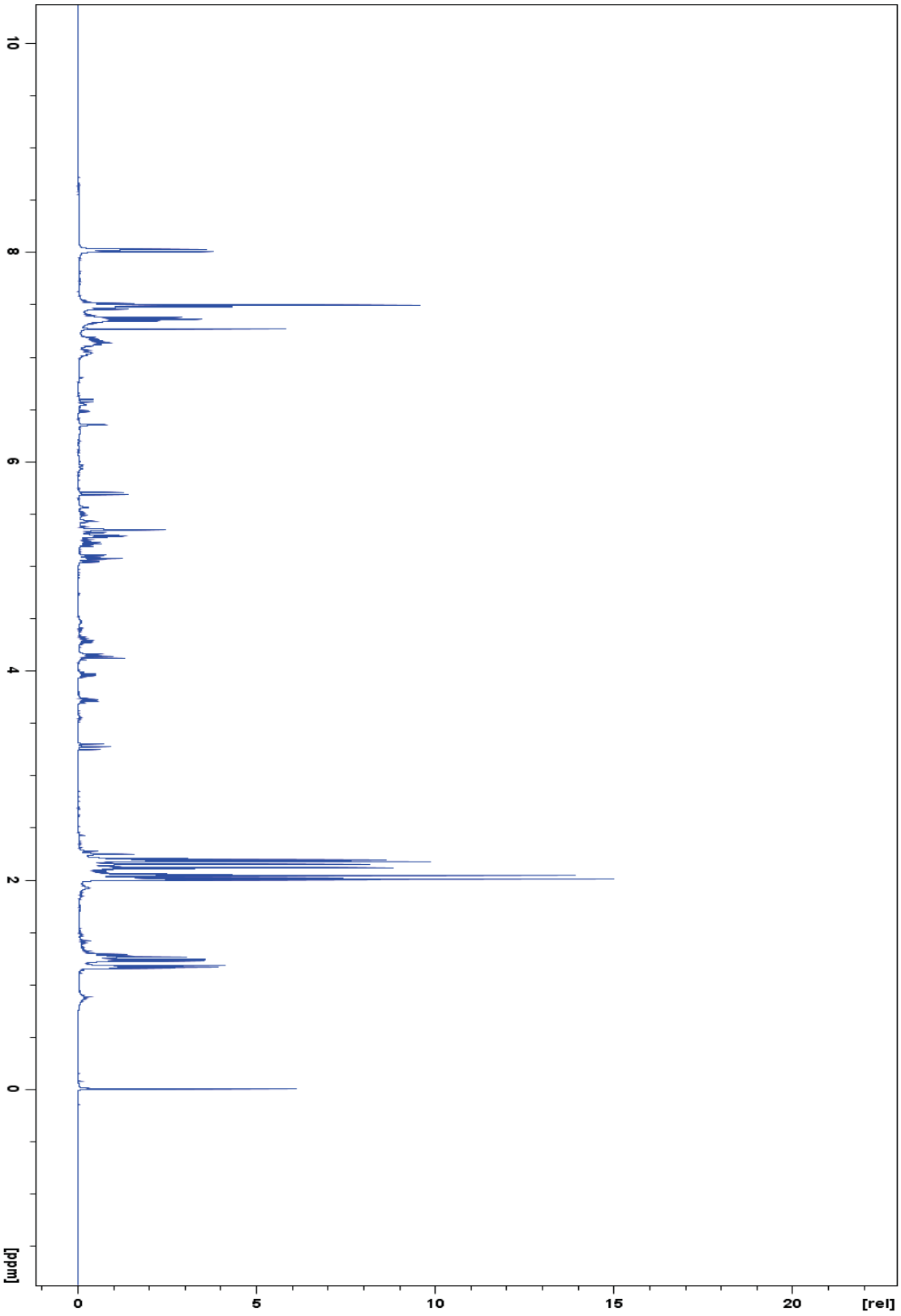


**Figure 35.** $^{1}$H NMR spectrum for 1,3,4-tri-*O*-acetyl-2-*N*-(2-chlorobezamido)-α,β-L-fucose **12**.

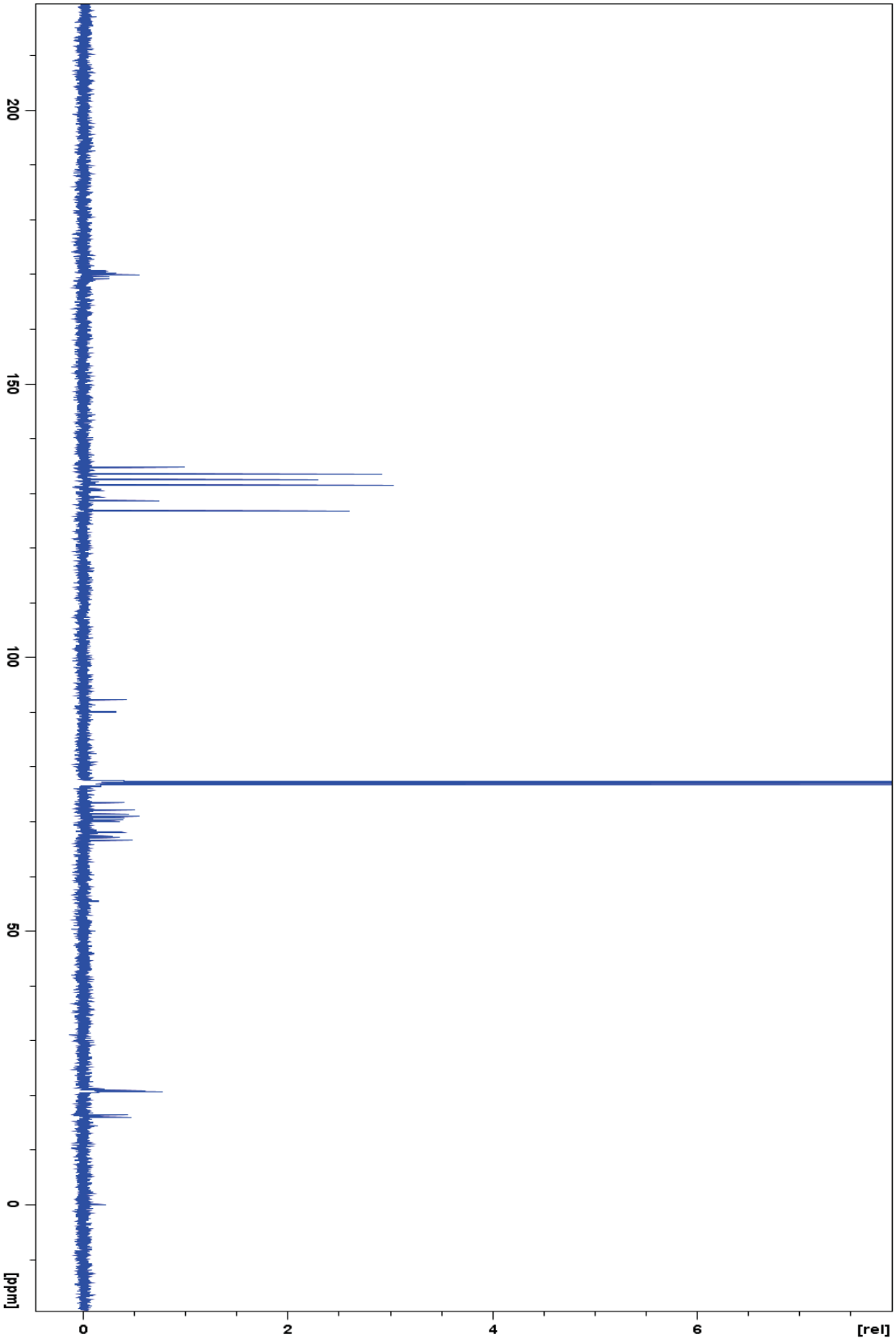


**Figure 36.** $^{13}$C NMR spectrum for 1,3,4-tri-*O*-acetyl-2-*N*-(2-chlorobenzamido)-α,β-L-fucose **12**.

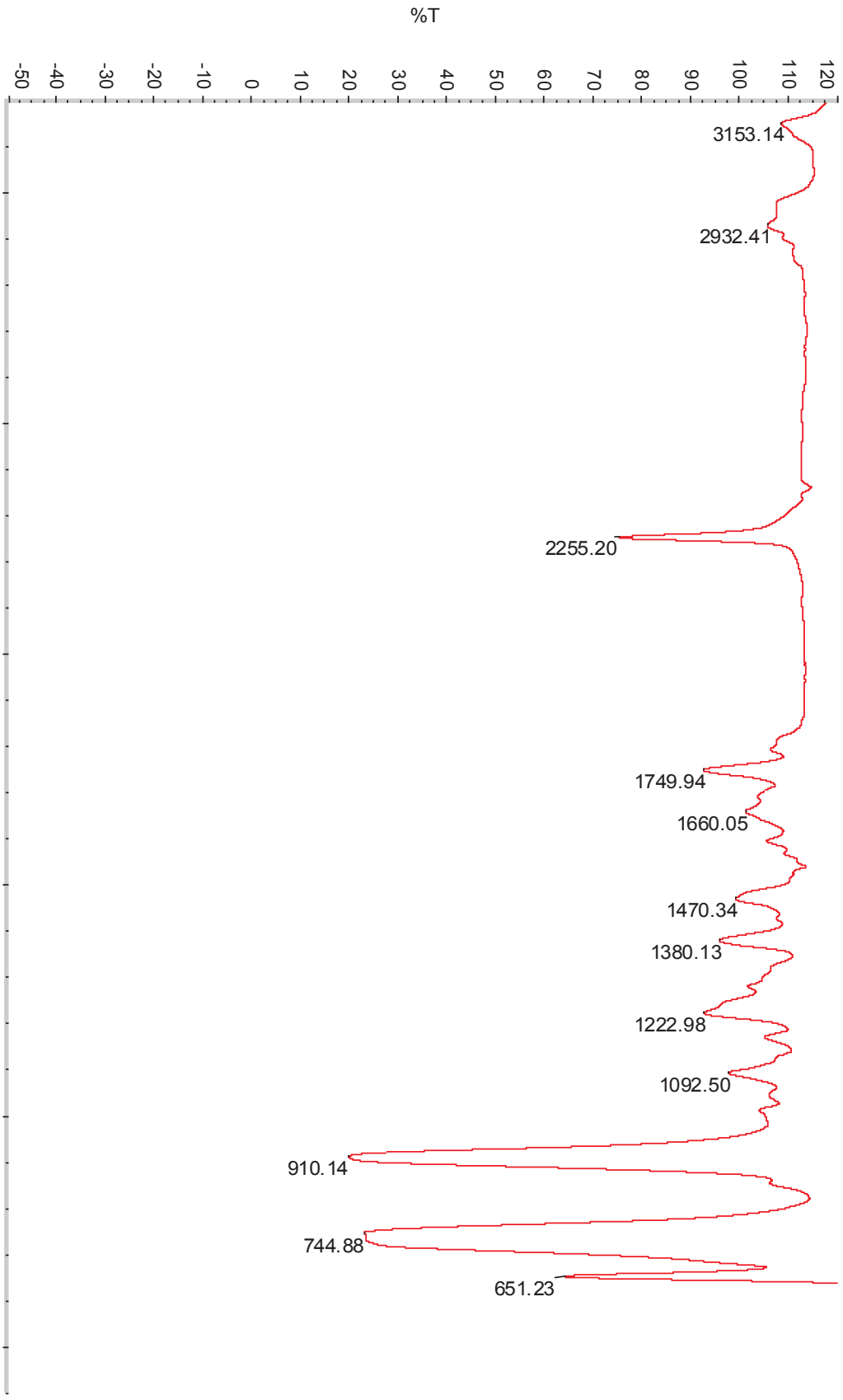


**Figure 37.** IR spectrum for 1,3,4-tri-*O*-acetyl-2-*N*-(2-chlorobenzamido)-α,β-L-fucose **12**.

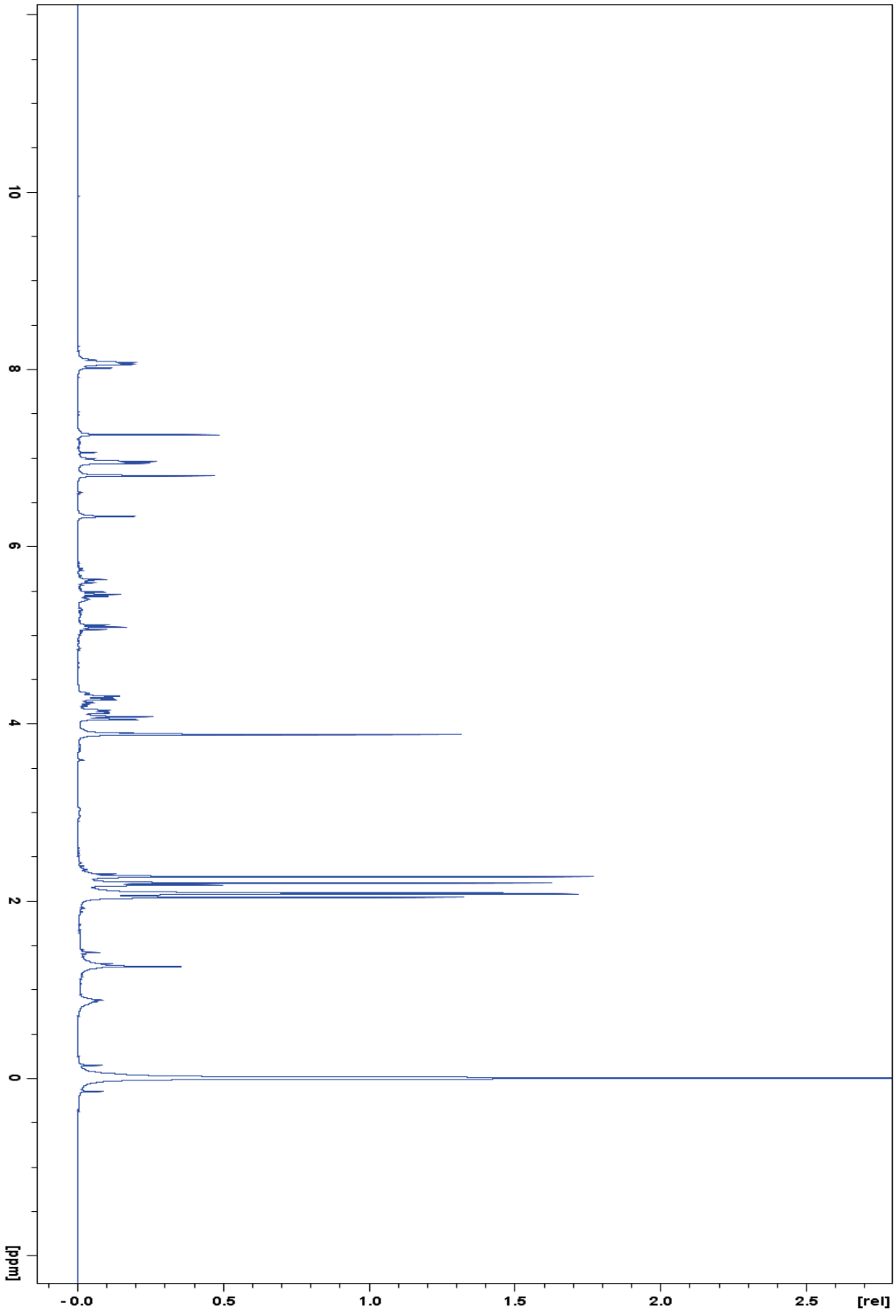


**Figure 38.** $^{1}$H NMR spectrum for 1,3,4,6-tetra-*O*-acetyl-2-*N*-(4-methoxybenzamido)-α,β-D-glucose **13**.

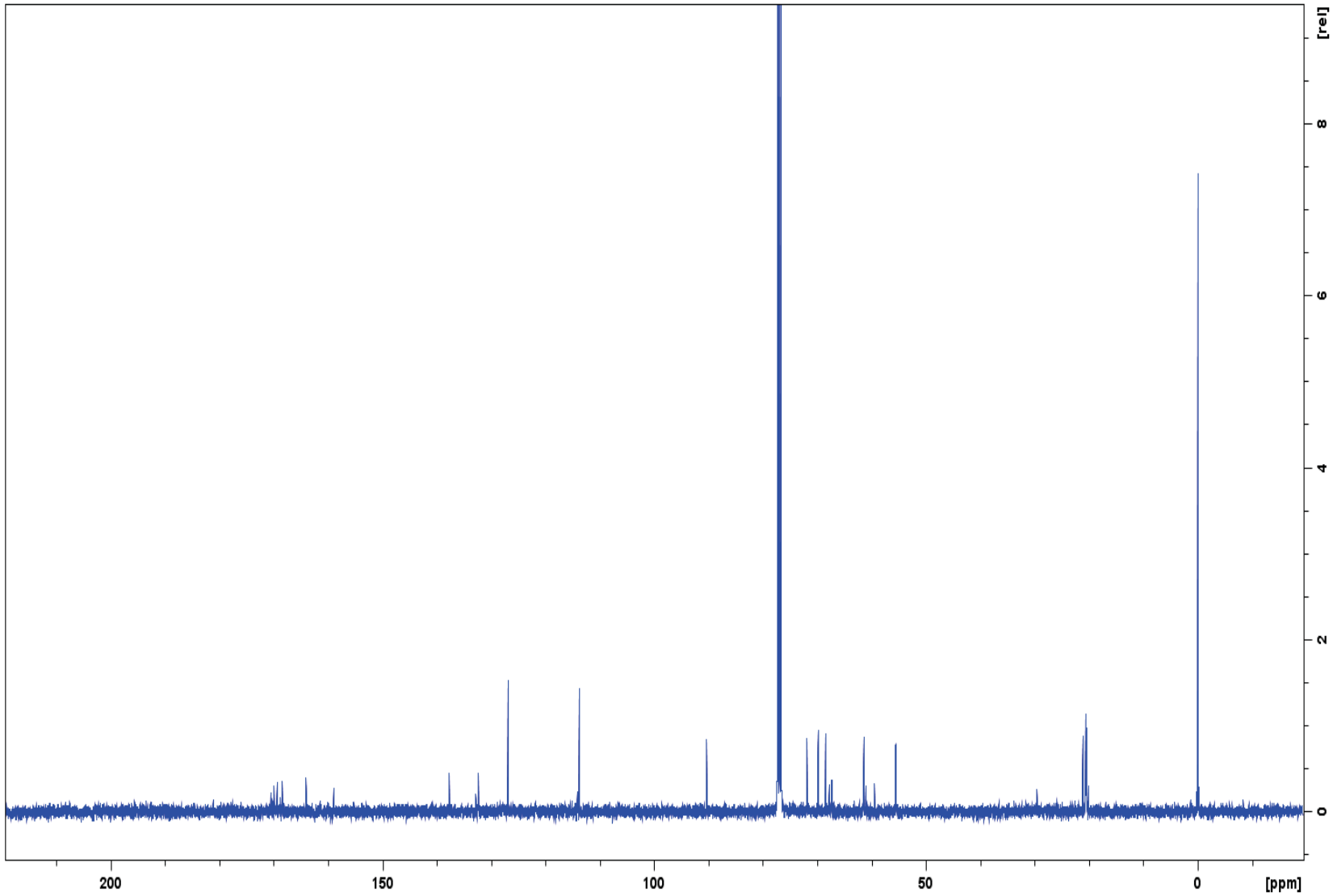


**Figure 39.** $^{13}$C NMR spectrum for 1,3,4,6-tetra-*O*-acetyl-2-*N*-(4-methoxybenzamido)-α,β-D-glucose **13**.

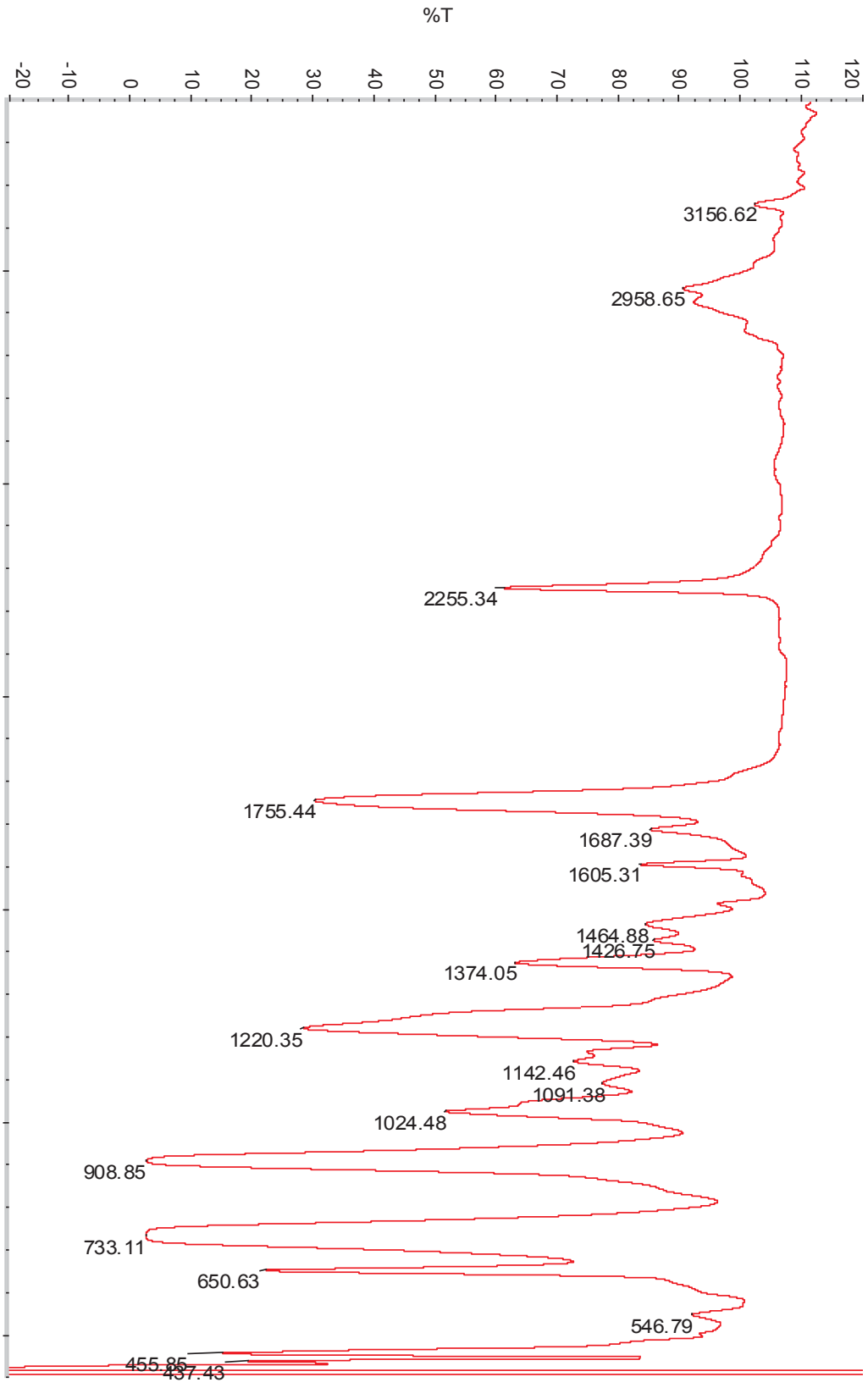


**Figure 40.** IR spectrum for 1,3,4,6-tetra-*O*-acetyl-2-*N*-(4-methoxybenzamido)-α,β-D-glucose **13**.

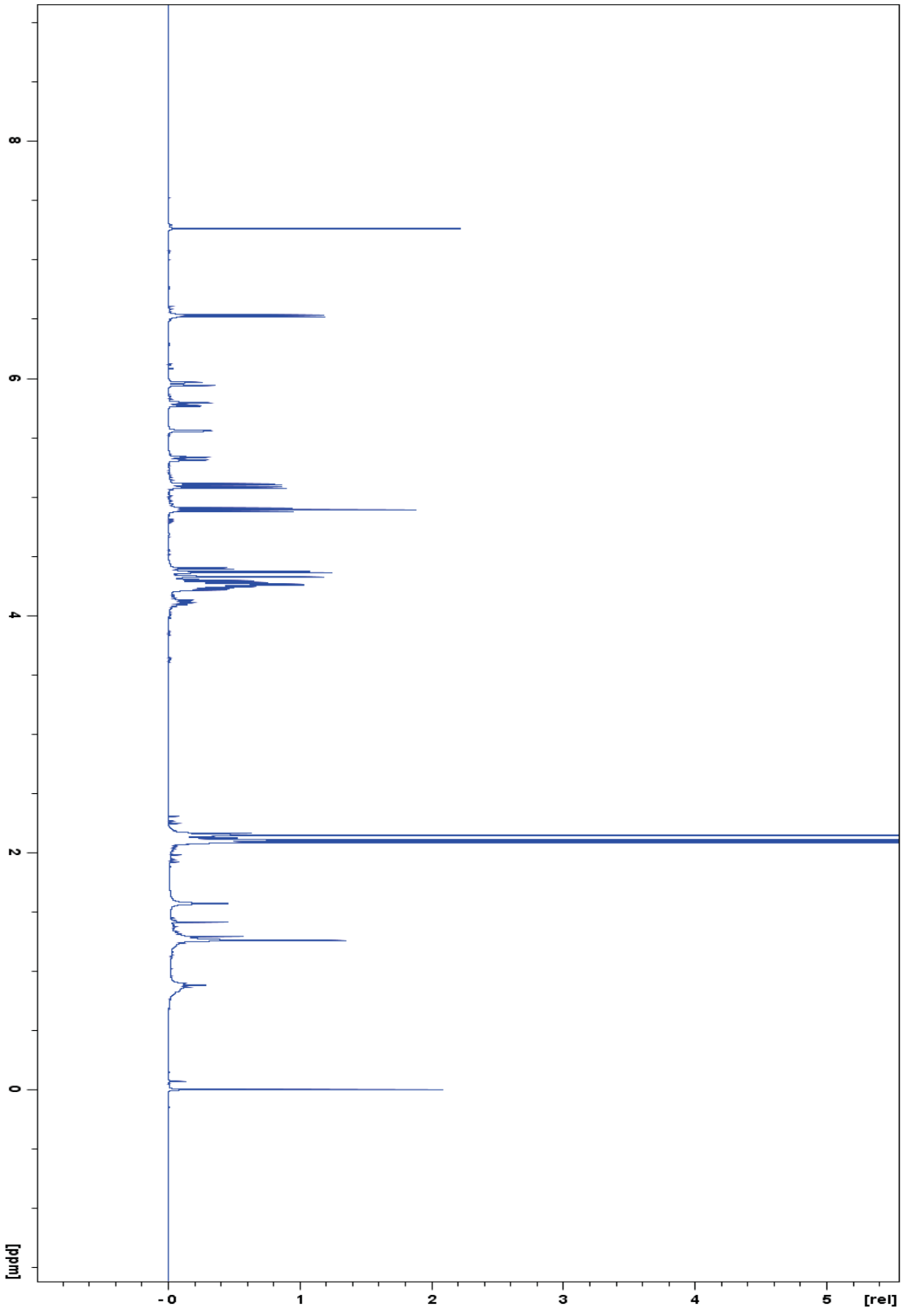


**Figure 41.** $^{1}$H NMR 1-chloro-3, 4,6-tri-*O*-acetyl-2-azidodeoxy-α-D-glucose **19**.

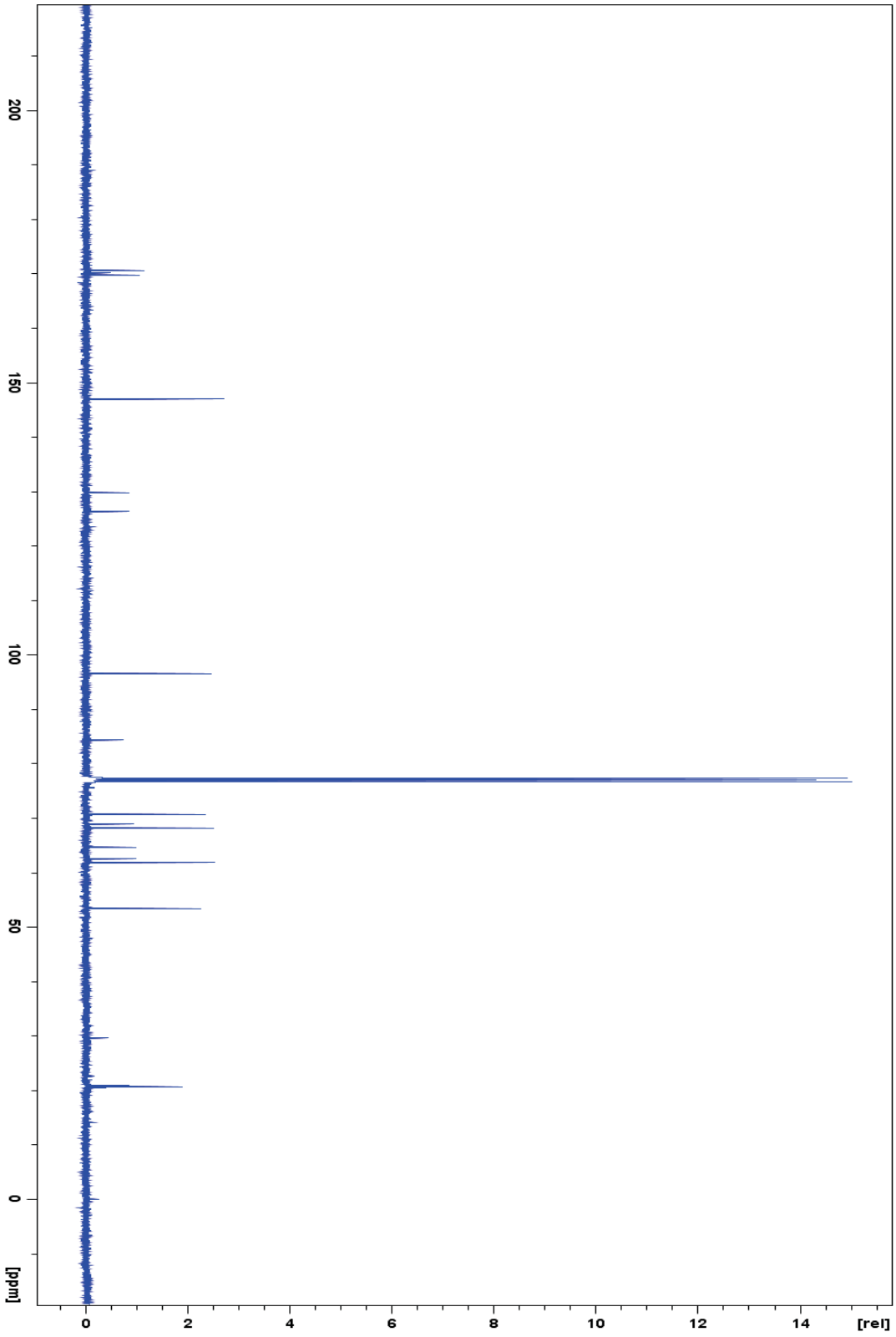


**Figure 42.** $^{13}$C NMR for 1-chloro-3,4,6-tri-*O*-acetyl-2-azidodeoxy-α-D-glucose **19**.

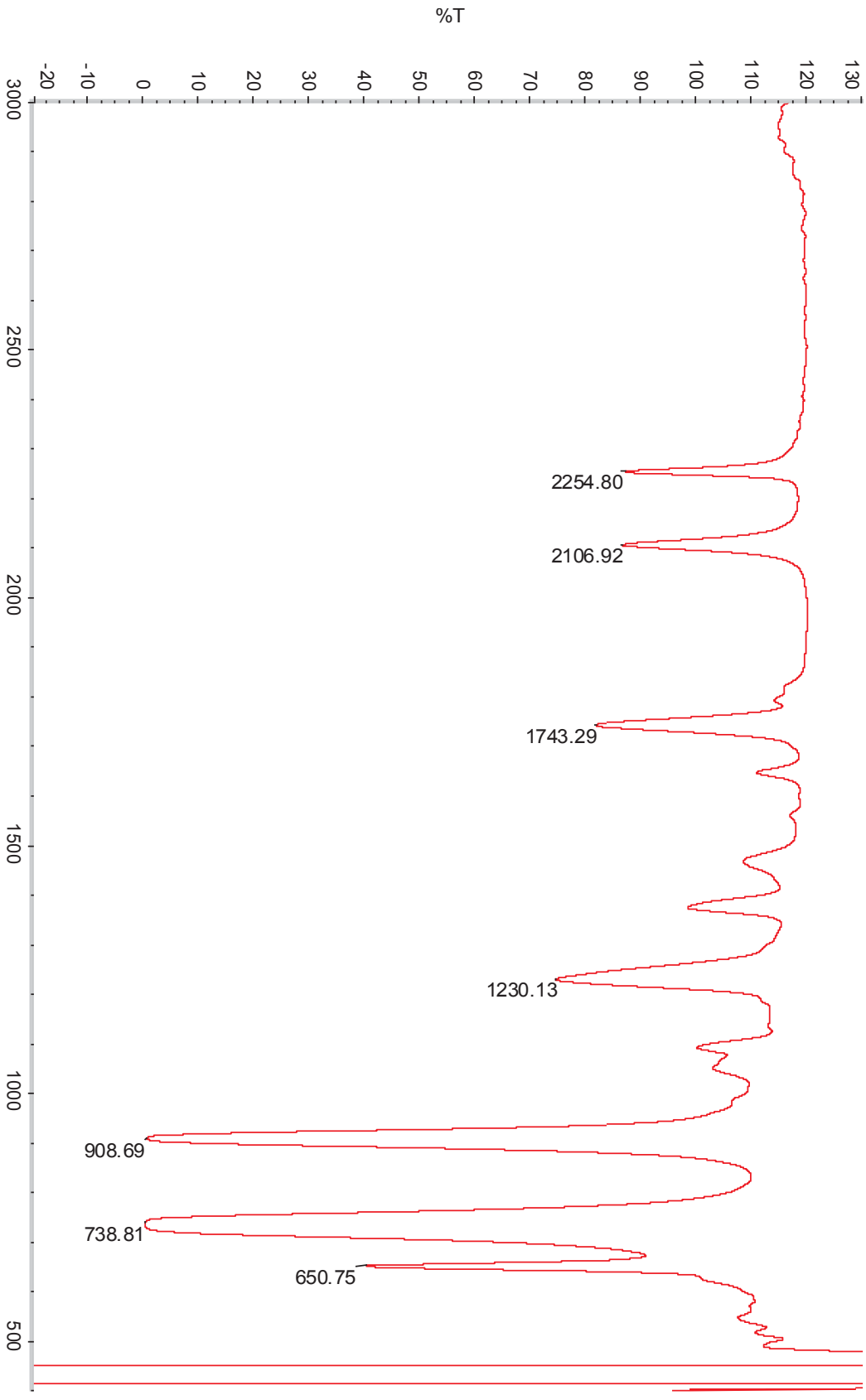


**Figure 43**. IR for 1-chloro-3,4,6-tri-*O*-acetyl-2-azidodeoxy-α-D-glucose **19**.